CHAPTER 4

Radiative Transitions between Electronic States

4.1 The Absorption and Emission of Light by Organic Molecules

Schemes 1.1–1.3 are key working paradigms used to initiate analysis of organic photophysics or organic photochemistry. In this chapter we are concerned with the portion of the working paradigm of molecular organic photochemistry that involves (1) the absorption ($R + h\nu \rightarrow {}^*R$) of light by an organic molecule (R) to produce an electronically excited state (*R), and (2) the emission (${}^*R \rightarrow R + h\nu$) of light from an electronically excited state (*R) to produce a ground state (R) (Scheme 4.1). In this chapter both spin-allowed and spin-forbidden radiative transitions will be discussed in detail. Of particular interest are the radiative transitions of light absorption and emission when *R is the lowest singlet (S_1) and triplet (T_1) state of an organic molecule (shown in the rectangle of Scheme 4.1).

4.2 The Nature of Light: A Series of Paradigm Shifts

The accepted paradigm that described the nature of light and its interaction with matter has changed dramatically three times since the 1700s. Each paradigm tried to answer the same questions: What is the nature of light, and What is the nature of the interaction of light with matter? Each paradigm answered the questions in a new and radically different way from that of the previous one, and each new one constituted a true *paradigm shift* for science. With each new paradigm shift, light was positioned as an ever more fundamental entity in the scientific universe; eventually, through the theory of relativity, light was placed at a level of significance equivalent to that of matter.

Historically, there was relatively little documented scientific study and discussion of the nature of light until the 1700s, when Newton proposed a paradigm that light was composed of a stream of *particles*. Newton employed concepts of the motion and

Radiative Processes

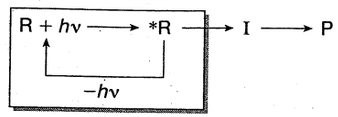

$^*R(S_1) \longrightarrow R(S_0) + h\nu_F$ (Flourescence, Spin Allowed Emission)

$^*R(T_1) \longrightarrow R(S_0) + h\nu_P$ (Phosphorescence, Spin Forbidden Emission)

$R(S_0) + h\nu \longrightarrow {}^*R(S_1)$ (Spin Allowed Absorption)

$R(S_0) + h\nu \longrightarrow {}^*R(T_1)$ (Spin Forbidden Absorption)

Scheme 4.1 Radiative transitions of organic molecules of greatest importance in organic photochemistry.

energy of point particles as a foundation for the hugely successful structure of classical mechanics. It was therefore natural for Newton to explain the properties of light by postulating that light also consisted of tiny particles emitted from light-producing objects such as the sun or a flame. These particles were imagined to move at great speeds through empty space or through transparent media. Newton's paradigm was supported by the action of a prism, which "decomposed" a ray of white light into its component "particles," possessing the diverse visible colors of the rainbow. Thus, each of the different particles of light could be associated with a color. The sensation of sight was interpreted as the result of the eye being excited by particles of light as they struck the eye. In large part (possibly because of Newton's towering reputation rather than the demonstration of a convincing array of experimental evidence), during the 1700s, the ruling paradigm of the nature of light was that it consisted of particles.

During the early 1800s, new experiments demonstrated aspects of light that Newton's particle theory completely failed to explain. In particular, Newton's theory could not explain the phenomena of *interference* by which two light rays can interact with one another *constructively* to make a more intense light ray or *destructively* to make a light ray completely disappear. On the other hand, interference was a well-known property of waves. For example, the interference of waves is commonly observed when one produces waves by disturbing the surface of a still sample of water. The theory of matter waves readily explained the phenomenon of interference. It seemed obvious that particles could commingle with one another, create a sort of constructive interference, and amplify each other's effect; on the other hand, there was no known way for particles to "cancel each other" and explain the phenomenon of destructive interference. The easily demonstrated and reproducible observation that light rays could interfere with one another was the beginning of the end for the paradigm of light as particles. A paradigm shift was about to occur.

In the mid-1800s, Maxwell put forward a new paradigm for the nature of light, proposing that light is composed of a *force field of oscillating electric charges that have the characteristics of waves, not particles.* If electric charges are oscillating, they

generate not only an oscillating electric field but also an associated oscillating magnetic field. In this paradigm, the wave nature of light was contained in an elegant set of mathematical equations (Maxwell's equations), which described light as a wave, driven by an oscillating electromagnetic field surrounding oscillating charged particles (later identified as negatively charged electrons and positively charged nuclei). Maxwell's paradigm for the nature of light also provided a beautiful, previously unrecognized synthesis of the electrical and magnetic forces in both light and matter. Maxwell's equations quantitatively explained the phenomena of interference, scattering, reflection, and refraction. Maxwell's paradigm probably possessed a special appeal to many scientists because it was formulated in an elegant mathematical language and because it integrated electrical and magnetic phenomena. By the end of the 1800s, Maxwell's paradigm for light as a form of electromagnetic waves was universally accepted by the scientific community and was widely considered a universal and unshakable paradigm of physics. Physicists refer to Maxwell's paradigm as the *classical paradigm of light as electromagnetic waves.*

In spite of its mathematical elegance and ability to integrate electricity and magnetism, Maxwell's paradigm for the wave nature of light ran into serious difficulties because of certain experiments that were unexplainable if light was fundamentally an electromagnetic wave. Toward the end of the 1800s, the validity of the classical paradigm for the electromagnetic wave nature of light was called into question because of its inability to explain two very simple experiments, one involving the *emission of light* and the other involving the *absorption of light*: (1) the first experiment dealt with the measurement of the wavelength dependence of the energy distribution for light *emitted* by a hot object, such as a heated metal bar (so-called *black-body* radiation, Fig. 4.1); and (2) the second experiment dealt with the measurement of the

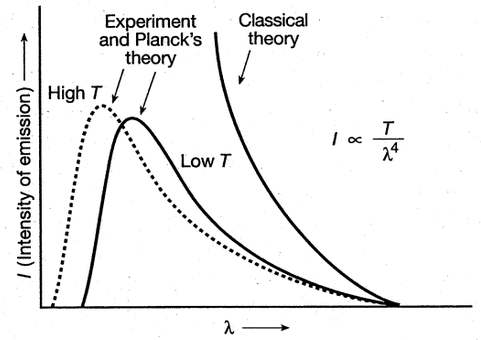

Figure 4.1 The UV catastrophe. The classical theory of light predicted that the intensity (I) of light emitted by a metal bar should be proportional to the temperature (T) of the bar and the inverse fourth power of the wavelength (λ) of the emitted light.

wavelength (or frequency) dependence of the kinetic energy (KE) for electrons emitted when light is *absorbed* by a metal (the so-called *photoelectric effect*, Fig. 4.2). At the beginning of the 1900s, the issue of the nature of light and its interaction with matter to produce the absorption and emission of light was a source of great debate among physicists.

4.3 Black-Body Radiation and the "Ultraviolet Catastrophe" and Planck's Quantization of Light Energy: The Energy Quantum Is Postulated

The energy distribution of light emitted from a heated metal bar is found experimentally (Fig. 4.1) to depend on temperature (T). At lower temperatures the heated bar emits at wavelengths, λ (or related frequencies, ν), that maximize in the infrared (IR) range; as the temperature of the metal is increased, the bar begins to glow red, green, then white, as all wavelengths in the visible (vis) region of the spectrum are emitted. A typical heated metal bar emits an energy distribution that possesses a maximum in the visible or ultraviolet (UV) region of the electromagnetic spectrum. The distribution of wavelengths emitted by the heated metal was modeled by a "black body," or a sample of matter that absorbs all of the light energy that strikes it. Black-body radiation is simply the emitted radiation of the electromagnetic field (light) that is in equilibrium with the body (matter) at a given temperature. The classical theory of light predicts that the electromagnetic field associated with the black body will possess a certain distribution of wavelengths (frequencies) characteristic of the temperature of the black body (Fig. 4.1).

In quantitative terms, the classical theory predicted (Fig. 4.1, right) that the intensity I (energy per unit time) of emitted light by a metal bar at a given temperature (T) is proportional to T/λ^4. Thus, according to classical theory, as $\lambda \rightarrow 0$, *the intensity of the emitted light should become infinite*, a preposterous prediction! If the intensity I indeed was proportional to $1/\lambda^4$, then a firefly, when it flashed its light, would release sufficient energy to cause the entire universe to be destroyed! The prediction of unlimited energy in the high-energy (UV) region of the spectrum was named (possibly by a perplexed physicist) the "ultraviolet catastrophe."

The beginning of a new paradigm shift for the nature of light was triggered by Planck's explanation of how to avoid the ultraviolet catastrophe and to theoretically fit the experimental data. Planck's radical paradigm-shifting contribution was to show *mathematically* that the energy distribution of a heated metal would have a maximum, in excellent agreement with experiment (Fig. 4.1), if the *energy of a light wave was quantized* and *if the energy of light was directly related to frequency* by a remarkably simple and now familiar relationship (Eq. 4.1). From this equation, the energy of a light is assumed to be directly proportional to its frequency (ν) through a *proportionality constant* (h), which *required* a value of 6.6×10^{-34} J s in order to fit the experimental data. We now know that this constant, h, is a fundamental quantity in quantum chemistry and its appearance in any unit indicates the quantity obeys the laws of quantum mechanics. In honor of his contribution, h is now known as Planck's constant

and the bit of energy, E (Eq. 4.1), that corresponds to the frequency ν is known as a *quantum*. When we say that the energy of the electromagnetic field is quantized we understand that this means light of a given frequency ν can only be absorbed (or emitted) in energy steps equal to $h\nu$ [i.e., light cannot be absorbed (or emitted) continuously]. However, there is no limitation to the value that ν can take.

$$E = h\nu \tag{4.1}$$

Recall that the classical theory viewed light as an electromagnetic field that was created by oscillating electric charges. Using the classical harmonic oscillator (Chapters 2 and 3) as a guide, it was assumed that the charges could be stationary or they could oscillate. Charges that were not oscillating were considered to be in a "ground state" and incapable of emitting light; charges that were oscillating were considered to be in an "excited state" and to be capable of emitting light energy on return to the ground state. Planck's basic idea, which solved the paradox of the ultraviolet catastrophe, was that a given temperature the *energy* ($h\nu$) associated with a quantum of very short-wavelength light (a very high-frequency oscillator) was so high that the electric oscillators contained in a light wave that are associated with very short wavelengths are not excited; the energy available to the black body was insufficient to excite very short-wavelength (high-frequency) oscillators. It was a very simple idea: As the wavelength, λ, of emitted light decreases, the energy, $E = h\nu$, associated with the quantum required to excite the oscillator increases. Thus it become less and less likely that the high-energy oscillator will be excited at a given temperature, since energy must be conserved. Since the high-energy oscillator is not excited, it cannot emit light (oscillators in their ground state cannot emit light according to the classical theory of a harmonic oscillator). The quantization of energy effectively discriminates against the population of the short-wavelength, high-frequency oscillators, and thereby mathematically eliminates the ultraviolet catastrophe by preventing the intensity of emitted light to approach infinity as the wavelength decreases. Of course, Planck's mathematical "trick," while impressive, was completely nonintuitive based on classical physics and completely at odds with the paradigm of the classical theory of light, which viewed the absorption or emission of light as being continuous, and therefore able to be associated with any arbitrary energy.

4.4 The "Photoelectric Effect" and Einstein's Quantization of Light—The Quantum of Light: Photons

For proponents of the classical paradigm of light, another experimental observation called the "photoelectric effect" (Fig. 4.2) was just as baffling as the ultraviolet catastrophe. The *photoelectric effect* was the name given to the following phenomenon: When light of a certain wavelength λ (or associated frequency, ν) is *absorbed* by a metal surface, electrons are emitted from the metal (the phenomenon is the basis for the common and familiar "electric eyes" that open and close "automatic" doors). The ejected electrons possess a certain amount of KE. The *maximum* KE of the ejected

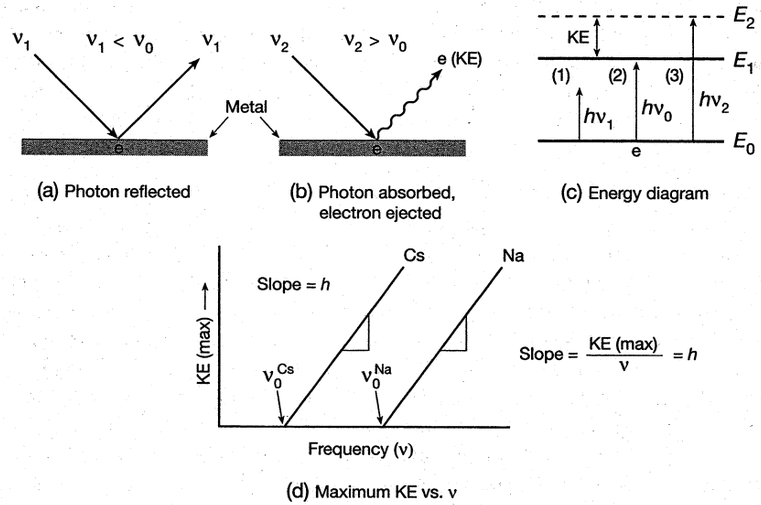

Figure 4.2 The photoelectric effect. (a) Light of frequency $\nu_1 < \nu_0$ is reflected from the surface of a metal. (b) Light of frequency $\nu_1 > \nu_0$ is absorbed by the metal and ejects an electron, which possesses a certain measurable KE. (c) Energy diagram showing the relationship of the frequency of light striking the metal, the energy (E_1) required to eject an electron from the surface of the metal, and the excess KE possessed by the ejected electron. For $h\nu_1$ there is insufficient energy to eject an electron; for $h\nu_0$ there is just enough energy for the light to be absorbed; for $h\nu_2$ the absorbed light contains sufficient energy to cause electrons to be ejected with excess KE. (d) Plots of the excess KE as a function of frequency of absorbed light for Cs (left) and Na (right).

electrons can be readily measured experimentally as a function of ν (or λ) for the absorbed light. However, the frequency of the light, ν, capable of emitting electrons had to be greater than a certain minimum value, ν_0.

Einstein showed that the simple relationships of Eqs. 4.2 and 4.3 provide a quantitative relationship between the maximum KE of the emitted electrons and the experimentally measured frequencies ν and ν_0.

$$\text{Maximum KE of emitted electrons} = h\nu - h\nu_0 \tag{4.2}$$

$$\text{Maximum KE of emitted electrons} = h(\nu - \nu_0) \tag{4.3}$$

According to Maxwell's classical theory, the energy of a light wave should be absorbed continuously by the metal (as more and more electron oscillators are excited) and, in addition, *the energy absorbed should depend only on the square of the amplitude, A, of the light wave, not on the frequency, ν, of the light wave.* However, the experimental measurements of the photoelectric effect demonstrated a number of surprises (Fig. 4.2) that could not be explained by classical theory:

1. Electrons are emitted from the metal surface only if the frequency of the light (ν) striking the metal is *larger* than a threshold value (ν_0).
2. The value of ν_0 is characteristic of the metal and differs for different metals (e.g., the value of ν_0 is smaller for Cs than for Na).
3. If the frequency of light, ν_1, striking the surface of the metal is less than the threshold value ($\nu_0 > \nu_1$), the light is completely reflected and is not absorbed (Fig. 4.2a) even at high intensities.
4. If the frequency of light, ν_2, striking the metal is greater than the threshold frequency ($\nu_2 > \nu_0$), electrons with a certain amount of KE are emitted "instantaneously" (Fig. 4.2b).
5. The *maximum* KE of the ejected electrons depends *linearly* on the frequency of the light once the threshold frequency, ν_0, is exceeded (Eq. 4.2c).
6. The slopes of plots of the maximum KE as a function of ν are *identical* for all metals (Fig. 4.2d). Most remarkable, the slope of such plots (KE_{max}/ν) are equal to the value of h (6.6×10^{-34} J s), Planck's constant!

Observations (1) and (3) taken together imply that energy is transferred from the light to the metal surface but that the energy transferred does not accumulate, as expected for a wave hitting a surface. Einstein interpreted these results in terms of the instantaneous absorption of energy of the light striking the metal surface, reminiscent of the instantaneous exchange of energy between two colliding particles. The colliding particles were viewed as photons of the light striking the electrons on the surface of the metal. Thus, Einstein concluded that not only is the energy of light quantized as *quanta*, as described by Planck, but light itself is quantized and consists of energy-carrying particles, termed "photons." Since a photon is a quantized particle, its energy can only be transferred to the electrons of the metal as an all-or-nothing event. In other words, when a photon strikes a metal surface, it can only eject an electron by transmitting *none (reflection of the photon) or all (absorption of the photon)* of its energy to the metal.

Furthermore, the energy imparted to the emitted electrons is directly related, by Eq. 4.1, to the frequency of the absorbed light (ν_2) after the threshold value, ν_0, has been achieved. Observations (2) and (5) imply that the threshold energy, $E = h\nu_0$, needed to remove an electron from a metal depends on the tendency of the metal to hold on to its electrons. Cesium (Cs) does not hold on to its electrons as effectively as sodium (Na), as expected from the lower position of Cs in the first column of the periodic table. Thus, the energy required to remove an electron from Cs metal is less (Fig. 4.2d) than the energy required to remove an electron from Na metal (the frequency of light required for electron ejection, ν_0, is lower for Cs than for Na). Observation (4) implies that a certain amount of energy (a threshold quantum, $E = h\nu_0$) is required to remove an electron from the surface of the metal, and that if the quantum of energy provided by the absorbed photon exceeds that required to do the work needed just to remove the electron, this excess light energy shows up as the KE of the electron (in order to obey the law of conservation of energy). Observation (6) is the most striking since it demonstrates that *there is a universal relationship of the energy, E, imparted to electrons by the absorption of light of a given frequency, ν; the proportionality constant between E and ν is Planck's constant, h.*

Thus, only five years after Planck's proposal of the quantization of the energy of light, Einstein connected Planck's ad hoc explanation of the quantization of light energy and the existence of the quantum with a proposal that light itself (and, by inference, all of electromagnetic radiation) was quantized and consisted of particles that possess discrete "bundles" of energy that he called photons. As a result, two crucial intellectual building blocks of a new paradigm of the nature for light and the beginning of quantum mechanics were put in place: quanta of energy and photons of light. (Most chemists do not use the word "quantized" to refer to matter, but in reality, matter had long been accepted by chemists as quantized in the form of atoms and molecules.) Einstein's brilliant idea was more than a speculation, since it could be used to "prove" the validity of Planck's Eq. 4.1 *quantitatively*.

4.5 If Light Waves Have the Properties of Particles, Do Particles Have the Properties of Waves? —de Broglie Integrates Matter and Light

If Planck and Einstein were correct and light consisted of particles (photons) with quantized energy (quanta) that was proportional to the light's frequency, ν, and if *at the same time* Maxwell was correct and light consists of waves, then there must be a correspondence between these two apparently incompatible views, however paradoxical the compatibility may seem at first. de Broglie postulated a fusion of the idea of particle and wave by postulating that *every* particle possesses some wavelike characteristics and that *every* wave possesses some particle characteristics. He hypothesized that the conditions of measurement determined whether the wave or particle characteristics were dominant in a given observation. In particular, de Broglie proposed that the wavelength (λ) of a particle is related to Planck's constant (h), and also to the mass (m) and velocity (v) of the particle through Eq. 4.4, termed the de Broglie equation. Since the product of mass and velocity (mv), is equal to the linear momentum of the particle, then the wavelength, λ, of a particle is inversely related to its linear momentum. The de Broglie equation elegantly connects the nature of particles and waves through h as a proportionality constant. Whenever h appears in an expression, we know that we are dealing with a quantum phenomenon.

$$\text{Wave property} \quad \lambda = h/mv \quad \text{Particle property} \tag{4.4}$$

The relationship between a photon's energy and its associated wavelength is given by connecting Eqs. 4.1 and 4.4 to yield Eq. 4.5:

$$E = h\nu = h(c/\lambda) \tag{4.5}$$

Algebraically manipulating Eqs. 4.4 and 4.5, the energy (E) can be related to the particle's momentum (mv), producing relationships among energy, frequency, wavelength, the speed of light, and momentum in Eq. 4.6:

$$E = h\nu = h(c/\lambda) = mvc \tag{4.6}$$

If we accept that the velocity (v) of a particle can be replaced with the velocity of light for a photon in Eq. 4.6 (i.e., $v = c$), then we can derive an expression (Eq. 4.7), that is, the remarkable and well-known Einstein equation. This equation couples the *paradigm of relativity to the paradigm of light as photons* and also demonstrates the equivalence of photons (light) and mass.

$$\text{Photons} \quad E = h\nu = mvc = mc^2 \quad \text{Relativity} \tag{4.7}$$

Note that the rather drastic paradigm shifts concerning the nature of light (from Newton's particles to Maxwell's oscillating electromagnetic waves to the wave particle of Planck–Einstein–de Broglie) should be a warning that *no matter how powerful a guiding paradigm may appear to be to a community, in the face of new results and new concepts, all current paradigms must be considered useful, but tentative and conditional—and subject to eventual replacement by more powerful or more universally governing paradigms.*

Finally, the classical electromagnetic wave theory of light as an oscillating electromagnetic field resulting from oscillating electrons in matter continues to be a useful quantitative paradigm to explain certain phenomena involving light, such as interference effects and the ability to assign light a wavelength (interference and wavelength both being signature properties of waves). On the other hand, the quantum mechanical theory of light, as bundles of photons possessing energy and momentum (both signature properties of particles), best explains phenomena such as the intensity of black-body emission of light by a heated metal and the KE of ejected electrons after light absorption by a metal in the photoelectric effect. The classical theory of light is at its worst in trying to explain phenomena associated with light absorption (the photoelectric effect) and emission (the ultraviolet catastrophe). In a qualitative manner, when light is unperturbed by strong interactions with matter, it is well characterized as a wave and displays wave properties that are completely explained by Maxwell's equations. In this model, light is part of the electromagnetic field that is spread out and fills the entire universe; the wave can be considered to propagate through the universe "at the speed of light." When light is absorbed by a molecule, the "spread out" wave is suddenly "localized" in the small space occupied by the molecule. The wave function of the photon can be viewed as "collapsing" from one that is very diffuse and spread out (infinite dimensions) and "wavelike" to one that is highly localized (molecular dimensions) and "particlelike." So a photon behaves more like a wave when it is not strongly interacting with matter and more like a particle when it is strongly interacting with matter (absorption and emission). We can view the initial, weak interactions of light and matter in terms of an electromagnetic *wave* weakly coupling with the electrons of a molecule; this weak coupling leads to scattering of light, which is well understood in terms of classical wave theory. On the other hand, as the strength of the interaction increases, we view the interactions in terms of a *photon* strongly interacting with the electrons of a molecule leading to absorption of a photon (emission is the reverse of the absorption process).

In closing this historical introduction to the nature of light, note that the *uncertainty principle* provides the ultimate quantum explanation of the apparent wave–particle

duality of light: For certain types of experiments, the measurement of a property that pins down light as a photon (absorption and emission) will cause complete lack of knowledge of all of its wave properties, and the measurement of a property that pins down light as a wave (interference) will cause complete lack of knowledge of all of its particle properties. Since this chapter is concerned with the absorption and emission of light (Scheme 4.1) by the electrons of molecules, from the above discussion it might seem that the photon model of light will be most useful. While this is true, we will see that describing the *initial interaction* of light with the electrons of a molecule is best modeled by considering light as an electromagnetic field that oscillates like a wave and interacts with electrons that can be driven into oscillation by the absorption of light.

4.6 Absorption and Emission Spectra of Organic Molecules: The State Energy Diagram as a Paradigm for Molecular Photophysics

The general paradigm of Scheme 4.1 can readily be integrated into the state energy diagram of Scheme 1.4, which is a very useful starting point for discussing radiative transitions. Electronic absorption and emission spectra provide important information concerning the structure, energetics, and dynamics of electronically excited states *R, in particular on the following parameters of *R: structures, energies, lifetimes, electron configurations, and quantum yields. For example, from knowledge of the $S_0 + h\nu \rightarrow S_1$ and $S_0 + h\nu \rightarrow T_1$ absorption processes, and of the $S_1 \rightarrow S_0 + h\nu$ and $T_1 \rightarrow S_0 + h\nu$ emission processes, one can often construct a fairly complete state energy diagram (Scheme 1.4), which includes the electron configurations of S_1 and T_1 and the energies of these two excited states relative to S_0. From measurements of the lifetimes of S_1 and T_1 and of the quantum efficiencies of emission Φ, we can deduce the rate constants (k) of the radiative and radiationless photophysical pathways available to S_1 and T_1. These energies and rates will set the stage against which photochemical processes must compete if they are to occur with significant efficiency.

4.7 Some Examples of Experimental Absorption and Emission Spectra of Organic Molecules: Benchmarks

In Chapter 1, we learned that for organic molecules the energy required to excite an electron from an occupied *valence* orbital (σ, π, or n) to an unoccupied antibonding orbital (π^* or σ^*) corresponds to light whose wavelength is typically in the range of 200 nm (UV light, 143 kcal mol^{-1}) to 700 nm (red light, 41 kcal mol^{-1}). In initiating a photochemical study of an organic molecule, the photochemist starts by measuring the electronic absorption and emission spectra of the starting materials (solutes, solvents, and reaction vessels). Saturated organic compounds (alkanes) are generally "transparent" to light in the region ~ 200–700 nm (Table 4.1). The lowest-energy absorption

corresponds to a HO → LU (highest occupied → lowest unoccupied) orbital jump of an electron; for saturated hydrocarbons this jump corresponds to a σ(HO) → σ^*(LU) orbital transition. The energy gap between σ and σ^* orbitals for saturated hydrocarbons corresponds to energies greater than that of a 200-nm photon (~ 143 kcal mol^{-1}).

On the other hand, unsaturated organic molecules (ketones, olefins, conjugated polyenes, enones, aromatic hydrocarbons, etc.) possess several absorption bands in the conventional "photochemical" region of the electromagnetic spectrum, 250 – –700 nm. Absorption of light in this region corresponds to π(HO) → π^*(LU) transitions for olefins and aromatic compounds that possess a π^* electron in the HO, or to n(HO) → π^*(LU) transitions for compounds, such as ketones, that possess an n electron in the HO.

The shorter wavelength limit of the photochemical region is set by the absorption of light by reaction vessels and solvents through which the light must pass (quartz and common organic solvents absorb strongly at 200-nm and shorter wavelengths). The longer wavelength limit is set by considerations of the minimum energy required to excite electrons (electronic excitation of organic molecules usually requires light of wavelengths < 700 nm). Wavelengths in the range of 700–10,000 nm correspond to near-IR and IR radiation. The energy of photons corresponding to these wavelengths is generally too small to excite electrons of organic molecules from a HO to a LU. However, such light excites fundamental vibrations or overtones of fundamental vibrations when absorbed.

A *chromophore* ("color bearer") is defined as an atom or group of atoms that behave as a unit in light absorption. A *lumophore* ("light bearer") is an atom or group of atoms that behave as a unit in light emission (fluorescence or phosphorescence, Schema 4.1). Typical organic chromophores and lumophores are the common organic functional groups, such as ketones (C=O), olefins (C=C), conjugated polyenes (C=C–C=C), conjugated enones (C=C–C=O), and aromatic compounds (benzene ring and condensed benzene rings). In this chapter and in Chapter 5, we concentrate on these common chromophores as exemplars for both the photophysical properties of organic molecules discussed in these chapters.

Table 4.1 lists some numerical benchmarks for the maximum of the longest-wavelength absorption bands (λ_{max}) and the extinction coefficient at maximum absorption (ε_{max}) of some common organic chromophores, and assigns an electron orbital transition to the band. The transitions listed generally correspond to the lowest-energy (longest-wavelength) electronic HO → LU orbital transition of the chromophore. The magnitude of ε_{max} determines the "absorption strength" of a chromophore; for organic molecules the value of ε_{max} for spin-allowed absorption may vary over several orders of magnitude. The usual units of ε_{max} are $cm^{-1}\,M^{-1}$ (a reciprocal length per mole). Since $M^{-1} = cm^3/mol^{-1}$, then an equivalent unit for ε is cm^2/mol^{-1} (area per mol). Thus, the units of ε are the same as a *surface area per mole of chromophore molecules*. These units suggest that we may interpret ε as the "cross-sectional area" that a mole of chromophores present to passing photons of a given wavelength, λ (as discussed in Section 4.15). The data in Table 4.1 show that the wavelength (λ) or corresponding frequency (ν) of absorption maxima vary greatly with the chromophore structure, as does the strength of the absorption as measured

Table 4.1 Long-Wavelength Absorption Bands (Corresponding to HO → LU Transitions) of Some Typical Organic Chromophores

Chromophore	λ_{max}(nm)	ε_{max}	Transition Type
C—C	<180	1000	σ,σ^*
C—H	<180	1000	σ,σ^*
C=C	180	10,000	π,π^*
C=C—C=C	220	20,000	π,π^*
Benzene	260	200	π,π^*
Napththalene	310	200	π,π^*
Anthracene	380	10,000	π,π^*
C=O	280	20	n,π^*
N=N	350	100	n,π^*
N=O	660	200	n,π^*
C=C—C=O	350	30	n,π^*
C=C—C=O	220	20,000	π,π^*

by ε_{max}. We shall postpone discussion of emission parameters until Section 4.16; we simply point out that both absorption and emission parameters vary widely as a function of molecular structure. *Note that the absorptions in Table 4.1 correspond to spin-allowed singlet–singlet transitions.* The values of ε_{max} for spin-forbidden, singlet–triplet transitions, while finite, are usually $\ll 1\,cm^{-1}M^{-1}$, so that a sample is effectively "transparent" at the wavelengths corresponding to the transition. For essentially all purposes, when an organic photochemist discusses absorption spectra, it is understood that spin-allowed singlet–singlet absorption is responsible for the absorption.

Inspection of Table 4.1 poses a number of interesting and important questions concerning $R + h\nu \rightarrow R$ (or $^*R \rightarrow R + h\nu$ transitions) that will be answered in this chapter:

1. Why is there such a wide variation in electronic absorption (and emission) parameters of λ_{max} and ε_{max} for the different chromophores?
2. Why is the value of ε_{max} smaller for some aromatic molecules (e.g., benzene, naphthalene) and larger for others (e.g., anthracene)?
3. How is the orbital configuration (HO → LU) for the electronic transition $R + h\nu \rightarrow {}^*R$ related to and assigned to a given absorption (or emission) band?
4. How are experimental absorption parameters related to theoretical quantities, such as quantum mechanical matrix elements?
5. How are the processes of electronic absorption and electronic emission related mechanistically?
6. How do vibrations influence electronic transition in absorption and emission?
7. What can we say about the interactions that provide a mechanism for "spin-forbidden" transitions in absorption ($S_0 + h\nu \rightarrow T_n$) and emission ($T_1 \rightarrow S_0 + h\nu$)?

In order to answer these and other related questions, we will construct a pictorial model of the radiative processes of Scheme 4.1 that relates the molecular structure of R and *R (electronic, nuclear, and spin configurations) to interactions with the electromagnetic field and to spectroscopic parameters. We will start by developing a simple paradigm for the structure of light and for the interactions of light with the electrons of molecules that are responsible for electronic absorption and emission.

4.8 The Nature of Light: From Particles to Waves to Wave Particles[1,2]

As discussed in Sections 4.2–4.5, the classical wave theory of light as a wave has been shown to be inadequate to explain the details of absorption and emission of light by molecules. Nevertheless, the classical theory of light is still a useful starting point for producing a qualitative pictorial representation of the initial, weak interaction between light as the oscillating electromagnetic wave and the electrons of a molecule. We start with Maxwell's model of light as an oscillating *electrical force field* resulting from oscillating electric charges (electrons) in molecules. This oscillating force field is used as a basis for constructing a quantum mechanical operator for the calculation of matrix elements for the absorption and emission of *photons* by organic molecules. A justification for using the classical theory of light as a starting point for the absorption and emission of light is that it provides a concrete pictorial explanation (and therefore an intuitive physical explanation) for the initial interaction of light and molecules, if not the overall process of absorption (or emission). This pictorial intuitive representation is generally much easier for the organic chemist to grasp than the highly mathematical quantum theory.

4.9 A Pictorial Representation of the Absorption of Light

The basic idea for visualizing the interaction of light and the electrons of a molecule is borrowed directly from the classical theory of light as a wave.[3] Photons are viewed as particles that allow the exchange of energy between the (electric portion of the) electromagnetic field and the electrons of a molecule under the rules of quantum mechanics. The most important interaction between the electromagnetic field and the electrons of a molecule can be modeled as the interaction of two oscillating electric dipole systems: *the oscillating electromagnetic field that fills the entire universe* and *the oscillating electrons that are fixed to the nuclear framework of a molecule in matter.* These two oscillating electric systems, when coupled to one another, behave as a reciprocally interacting and coupled system of potential energy (PE) donor and acceptor attempting to participate in a common resonance if a common frequency (ν) can be found. The electromagnetic field is visualized as a field of electric dipoles that pervade the universe and oscillate at a range of frequencies (ν). If the electrons of a molecule possess a "natural" (resonance) oscillation frequency (ν) that corresponds to a "natural" (resonance) oscillation frequency (ν) of one of the oscillating dipoles

(photons) in the available electromagnetic field, and if the electrons and the field are coupled by a significant dipole–dipole interaction, the electromagnetic field can interact with the electrons and exchange energy with the electrons by driving the electrons into oscillation and result in absorption of photons from the electromagnetic field.

The interactions are completely analogous to that of two interacting antennae, one an energy transmitter and the other an energy acceptor. The dipole–dipole interaction can cause a coupling of the two antennae (i.e., a *resonance results between the two antennae*). This resonance is most efficient when there exists a frequency (ν) that is common to both the electromagnetic field and the electronic transition for the photon ($E = h\nu$) and for the energy gap for the transition of the electron from one state to another ($\Delta E = h\nu$). In the classical harmonic oscillator model for the electromagnetic field, the field contains energy by virtue of its oscillating electrons (oscillating electrons are excited, and therefore possess energy that can be transferred). Transfer of energy from the field (absorption of a photon by a molecule, R) reduces the oscillations and energy of the electromagnetic field, whereas transfer of energy to the field (emission of a photon by an electronically excited molecule, *R) increases the oscillations (energy) of the field. *In the ground state (*R*) the electrons of a molecule are considered to be at rest, and in the excited state (*R*) the electrons of a molecule are considered to be oscillating along the molecular framework in some manner.*

At the special resonance frequency (ν) corresponding to $\Delta E = h\nu$, the electrons of a molecule (R) can absorb energy from the electromagnetic field (by absorbing a photon). The electromagnetic field is then impoverished by one photon, and an excited oscillating electron of a molecule takes all of the energy of the photon and becomes an electronically excited molecular (*R). Emission is viewed as the reverse process, in which an excited oscillating electron interacts through dipole–dipole coupling with the electromagnetic field and the electromagnetic field becomes excited by the photon emitted by the molecule (*R). The photon is transferred from the oscillating electron of the excited molecule to the electromagnetic field; the field's energy is increased by the energy of one more photon and an electron of the molecule returns from an excited state (*R) to its ground state (R). From the above qualitative, intuitive classical description, it is now relatively easy to make a simple quantum modification of the classical picture of energy transfer from the electromagnetic field to the electrons of a molecule, and vice versa, as follows: *The absorption of energy from the electromagnetic field corresponds to the removal of a photon from the electromagnetic field, and the emission of energy from a molecule corresponds to the addition of a photon to the electromagnetic field.* Both pictures involve the coupling and resonance of two oscillating electric fields.

4.10 The Interaction of Electrons with the Electric and Magnetic Forces of Light

The absorption and emission of energy from the *electric* portion of the *electro*magnetic field by electrons are described by the field of *electronic molecular spectroscopy*; the absorption and emission of the electric portion of electromagnetic radiation by

vibrating nuclei are the basis for the field of *vibrational molecular spectroscopy*. The absorption and emission of energy from the *magnetic* portion of the electro*magnetic* field by the electrons are the basis for the field of *magnetic resonance spectroscopy*. All three forms of spectroscopy have relevance for an understanding of molecular organic photophysics and photochemistry.

Now, we analyze more deeply the resonance condition that is required for the absorption or emission of light by molecules. The absorption or emission of light, as for all transitions of molecules, requires the conservation of energy. When two electronic states separated by an energy, $\Delta E = E_1 - E_2$, are coupled by some interaction, the electron density (square of the wave function) appears to oscillate and vary with time. From the Einstein resonance relation (Eq. 4.8a), an energy separation of $E_1 - E_2$ corresponds to a frequency of oscillation of $\nu = (E_1 - E_2)/\mathrm{h}$. This oscillation of electric charge, or electric dipole moment (at the frequency ν) interacts with the oscillating dipolar electric field of electromagnetic radiation at this frequency and corresponds to the resonance condition for the absorption or emission of light (Eq. 4.8b).

$$\Delta E = E_1 - E_2 = h\nu \tag{4.8a}$$

$$\nu = (E_1 - E_2)/h \tag{4.8b}$$

Now, we describe a concrete classical picture (Fig. 4.3) of an electromagnetic wave and analyze the electric and magnetic features of the *initial* interactions of the electric and magnetic fields of light with the electrons of a molecule.

An electromagnetic wave exerts both electric and magnetic forces on charged particles (e.g., electrons and nuclei) and on magnetic dipoles (e.g., the magnetic

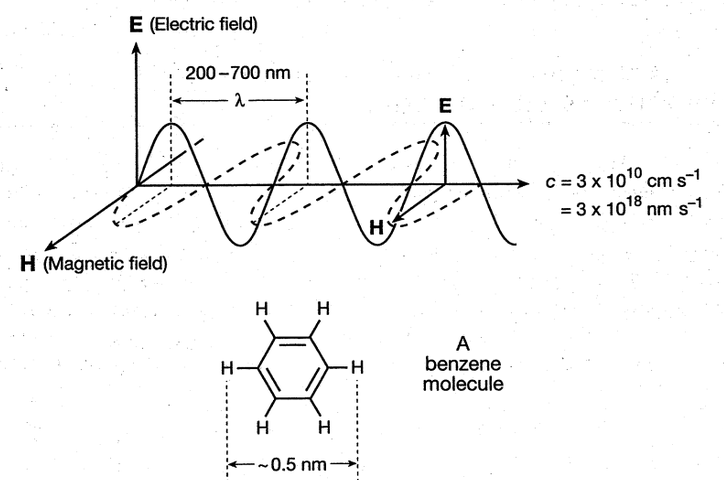

Figure 4.3 An electromagnetic wave. The electric field (**E**) is imagined to be in the plane of the page, and the magnetic field (**H**) is imagined to be perpendicular to the plane of the page.

moments associated with electron and nuclear spins). We can view light as mapping oscillating dipolar electric and magnetic force fields into the neighborhood of space about its direction of propagation (Fig. 4.3). In the volume of this space, two vectors can be drawn: an electric vector (**E**) that represents the source of the *electrostatic force* of the light wave, and a magnetic vector (**H**) that represents the source of the *magnetic force* of the light wave. The magnitudes of **E** and **H** at any point in space vary as a function of time and oscillate from mathematically positive (attractive) to mathematically negative (repulsive) values. A stationary spectator measuring the magnitude of **E** (or **H**), as the wave passes, would thus record oscillating values of **E** (or **H**) as a function of time. A test electric charge in space that can be coupled to **E** and that possesses the frequency ν can be set into oscillation by the oscillating values of **E**. To both the spectator and the test charge, the light wave appears to have the characteristics of a *harmonically oscillating electric and magnetic dipole*. A characteristic of this harmonic motion is the back-and-forth *linear oscillation* of the electric force field of the light wave and the electron cloud of the molecule.

A key idea in understanding the interaction of light with organic molecules is that electrons can be set into resonant oscillation (resonance) by the oscillating dipolar electric field of light *only* when Eq. 4.8 is obeyed. Under the condition of resonance, an electron (of R) may absorb energy from the electromagnetic field set up by the light wave, or an electron of *R may emit a photon as electromagnetic radiation. Thus, we can visualize the interaction of light by molecules as a process in which energy is exchanged *by resonance* between a collection of oscillating dipoles (electrons) that are coupled to a radiation field (an oscillating electric field that pervades the universe). *In more concrete chemical terms, the oscillation of the dipoles corresponds to the movements of electrons in bonds relative to positively charged nuclei in matter; that is, electrons oscillate about the nuclear framework of molecules.*

4.11 A Mechanistic View of the Interaction of Light with Molecules: Light as a Wave

Now, let's take a closer, more quantitative view on how the oscillating light wave (the electromagnetic field containing photons) makes a ground-state electronic configuration of R look like an excited-state electronic configuration of *R according to the classical theory of light. Imagine a light wave passing a stationary molecule.[3] As we have seen above, the electromagnetic wave causes both periodic electrical and magnetic disturbances in the region of space through which it passes, particularly in the region occupied by our exemplar stationary molecule (Fig. 4.4). The magnitude of force (**F**) exerted on an electron in a molecule by the light wave is given by Eq. 4.9:

Total force exerted on an electron by a light wave

$$\mathbf{F} = e\mathbf{E} + \frac{e[\mathbf{H}v]}{c} \qquad (4.9)$$

Electrical force

Magnetic force

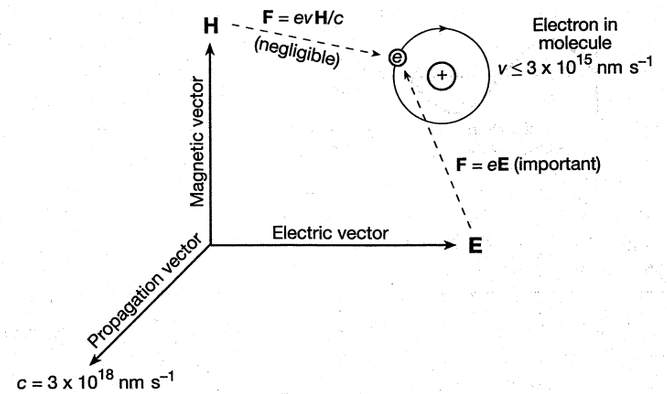

Figure 4.4 Interaction of the electric field **E** and the magnetic field **H** of an electromagnetic wave on an electron in an orbit about a nucleus.

where e is the charge of an electron, **E** is the electric field strength, **H** is the magnetic field strength, v is the velocity of an electron, and c is the speed of light. Since the speed of light (3×10^{10} cm s$^{-1} = 3 \times 10^{17}$ nm s^{-1}) is much greater than the possible speed of an orbiting electron ($v_{max} \sim 10^8$ cm s$^{-1} = 10^{15}$ nm s^{-1}, from the Bohr atom model), the magnitude of $e\mathbf{E}$, in general, *will be considerably greater* than the value of the magnetic force $(e/c)[\mathbf{H}v]$; that is, $e\mathbf{E} \gg (e/c)[\mathbf{H}v]$. Therefore, we conclude that the electric force of the oscillating light wave operating on electrons is much larger than the magnetic force operating on the electrons. Therefore, we can ignore the magnetic force to a good first approximation when we are dealing with electronic excitation by the electromagnetic field. Thus, because $e\mathbf{E} \gg (e/c)[\mathbf{H}v]$, Eq. 4.9 is approximated by Eq. 4.10, if the magnetic term of Eq. 4.9 is ignored.

Force on electron ignoring magnetic interaction

$$\mathbf{F} \cong e\mathbf{E} \qquad (4.10)$$

Thus, although there is a simultaneous interaction of the electrons with the oscillating magnetic field (**H**), this interaction is negligible compared to the electrical interaction. However, the oscillating magnetic field of electromagnetic radiation interacts strongly with the *magnetic* dipoles of electron and nuclear spins and is the basis of magnetic resonance spectroscopy.

4.12 An Exemplar of the Interaction of Light with Matter: The Hydrogen Atom

Let us consider the simple exemplar of an electron in a Bohr orbit of a hydrogen atom interacting with the oscillating electromagnetic field (Fig. 4.5a). Here, we assume that

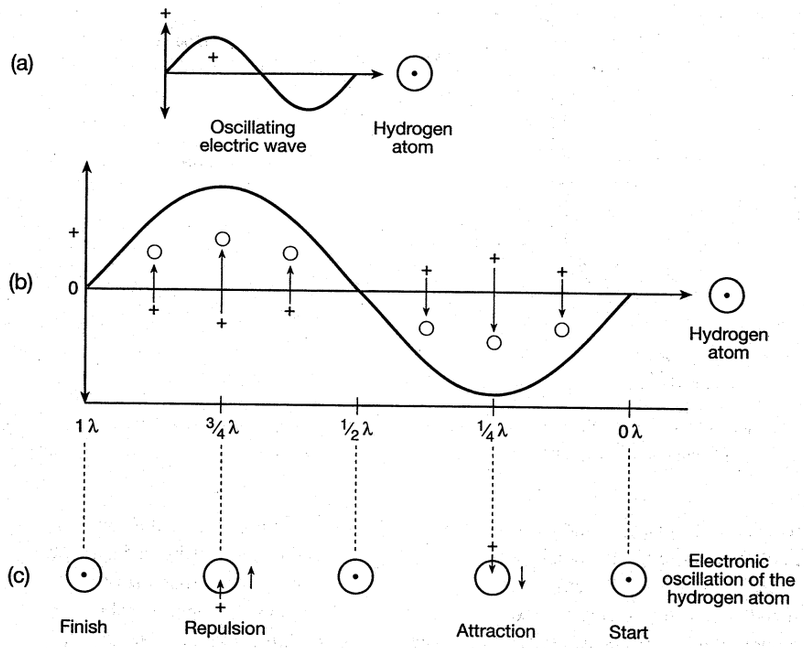

Figure 4.5 Schematic of the electric portion of the light wave interacting with a hydrogen atom.

the massive nucleus holds the atom fixed in space as the light wave zips by, but the electron of the atom can interact with and follow to some extent the oscillating electric field of the passing light wave. The maximum interaction between **E** and the electron will occur if the electron possesses a natural resonance frequency of oscillation (ν) that is equal to the frequency of oscillation of the passing light wave. Suppose that the frequency ν of the passing light wave corresponds to that of some natural frequency of the hydrogen atom; this frequency corresponds to an energy gap ($\Delta E = E_1 - E_2$) through Eq. 4.8b.

At the start of the interaction (Fig. 4.5b, right, 0 λ), for the sake of argument, let us imagine that the electric field **E** has a value of zero; that is, at this particular point of its period, the light wave does not exert an attractive or a repulsive force on the electrons of the hydrogen atom and the shape of the atom is spherical (Fig. 4.5c, right). One-quarter of a wavelength ($\lambda/4$) later, we imagine that the value of **E** has decreased to a negative maximum (defined as a repulsive electrical force on the electron) value and that the light wave exerts the same force on the electron of the hydrogen atom as an electric dipole with its negative end closest to the electron. This repulsion between negative charges continues until one-half of a period ($\lambda/2$) is completed. Thus, during the first half-cycle of the passing light wave, the hydrogen atom's electron is repelled

away from the passing light wave with the maximum force occurring after $\lambda/4$ of the wave has passed. When exactly one-half of a wavelength ($\lambda/2$) has passed the atom, the force on the electrical force on the electron has dropped to 0. After $3\lambda/4$ has passed, we imagine that the value of **E** has increased to a positive (defined as an attractive force on the electron) maximum value and that the light wave exerts the same force on the electron of the hydrogen atom as an electric dipole with its positive end closest to the electron. During the second half-cycle of the passing light wave, the hydrogen atom's electron is attracted toward the passing light wave, with the maximum force occurring when $3\lambda/4$ has passed. When one full wavelength λ of the light wave has passed, the value of **E** is back to 0, and the electromagnetic field exerts no force on the electron.

What is the positive nucleus doing during the passing of the light wave? After all, the nucleus is a charged electrical particle just like the electron. Surely the electromagnetic field was also exerting a force on the nucleus as the wave passed. Indeed, this is correct: The nucleus does feel the force of the passing electromagnetic wave. However, because the nucleus is so massive compared to the electron that its electrical interactions with electromagnetic radiation occur at much lower frequencies ($\nu \sim 10^{13}$–10^{14} s^{-1}) than those that set electrons into oscillation ($\nu \sim 10^{15}$–10^{16} s^{-1}). This conclusion is easily deduced from the harmonic oscillator model (Eq. 2.25), for which the frequency of oscillation is inversely proportional to the mass of the particle undergoing oscillation. Thus, *the nucleus is not set into resonance by frequencies that set the electrons to resonance*. In fact, the nucleus is set into vibrational resonance at frequencies in the IR portion of the electromagnetic field and is the basis of vibrational spectroscopy.

The effect of **E** on the electrons of a hydrogen atom may be compared to the effect on an electron cloud of a hydrogen atom that is "fixed" in space between two charged plates. If one plate is charged positive and the other is charged negative, an induced dipole is produced in the hydrogen atom, with the negative end of the electric dipole pointing toward the positively charged plate. The important picture that emerges is that as far as the electron of an atom is concerned, the oscillating **E** of the light wave is an oscillating dipole that can interact with the electrons of a molecule; if the electron can oscillate at the correct frequency (ν), a resonance occurs and energy moves back and forth from the electromagnetic field to the electron's motion about the nucleus (and back and forth with the electromagnetic field). In the Bohr model, the electron in resonance with the electromagnetic field would be viewed as making harmonic oscillations back and forth between two Bohr orbits during the resonance period. We say that the interaction between **E** and the electron produces a transitory (or *transition*) *dipole moment* in the hydrogen atom as it oscillates between the two Bohr orbits. The greater the strength of the interaction of the charged plates with the hydrogen atom, the greater the size of the transition dipole. The greater the ease with which the electron can oscillate between two orbits, the more "polarizable" the electron and the larger the transition dipole moment. We shall see how this classical idea of a transition dipole carries over to help us understand the probability of absorption and emission of light by molecules.

4.13 From the Classical Representation to a Quantum Mechanical Representation of Light Absorption by a Hydrogen Atom and a Hydrogen Molecule[4,5]

Now, let now modify the classical picture of the interaction of light and introduce the required quantum mechanical features of wave functions so that we can obtain some quantum intuition and can deduce the basis for the important selection rules for the absorption and emission of light. Instead of an electron in a Bohr orbit (Fig. 4.5), now we consider the electron of the hydrogen atom to be in a 1 s orbital. The wave function of a 1s state is spherically symmetric about the nucleus, and therefore does not possess a net dipole moment. Figure 4.6a shows schematically how the oscillating **E** force will alternately cause the 1s electron cloud of the hydrogen atom to move toward and away from the passing light wave (in an analogous manner to that in which the oscillating **E** force causes a distortion of an electron in a Bohr orbit in Fig. 4.5). As a result, the light wave "reshapes" the electron distribution from one that is spherically symmetric about the nucleus to one that is alternatively more concentrated on one side of the nucleus, closer to the light wave, and then is more concentrated on the other side of the nucleus, farther away from the light wave (Fig. 4.6a). The oscillation of negative charge back and forth from one side of the atom to the other has the appearance of a transitory oscillating dipole. The *time average* of the oscillating electron "looks like" a p orbital (Fig. 4.6a, right), which possesses an electron distribution above and below a nodal plane containing the nucleus. This picture provides the intuition that the resonance interaction of an electromagnetic wave with a hydrogen atom in a spherically shaped 1s orbital will change the shape of the orbital and make it "look like" a 2p orbital. The tuition gained is that there must be a selection rule saying that this sort of shape change in the electron cloud corresponds to an "allowed" absorption.

In the above pictorial representation, the electron *vibrates* back and forth, just like a *harmonic oscillator according to the classical theory of light!* In the 1s state, the electron corresponds to a classical oscillator *that is not vibrating*. Translating this classical picture into a quantum mechanical one, we say that, in the 1s orbital, the electron has zero orbital angular momentum ($l = 0$) and that the interaction with the light wave causes the electron to pick up exactly one unit of orbital angular momentum as it is excited to a 2p orbital ($l = 1$). At this point, it is important to recognize that a photon possesses one unit of spin angular momentum. The excitation process requires both the conservation of energy ($\Delta E = 0$, because $E = h\nu =$ energy gap of 1s $\rightarrow$ 2p transition, exactly) and the conservation of angular momentum ($\Delta l = 0$, because angular momentum change increase for the 1s $\rightarrow$ 2p transition must equal the loss of one unit of angular momentum of the absorbed photon). Experimentally, the wavelength of the 1s $\rightarrow$ 2p transition in the hydrogen atom is 122 nm (deep UV) and corresponds to an energy gap of 234 kcal mol^{-1}.

From the above description of examining the interaction of a light with the hydrogen atom's 1s wave function, we deduce (Fig. 4.6a) that a nodal plane of the 2p orbital is produced at right angles to the oscillating electric vector (**E**). Thus, we conclude that the interaction of **E** sets the electron into a harmonic oscillation (vibration) selectively along the direction of motion of the electric vector. This idea, in turn, provides

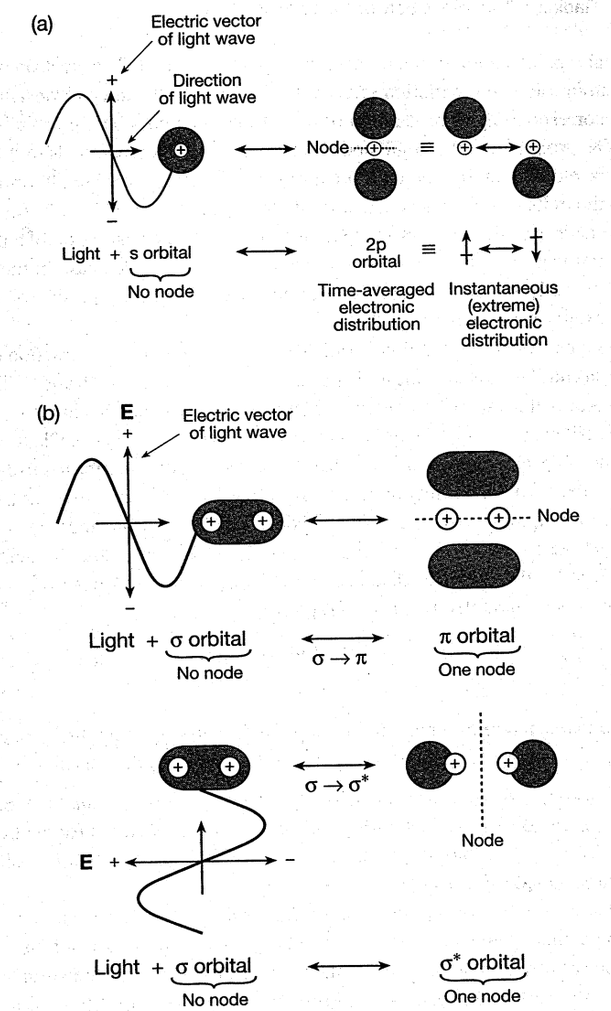

Figure 4.6 (a) Pictorial representation of light absorption by a hydrogen atom. The light wave and the 1s state of hydrogen are viewed as being in resonance with the 2p state. The latter may be represented as a time-averaged dumbbell shaped electron cloud or as an oscillating dipole. The transition is found experimentally at 122 nm. (b) Pictorial representation of light absorption by a hydrogen molecule. The light wave and the 1σ state have two possible resonances: a $\sigma \rightarrow \pi$ transition (at 90 nm) and a $\sigma \rightarrow \sigma^*$ transition (at 100 nm). One interaction of the electric field (upper drawing) drives the electron into oscillations perpendicular to the bond axis; the other interaction (lower drawing) drives the electron into oscillations along the bond axis.

a pictorial representation of the absorption of *polarized* light: The electron of the hydrogen atom can be set in motion selectively along one of the three Cartesian axes (x, y, or z) corresponding to production of one of the three possible 2p orbitals (p_x, p_y, or p_z). The production of a single node in a wave function corresponds to the change of angular momentum by one unit, $\hbar$ (this symbol characterizes angular momentum that has the units of Planck's constant h divided by 2π, i.e., $\hbar = h/2\pi$). An increase in the number of nodes (e.g., 1s → 2p transition) during the absorption of a photon is an essential feature of the absorption process. Conversely, a decrease in the number of nodes (e.g., 2p → 1s transition) is an essential feature of the emission of a photon from an excited hydrogen atom.

When the resonance condition is satisfied, the strength of the interaction between an electron and **E** is related to the ability of the electron to couple with and "follow" the electric force of the light wave, and to the magnitude of the maximal charge separation, Δr, effected by the interaction of **E** and the charge on the electron, e. Classically, the magnitude of development of charge separation as one proceeds from an s to a p orbital is related to α, the polarizability of the electron cloud, which is defined as the transitory (or transition) dipole moment ($\boldsymbol{\mu}_i$) that is induced in the electron cloud by an applied electric field (**E**) (Eq. 4.11). The magnitude of the transition dipole moment ($\boldsymbol{\mu}_i$) in turn is given by the extent of displacement of the positive and negative centers of charge (**r**) times a unit electric charge (Eq. 4.12).

$$\alpha = \boldsymbol{\mu}_i/\mathbf{E} \tag{4.11}$$

$$\boldsymbol{\mu}_i = e\mathbf{r} \tag{4.12}$$

The fundamental requirement for absorption or emission of light by an atom or a molecule may now be summarized in terms of the simple models discussed above:

1. The *energy conservation rule* (Eq. 4.8): There must be an exact matching of the energy difference that corresponds to the energy required for the transition (ΔE) between orbitals and the energy of the photon ($h\nu$); that is, ΔE must exactly equal $h\nu$ (Eq. 4.8).
2. The *momentum conservation rule*: There must be an exact matching of the angular momentum gained (or lost) during the transition and the angular momentum of the photon; in quantum mechanical terms, the transition between orbitals must generate a node (absorption) or destroy a node (emission).
3. The *finite interaction rule*: The transition dipole moment ($\boldsymbol{\mu}_i$) created by the interaction of the electron with the electromagnetic field must be finite. The larger the value of $\boldsymbol{\mu}_i$, the more probable the absorption of light by R, and conversely the more probable (the faster) the emission of light from *R.
4. The *frequency matching (resonance) rule*: There must be a matching of a frequency (ν) of the oscillating light wave and a frequency that corresponds to the formation of a transition dipole moment. Since $\Delta E = h\nu$ and $\nu = \Delta E/h$, this rule is related to rule 1 above, the energy conservation rule. A matching of energy, when there is an energy gap of ΔE, is equivalent to a matching of frequency, which is the resonance condition.

Now, let us extend the ideas we have developed for a hydrogen atom and apply them to the simplest molecular system, the H_2 molecule (Fig. 4.6b). In going from atoms to

diatomic molecules, the atomic s and p orbitals are replaced with molecular σ and π orbitals. In the simple case of H_2, the absorption of a photon promotes an electron in the ground-state HO(σ) orbital, which does not possess a node, into one of two low-energy unoccupied orbitals containing a single node (for convenience we refer to both of these orbitals as LU orbitals): a π orbital or a σ^* orbital. The bonding π LU orbital (not an antibonding π^* orbital!) possesses a single node along the bond axis, and the σ^* LU orbital possesses a single node perpendicular to the bond axis (Fig. 4.6b).

In the ground state, the hydrogen molecule possesses two electrons in the σ HO orbital, which is cylindrically symmetric about the internuclear axis. Compared to an atom, the nuclear axis imbues the molecule with an inherent axial asymmetry, and one can imagine electronic oscillations of two types: one oscillation that is parallel and one oscillation that is perpendicular to the bond axis.

Notice that both the $\sigma \rightarrow \pi$ and the $\sigma \rightarrow \sigma^*$ transitions are similar to the 1s → 2p transformation of atoms, respectively, in that a node is produced when the HO → LU transition occurs for each. The major difference is that two symmetry-distinct electronic oscillations are possible for the molecule: One oscillation (corresponding to the transition dipole of the $\sigma \rightarrow \sigma^*$ transition) is in a plane perpendicular to the bond axis and between the two nuclei (Fig. 4.6b, lower drawing) and the other oscillation (corresponding to the transition dipole of the $\sigma \rightarrow \pi$ transition) is in a plane containing the bond axis and the nuclei (Fig. 4.6b, upper drawing). Experimentally, the wavelength of the $\sigma \rightarrow \pi$ transition in the hydrogen molecule is 100 nm (very deep UV), which corresponds to an energy gap of 286 kcal mol^{-1}, and the wavelength of the $\sigma \rightarrow \sigma^*$ is 110 nm (deep UV), which corresponds to an energy gap of 264 kcal mol^{-1}.

Although an organic molecule is much more complex than a hydrogen atom or a hydrogen molecule, the two systems provide exemplars such that the basic ideas we have developed for these two simple species shall be sufficient as a starting point to develop a working paradigm for the absorption and emission of light by organic molecules.

In summary, an atom (or molecule) and the electromagnetic field of light are viewed as analogous to two coupled harmonic oscillators, such as two coupled pendulums. The electrons of the molecule possess a set of "natural transition frequencies," which correspond to the values of $\nu_i = \Delta E_i/h$, where ΔE_i correspond to the energy gap between two allowed electronic energy levels. We imagine that by changing the frequencies of the incident light passing by a molecule we can achieve values of ν for the light that correspond to the values ν_i of the electrons of the molecule. When a matching of the value of ν of the light and the value of ν_i of the electrons of the molecules occur, the electrons of the molecule behave like two coupled pendulums and energy is transferred from the light field (absorption of a photon by the molecule) or is transferred from an excited electron to the light field (emission of a photon by the molecule).

4.14 Photons as Massless Reagents

In spite of its shortcomings in describing the details of the *weak initial* interaction of light with electrons, the concept of a photon has the concreteness that is associated with

the concept of a particle and provides a powerful intuition in dealing with quantum phenomena. The concept of a photon works well when the interaction of light with electrons is strong and absorption occurs. Indeed, the concept of a photon as a particle allows the organic chemist to consider the photon as a "massless reagent." A photon reagent may "collide" with molecules and "react" with them (i.e., be absorbed). Since *R is clearly a completely different species than R in terms of its energy, its electronic distribution, and its chemical reactivity, the photon reagent has certainly caused a chemical reaction, $R + h\nu \rightarrow {}^*R$, to occur! Like the molecules of an organic reagent, which can be counted, we can also count photons. A source of light of frequency ν can be regarded as being composed of N photons, each of which possesses the energy $h\nu$. Each photon of wavelength $\lambda = c/\nu$ carries an energy $h\nu$ and a linear momentum $h\nu/c$. *Low-frequency (long-wavelength) photons carry little energy and momentum; high-frequency (short-wavelength) photons carry a great deal of both energy and momentum.* Eq. 4.13 provides a quantitative connection between the energy (E) for Avogadro's number (N_0) of photons with a light source of frequency ν (wavelength λ).

$$E = N_0 h\nu = N_0(c/\lambda) \tag{4.13}$$

From Eq. 4.13, Table 4.2 can be constructed to describe the relationship between the number of photons (N) that correspond to 100 kcal of energy (selected as an arbitrary numerical benchmark energy for photons of varying frequency and wavelength over the entire electromagnetic spectrum). From Table 4.2, it can be seen that 100 kcal corresponds to about an einstein (a mole of photons) for the special case of 1 mol of photons whose $\lambda = 286$ nm ($\nu = 1 \times 10^{15}\ s^{-1}$). However, for light of $\lambda = 1000$ nm (IR), the same 100 kcal of energy corresponds to over 3 mol of photons, and for radiowaves ($\lambda = 10^{11}$ nm) 100 kcal of energy corresponds to 10^7 mol of photons! On the other hand, for X Rays, 100 kcal mol^{-1} of energy corresponds to < 1 millimole of photons, and for γ-rays 100 kcal mol^{-1} of energy corresponds to a few micromoles of photons! The concentration of photons can be computed from knowledge of the number of photons absorbed in a volume.

It is very important in photochemistry to understand the difference between the *energy* and *intensity* of photons. The intensity of a beam of monochromatic light of frequency ν refers to the *number* of photons in the beam. The greater the intensity of a beam of monochromatic light, the greater the number of photons in the beam. No matter what the intensity of the beam, each photon carries the energy $E = h\nu$. The greater the frequency of a beam of monochromatic light, the greater the energy of the photons in the beam. Thus, a weak light beam of high frequency may possess sufficient energy to break strong bonds, whereas a strong beam of light of low frequency may not be able to break even weak bonds. This difference between energy and intensity was noted by Einstein in his explanation of the photoelectric effect (Fig. 4.2).

Analogous to organic reagents, photons may be viewed as *chiral* reagents in that they may possess a quality of "handedness" or "helical circularity" analogous to that of optically active molecules.[6] In the discussion of light absorption, we noted that a photon possesses one unit of angular momentum, $\hbar$. A photon's angular momentum is due to its inherent spin. *The existence of left- and right-circularly polarized light*

Table 4.2 Relationship of Number of Photons (einsteins) Corresponding to 100 kcal mol^{-1}

Spectra Region	λ (nm)	ν (s^{-1})	einsteins (N)
Gamma	0.001	1.0×10^{20}	3.5×10^{-6}
X Ray	0.1	1.0×10^{18}	3.5×10^{-4}
UV	300	1.0×10^{15}	1.1
Violet	400	7.5×10^{14}	1.5
Green	500	6.0×10^{14}	1.8
Red	700	4.3×10^{14}	2.5
NIR	1000	3.0×10^{14}	3.5
IR	5000	0.6×10^{14}	17.3
Microwave	10^7	3.0×10^{10}	3.3×10^4
Radiowave	10^{11}	3.0×10^6	3.3×10^7

is a manifestation of the spin angular momentum of a photon. A beam of circularly polarized light passing through a quartz crystal (which itself has right or left chirality) produces a torque that causes the crystal to acquire an angular momentum and turn to the left or to the right! As we have seen in the above description of light absorption, in any absorption or emission process, the photon and the electrons of the molecule "exchange" angular momentum, and the total system of photon-plus-molecule experiences no *net* change in angular momentum. The fact that a photon possesses an angular momentum is the basis of the selection rule that requires the creation or destruction of nodes in the electron cloud of a molecule as the result of absorption or emission of light (Section 4.13). Perhaps the most convincing evidence for the chirality of photons is the observation that racemic mixtures of organic molecules may be resolved if one enantiomer of a racemic pair absorbs circularly polarized light more efficiently than the other enantiomer, and if a reaction follows the act of absorption.[6]

Viewing the photon as a particle elicits a picture of absorption as an energy and momentum transfer between two colliding particles, the photon and the electron. It is possible to evaluate the "cross section," or size of the "target," that the electrons of a molecule present for being struck by the photon. By cross section, we mean the area of space around a molecule that is accessible to being struck by a passing photon. If we view the molecule as a target of a given diameter (d), then the experimental extinction coefficient (ε, in $cm^{-1}M^{-1}$) for absorption is given by Eq. 4.14.[5,7]

$$\varepsilon = 10^{20} d^2 \tag{4.14}$$

In Eq. 4.14, d^2 is the area or cross section of the molecule in squared centimeters (cm^2). From the experimentally maximal value of ε_{max}, which is on the order of $10^5\ cm^{-1}\ M^{-1}$ for organic molecules, we calculate (Eq. 4.15) d^2_{max} to be

$$d^2_{max} \sim 10^5/10^{20} = 10 \times 10^{-16} cm^2 \sim 10\ Å^2 \tag{4.15}$$

According to this evaluation, we have a numerical benchmark for the largest cross section of an individual chromophore to be on the order of 10 Å^2, which corresponds to a diameter of 3.2 Å. The latter value is on the order of one or two bond lengths. This is on the correct order of the size of typical organic chromophores (Table 4.1).

4.15 Relationship of Experimental Spectroscopic Quantities to Theoretical Quantities[4]

Now, we use the qualitative classical model for the interaction of light with electrons as an intuitive basis for developing a quantum mechanical picture that will allow us to establish a relationship between experimental quantities and theoretical electronic wave functions (and matrix elements) for the radiative processes shown in Scheme 4.1. Let us consider the simplest case for radiative processes between two energy levels, one corresponding to the energy of R and one corresponding to the energy of *R. The fundamental experimental spectroscopic quantities related to absorption and emission of light between two energy levels are (1) the extinction coefficient for absorption (ε) for the R + $h\nu \rightarrow$ *R process as a function of wavelength, λ; (2) the intensity of emission (I) for the *R $\rightarrow$ R + $h\nu$ process as a function of wavelength, λ; and (3) the inherent rate constant of decay of emission (k_e^0), the *R $\rightarrow$ R + $h\nu$ process (which is usually independent of the emission wavelength). From the full state energy diagram (Fig. 1.4), we understand that an important issue in understanding photophysical phenomena is the fact that there generally will be a competition between radiative *R $\rightarrow$ R + $h\nu$ processes and radiationless (physical and chemical) processes. However, for simplicity, we start our discussion by assuming that emission is the only pathway for excited-state deactivation of *R. This means that there are no competitive radiationless pathways from the emitting state; in this special case k_e^0 represents the rate constant for deactivation of the state by emission. By definition, the *lifetime* of a state is equal to the reciprocal of the rate for deactivation of the state; for a unimolecular decay $k = 1/\tau$. Thus, $k_e^0 = 1/\tau_e^0$, so that we immediately know the decay time of emission τ_e^0 if we know k_e^0, the rate of decay of emission, and vice versa. Now, we seek to answer the question, How do these experimentally measurable quantities ε and k_e^0 relate to theoretical quantum mechanical quantities (matrix elements) for absorption or emission of light?

According to quantum mechanics (Section 3.4), the rate of a measurable experimental transition, P_{12}, such as ε or k_e^0, may be computed in terms of the square of a theoretical quantity, a matrix element (i.e., for transitions between an initial state, Ψ_1, and a final state, Ψ_2), as shown in Eq. 4.16:

$$\underset{\text{transition rate } (\varepsilon \text{ or } k_e^0)}{\text{Experimental quantity:}} \quad P_{12} \rightarrow \langle \Psi_1 | P | \Psi_2 \rangle^2 \quad \underset{\langle \text{matrix element} \rangle^2}{\text{Theoretical quantity:}} \tag{4.16}$$

To qualitatively or pictorially determine the value of P_{12}, we need to answer the questions: In the matrix element of Eq. 4.16, to what electronic states of a molecule do Ψ_1 and Ψ_2 correspond, and what is the nature of the operator P_{12} that triggers the transition? If we can compute or approximate Ψ_1 and Ψ_2, and if we have identified an appropriate operator P_{12}, we can then proceed to evaluate the matrix element given in Eq. 4.16. Then, we may set up the calculation of a matrix element such that the result allows us to compute the probability of absorption or the rate of emission, ε or k_e^0, respectively. From the results of the classical theory of light absorption,[4,5] which considers electrons as negative charges that can oscillate in specified ways along a molecular framework,[8] the values of ε and k_e^0 can be related by way of Eq. 4.16.

4.16 The Oscillator Strength Concept[4,5]

In classical theory, light is viewed as a harmonically oscillating electromagnetic wave, and the electrons of a molecule are viewed as negatively charged harmonic oscillators that can be driven into oscillation by interactions with light of certain frequencies corresponding to the resonance condition. In the classical theory of light, the *oscillator strength* (f) is defined as a quantity that measures the intensity or probability of an electronic transition that is induced by the interaction of electrons in matter with the electromagnetic field of a light wave. In a simple model, f may be viewed as the ratio of the intensity or radiation absorbed or emitted by an actual molecule compared to a single electron behaving as a "perfect" harmonic oscillator bound to a molecule. For such an idealized electron, $f = 1$; that is, the electron is considered a "perfect" harmonic oscillator. The basic idea is that for an electron with $f = 1$, when light interacts with this electron, the probability that light is absorbed at the correct resonance frequency, ν_i, will be very close to a maximal value (in the limit a probability of light absorption of a passing photon will be equal to 1 and every photon that interacts with the electron will be absorbed). In classical theory, electrons in the ground state of a molecule, R, are not oscillating, and are motionless (a situation that is forbidden by quantum mechanics!). The process of light absorption causes the excitation of an electron; the excited electron is viewed as an oscillating electron, but an unexcited electron is viewed as not oscillating. In the language of photons, the process of light absorption removes a photon from the electromagnetic field and causes an electron to oscillate; the process of light emission adds a photon to the electromagnetic field and causes an electron to stop oscillating.

As a concrete exemplar capable of relating the quantities ε and k_e^0 to the oscillator strength (f), an excited oscillating electron is approximated as a one-dimensional harmonic oscillator,[4c] that is, an oscillating dipole. For this simple case, the *theoretical quantity* of oscillator strength f in the classical theory of light absorption is related qualitatively to the experimental quantity ε by the expression given in Eq. 4.17:[4]

$$\underset{\text{strength}}{\text{Theoretical oscillator}} \quad f \equiv 4.3 \times 10^{-9} \int \varepsilon d\bar{\nu} \quad \underset{\text{absorption}}{\text{Experimental}} \tag{4.17}$$

In Eq. 4.17, ε is the experimental extinction coefficient and $\bar{\nu}$ is the energy (conventionally given in units of $1/\lambda$, typically in reciprocal centimeters cm^{-1}, termed wavenumbers) of the absorption in question.

Experimentally, the integral $\int \varepsilon d\bar{\nu}$ in Eq. 4.17 corresponds to the value of the area under a curve of a plot of the molecular extinction coefficient ε against wavenumber

$\bar{\nu}$ corresponding to a single electron oscillator. The rate constant (k_e^0) for emission (probability of emission of photons per unit time), according to classical theory, is related to the extinction coefficient for absorption[8,9] by Eq. 4.18.

$$\text{Radiative rate constant} \quad k_e^0 = 3 \times 10^{-9} \bar{\nu}_0^2 \int \varepsilon d\bar{\nu} \cong \bar{\nu}_0^2 f \tag{4.18}$$

In Eq. 4.18, $\bar{\nu}_0$ is the wavenumber (energy in $1/\lambda$ units) corresponding to the maximum wavelength of absorption, and the integral $\int \varepsilon d\bar{\nu}$ is the same as that given in Eq. 4.17. We can see from Eq. 4.18 that the probability of light absorption as measured by f is directly related to the experimental extinction coefficient, ε, and the radiative rate, k_e^0, and depends on the *square* of the frequency of the absorption (since $\bar{\nu}$ is directly proportional to $1/\lambda$). Immediately, we deduce from Eq. 4.18 that all other factors being equal, the rate of emission of light will be faster for an emission at a shorter wavelength.

The perfect electron oscillator in a molecule is predicted to have an oscillator strength of 1, corresponding to the maximum values of f (and the related values of ε). However, from Table 4.1, the experimental values of f, calculated from Eq. 4.17, are found to vary over an enormous range (from values near $1\text{–}10^{-10}$ $cm^{-1}M^{-1}$). One of the major failings of the classical theory of light absorption and emission was its inability to provide an adequate basis for understanding the wide variation in the observed values of f computed from Eq. 4.17. Nonetheless, the oscillator strength concept possesses the fundamentally correct form of the initial interaction of light with electrons, and upon reinterpretation in quantum mechanical terms, the wide variation in the value of f (and of experimental values of ε and k_e^0) can be explained in terms of the wave functions of the initial and final states involved in a radiative transition, as well as an operator representing the dipolar electric forces that an oscillating electromagnetic field imposes on an electron. Wave functions possess properties that must reflect the *electronic symmetries* of R and *R. In addition, they must reflect the *vibrational and spin properties* of these states. Since these important features were not considered at all in the classical theory of light absorption and emission, it is not surprising that the wide range of experimental values of f could not be predicted by classical theory and that the spread will be due at least in part to considerations of molecular symmetry, molecular vibrations, and electron spins.

4.17 The Relationship between the Classical Concept of Oscillator Strength and the Quantum Mechanical Transition Dipole Moment

The classical theory of light approximates the excited electron in a molecule as a linear harmonic oscillator or oscillating electric dipole. Let us consider some properties of electric dipoles in order to obtain some insight into the connection between f and the magnitude (strength) of an electric dipole. Then, we exploit this classical intuition to understand how the values of ε and k_e^0 can be related to the dipole strength of a radiative

transition. If two equal and opposite electric charges (e) are separated by a (vectorial) distance (**r**), a dipole moment ($\boldsymbol{\mu}$) of magnitude equal to **er** is created (Eq. 4.12). For an electronic transition of the type $R + h\nu \rightarrow {}^*R$, an oscillating dipole must be induced by the interaction of an electron with the electromagnetic field. According to classical theory,[4,5] the magnitude of f is proportional to the *square* of the induced (or transition) dipole moment ($\boldsymbol{\mu}_i$) produced by the action of a light wave on an electric dipole (Eq. 4.19):

$$\text{Oscillator strength } f \propto \boldsymbol{\mu}_i^2 = (\mathbf{er})^2 \quad \text{Transition dipole moment} \tag{4.19}$$

In Eq. 4.19, $\boldsymbol{\mu}_i$ is the induced *transition dipole moment* (or *dipole strength*) corresponding to the electronic transition (absorption or emission). The dipole strength of a transition may be set equal to **er**, which can be viewed as the average size of the transition dipole, where **r** is the dipole length. By combining the classical oscillator strength with the quantization of the oscillation of electrons, we have an expression relating f and $\boldsymbol{\mu}_i$, which is given by

$$f = \left(\frac{8\pi m_e \bar{\nu}}{3he^2}\right) \boldsymbol{\mu}_i^2 \cong 10^{-5} \bar{\nu} |\mathbf{er}_i|^2 \tag{4.20}$$

Eq. 4.20, where m_e is the mass of the electron, $\bar{\nu}$ is the energy of the transition (in cm^{-1}), h is Planck's constant, and **r** is the length (in cm) of the transition dipole.

Now, we can identify $\boldsymbol{\mu}_i$ with an observable quantity that can be computed as a matrix element, that is, $\boldsymbol{\mu}_i = <\psi_1|P|\psi_2>$, and produce Eq. 4.21:

$$\text{Classical} \rightarrow f = \left(\frac{8\pi m_e \bar{\nu}}{3he^2}\right) <P>^2 \leftarrow \text{Quantum mechanical} \tag{4.21}$$

Equation 4.21 connects the classical mechanical oscillator strength (f) to the quantum mechanical square of the matrix element, $<\Psi_1|P|\Psi_2>^2$ of Eq. 4.16. We are now in a position to derive the relationships between the quantum mechanical quantity, $<\Psi_1|P|\Psi_2>$, and experimental quantities, since both f and $<\Psi_1|P|\Psi_2>$ may be directly related to experimental quantities, such as ε, k_e^0 ($= \tau_e^0$) through Eq. 4.18.

4.18 Examples of the Relationships of ε, k_e^0, τ_e^0, $<\Psi_1|P|\Psi_2>$, and f

Note that the expressions given above that relate theory and experiment are simplified and given only to provide quantum insight into the important factors controlling the nature of the radiative transitions $R + h\nu \rightarrow {}^*R$ and ${}^*R \rightarrow R + h\nu$. Nevertheless, the use of these equations is expected to provide at least a *qualitative order-of-magnitude* agreement with experiment and to serve as calibration points and numerical benchmarks for expectations and comparison with experimental results. With these qualifications in mind, let us present some exemplars as numerical benchmarks in

order to acquire a feel for the orders and limits of magnitude of quantities associated with various radiative transitions.

A molecular absorption spectrum corresponds to the absorption of light over a range of many wavelengths. Consequently, Eq. 4.18 must be integrated over all of the wavelengths at which absorption occurs. The integration of Eq. 4.18 is simplified by the assumption that the absorption spectrum is a symmetrical curve that can be approximated by an isosceles triangle.[9] With this assumption, we have Eq. 4.22:

$$\int \varepsilon d\bar{\nu} \sim \varepsilon_{max} \Delta\bar{\nu}_{1/2} \tag{4.22}$$

In Eq. 4.22, ε_{max} is the value of ε at the absorption maximum and $\Delta\bar{\nu}_{1/2}$ is the width of the absorption band at a value of 1/2 ε_{max} in wavenumber (energy) units.

As an example, let us take the absorption spectrum of a molecule with $\varepsilon_{max} = 5 \times 10^4\ M^{-1}\ cm^{-1}$ at $\bar{\nu} = 20{,}000\ cm^{-1}$ (500 nm) and a half-width of $\Delta\bar{\nu}_{1/2} = 5000\ cm^{-1}$. Such a half-width for an absorption band is typical for organic molecules, and the extinction of maximum absorption in the example is close to the maximum found for typical organic molecules. In other words, *this example is an exemplar for a fully allowed electronic absorption* and would correspond closely to the classical case of an oscillator strength, $f = 1$.

Now, let us relate the experimental quantity ε to its theoretical counterparts, namely, f and $< \Psi_1|P|\Psi_2 >^2$ of Eq. 4.16. Guided by the classical model, the matrix element $< \Psi_1|P|\Psi_2 >$ is identified with a transition dipole moment, $\boldsymbol{\mu}_i = e\mathbf{r}$. The value of the matrix element $< \Psi_1|P|\Psi_2 >$ is then directly related to the value of the transition dipole e$<\mathbf{r}>$. Approximate expressions relating f and $<\mathbf{r}>^2$ are given by Eqs. 4.23 and 4.24:

$$f \sim \frac{\varepsilon_{max} \Delta\bar{\nu}_{1/2}}{2.5 \times 10^8} \quad \text{(unitless)} \tag{4.23}$$

$$<\mathbf{r}>^2 \sim \frac{\varepsilon_{max} \Delta\bar{\nu}_{1/2}}{2.5 \times 10^{19} \bar{\nu}} \quad (\text{units cm}^2) \tag{4.24}$$

Evaluating for $\varepsilon_{max} = 5 \times 10^4\ M^{-1}\ cm^{-1}$ at $20{,}000\ cm^{-1}$ with $\Delta\bar{\nu}_{1/2} = 5000\ cm^{-1}$, we find for f and $\mathbf{r}$:

$$f \sim \frac{(5 \times 10^4)(5 \times 10^3)}{2.5 \times 10^8} = 1.0 \tag{4.25}$$

$$<\mathbf{r}>^2 \sim \frac{(5 \times 10^4)(5 \times 10^3)}{(2.5 \times 10^{19})(2 \times 10^4)} = 5 \times 10^{-16} \quad (\text{units cm}^2) \tag{4.26}$$

Thus, we see (Eq. 4.25) that indeed such a large value for ε_{max} corresponds to an *oscillator strength f of the order of* 1.0.

In classical theory, such an exemplar system would correspond to an ideal electron harmonic oscillator.[4c] The transition dipole length $\mathbf{r}$ for the exemplar under discussion is 2.2×10^{-8} cm = 2.2 Å. Thus, according to quantum theory, our exemplar system

would have a transition dipole moment length of 2.2 Å, corresponding to a transition dipole moment $e\mathbf{r}$ of 2.2×10^{-8} cm $\times\ 4.8 \times 10^{-10} \sim 10$ D (the symbol D here stands for debye, the conventional unit for dipole moments). Thus, the strong electronic transition in the exemplar has associated with it a transition dipole moment of ~ 10 D. In other words, during the interaction of the light wave and the molecule, the electron cloud is distorted enough to produce a transition dipole moment of 10 D. For a numerical benchmark comparison, the permanent dipole moment of water is ~ 2 D.

Now, let us estimate the value of the radiative rate constant (k_e^0) associated with emission of light from the state producing the absorption spectrum we have just discussed. From our calculation of f and with the use of Eq. 4.18, we have Eq. 4.27:

$$k_e^0 \ (\equiv 1/\tau^0) \sim \bar{\nu}_0^2 f \sim (2 \times 10^4)^2 \sim 4 \times 10^8\ s^{-1} \tag{4.27}$$

In the calculation of k_e^0, we take the *theoretical* relationship of absorption to emission through the oscillator strength, f, and then make a prediction of the relationship between *experimental* quantities, that is, the integrated absorption spectrum and the inherent emission lifetime τ^0 (which is defined as $1/k_e^0$) for a corresponding radiative transition.

Now, consider a second exemplar of a molecule whose absorption spectrum is identical in shape and spectral position (same frequency) to our first case, but whose ε_{max} is only ~ 10. We find that

$$f = 2 \times 10^{-4} \quad \mathbf{r} = 0.3\ \text{Å} \quad k_e^0 \sim 10^5\ s^{-1} \tag{4.28}$$

Note that the value of the oscillator strength f is orders of magnitude smaller than the maximum value of 1.0, as are the associated dipole strength and radiative rate, and that the size of the transition dipole is correspondingly also much smaller.

These order-of-magnitude calculations for exemplars allow us to generate numerical benchmark estimates of the most intense radiative absorptions (measured by ε_{max}) or the fastest radiative emissions (measured to k_e^0) that we expect to encounter experimentally for organic molecules. How large can the value of ε_{max} be for an organic molecule? If one uses arguments derived from the classical theory of light absorption, the largest value of ε_{max} is associated with an oscillator strength of 1.0. A limiting value of $\varepsilon_{max} \sim 100{,}000$ is predicted for absorptions occurring near 400 nm (20,000 cm^{-1}). The corresponding radiative rate is $\sim 10^9\ s^{-1}$. Thus we have the values given in Eq. 4.29:

$$\text{Spin-allowed absorption} \quad \varepsilon_{max} \rightarrow 10^5\ cm^2\ M^{-1} \quad \text{(limit)} \tag{4.29a}$$

$$\text{Spin-allowed emission} \quad k_e^0 \rightarrow 10^9\ s^{-1} \quad \text{(limit)} \tag{4.29b}$$

The typical bandwidths ($\Delta\bar{\nu}_{1/2}$) of many absorption bands in the vis and near-UV regions are on average $\sim 3000\ cm^{-1}$ (at room temperature), so that from Eqs. 4.23

and 4.27 a convenient approximate relationship between the rate of emission, k_e^0, and ε_{max} is given by

$$k_e^0 \sim \varepsilon_{max} \Delta \bar{\nu}_{1/2} \sim 10^4 \varepsilon_{max} = 1/\tau^0 \tag{4.30}$$

Note that lifetimes calculated in this way are *pure radiative* lifetimes (τ^0) that is, lifetimes that would be observed in the absence of all radiationless processes by which the excited molecule *R could return to the ground state. The values of $1/\tau^0$ in turn are associated with rate constants (k_e^0), which correspond to pure radiative processes from *R. The experimentally observed lifetimes, τ_{obs}, are almost always less than the calculated values because of competing radiationless processes, both photophysical (*R → R) and photochemical (*R → I, *R → F), which compete with the *R → R + $h\nu$ radiative process.

Now, let us seek a benchmark for the smallest value of ε_{max} (smallest value of k_e^0). The smallest values of the matrix element for ε are expected when the R + $h\nu$ → *R process is spin forbidden (classical theory is of no help here because it does not consider an electron's spin at all). Of course, the theoretical limit for a spin-forbidden process is precisely zero. However, finite perturbations due to spin-orbit coupling[10] will always be present in organic molecules, so that, although the value of ε for a spin-forbidden radiative transition will always be much smaller than the value for an analogous spin allowed transition, the value is finite. The experimental lower limit for ε for organic molecules is in the range of $\varepsilon_{max} \sim 10^{-4}$. This corresponds to a radiative rate $k_e^0 \sim 10^{-1}$–10^{-2} s, which is the benchmark for spin-forbidden radiative transitions. When spin–orbit coupling is particularly strong, an upper limit of $\varepsilon_{max} \sim 10^0$ may be observed (molecules possessing heavy atoms).

4.19 Experimental Tests of the Quantitative Theory Relating Emission and Absorption to Spectroscopic Quantities

Experimental tests[9] of a slightly modified form of Eq. 4.18 have been made for singlet–singlet transitions; the results are given in Table 4.3. The agreement between the calculated and experimental values is excellent when the geometries of the ground and excited states are not significantly different and when the symmetry of the molecule is not too high. Large geometry changes between R and *R result in a breakdown in the assumptions of the above equations. High symmetry (e.g., benzene) may cause an "orbital" forbiddeness in a transition to cause a lower experimental value of ε than expected. The reason for this can be understood qualitatively as being due to the inability of the light wave to find a suitable molecular axis along which to generate a transition dipole by a HO → LU transition. This is the situation for the lowest-energy transition of benzene, naphthalene, and pyrene and other molecules possessing high symmetry. An important collateral property of these molecules is that they possess very long fluorescence lifetimes!

Although application of Eq. 4.18 to electronically forbidden singlet–singlet and spin–forbidden singlet–triplet radiative transitions is not theoretically justified, since

Table 4.3 Experimental and Calculated Radiative Lifetimes for Singlet–Singlet Transitions

Compound	$\tau^0(\times 10^9)^a$	$\tau(\times 10^9)^b$
Rubrene	22	16
Anthracene	13	17
Perylene	4	5
9,10-Diphenylanthracene	9	9
9,10-Dichloroanthracene	11	14
Acridone	15	14
Fluorescein	5	4
9-Aminoacridine	15	14
Rhodamine B	6	6
Acetone	10,000	1,000
Benzene	140	60

a. Calculated
b. Experimental

the classical theory does not consider the influence of molecular symmetry or electron spin on radiative transitions,[10] nonetheless it appears that relative values of k_e^0 still may be approximately derived from absorption data.[11]

4.20 The Shapes of Absorption and Emission Spectra[12]

We will examine a number of electronic absorption and emission spectra of several exemplar organic molecules. Some of these spectra show relatively "broad" bands, while others show a number of "sharp" bands. Now, we provide a qualitative description of the shape of the bands in an absorption or emission spectrum and provide a structural interpretation of the basis for their shapes.

Let the energy of the ground state R be E and the energy of the excited state *R be $^*E$. The resonance equation $\Delta E = h\nu$ then corresponds to transitions between two energy levels, E and $^*E$, with an energy gap, $\Delta E = {}^*E - E$. For the absorption (R + $h\nu$ → *R), the energy change corresponds to $\Delta E = h\nu = |E \rightarrow {}^*E|$, and for the emission (*R → R + $h\nu$), the energy change corresponds to $\Delta E = h\nu = |{}^*E \rightarrow E|$. We might expect that absorption and emission spectra will be observed experimentally as "sharp lines" with respect to the frequency ν of the absorbed or emitted light. In fact, only the absorption and emission spectra of atoms are close to being "sharp lines" (see Fig. 4.7a).

This sharpness of an atomic spectrum appears because the energies E and $^*E$ of the electronic states of atoms can be accurately described by specifying the *electronic energies* of the electronic orbitals. At low pressures in the gas phase for an atom, there are no rotations, vibrations, or collisions that "broaden" the values of E and $^*E$ for the ground and excited states of R and *R for atoms, and the value of $\Delta E = |{}^*E \rightarrow E| =$

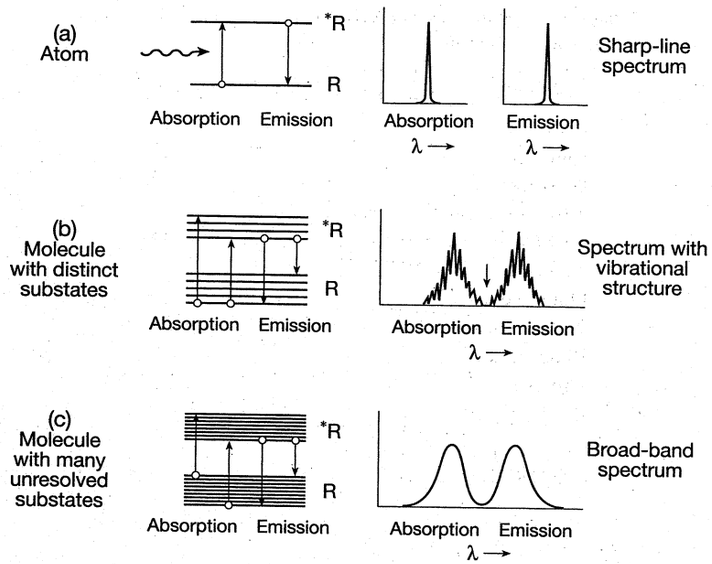

Figure 4.7 (a) Sharp-line absorption and emission spectrum typical of atoms at low pressure in the vapor phase. (b) Broad-band absorption and emission spectrum possessing vibrational typical of certain rigid molecules at low pressure in the vapor phase. (c) Structureless broad absorption and emission spectrum typical of molecules in solvents. Each absorption or emission corresponds to a single electronic transition.

$h\nu$ has a sharply and precisely defined magnitude since E and $^*E$ are sharply defined. Thus, at low pressure in the gas phase, atomic absorption and atomic emission spectra show very sharp lines, since the values of E and $^*E$ are sharply defined and the value of $\Delta E = h\nu$ is therefore sharply defined. An atomic electronic transition from the ground state, R, to an excited state, *R, requires a quantum of well-defined energy; consequently, the absorption ($R + h\nu \rightarrow R$) or emission ($^*R \rightarrow R + h\nu$) spectrum of an atom in the gas phase is a very narrow band of wavelengths (Fig. 4.7a). For example, both the absorption and emission spectra of the gaseous H atom in the *visible* region of the spectrum (corresponding to transitions between the $n = 2$ (2s, 2p) and $n = 3$ (3s, 3p, 3d) states of the H atom) consists of four sharp lines at 410, 434, 486, and 656 nm, respectively. There is nearly an exact correspondence between positions of the absorption and emission, because the energy of orbitals involved for R and *R in the transitions do not change significantly for an atom.

For a molecule, even in the gas phase at low pressures, because of coupling between the electrons and vibrations, the transitions between R and *R are not "pure" electronic transitions, but rather are "vibronic" transitions that can possess a range of energies. In order to describe the electronic states of a molecule, one must consider not only the motions of the electrons, but also the motions of nuclei relative to one another and

the molecules as a whole (e.g., vibrations and rotations). Thus, a molecular electronic transition between R and *R does not correspond to a well-defined single quantum of energy, because an instantaneous *ensemble* of different nuclear shapes may correspond to the initial or the final states (Chapter 3). As a result, the absorption (and emission) spectrum for a HO → LU transition of a molecule may involve many vibrational transitions over a range of energies corresponding to slightly different conformations of R and *R, even in the vapor phase at low pressures (Fig. 4.7b). The sharp "line" that characterized atomic transitions is replaced in molecular absorption by a set of closely spaced lines characterizing the molecular vibrations. Usually, these sets of closely spaced lines cannot be resolved and are termed an absorption or emission "band."

For organic molecules in solution, the situation becomes even more complex (Fig. 4.7c). In solution, R and *R are surrounded by solvent molecules that may be instantaneously intermolecularly oriented about R and *R in many different *supramolecular configurations*; in addition, the vibrations are coupled to within the molecule and to some extent to the solvent molecules. These supramolecular configurations of solvent molecules around R may be described by the supramolecular terminology R@solvent. Each one of these supramolecular configurations for the R@solvent + $h\nu \rightarrow$ *R@solvent transitions will have a slightly different energy gap for absorption or emission, so that compared to the gas phase, the molecular spectrum is greatly broadened and the molecular vibrational structure (Fig. 4.7b) is further broadened, or may be blurred out (Fig. 4.7c) or lost completely (termed a "featureless band with a single maximum). Similarly, for *R@solvent, the energy levels are broadened by the range of solvent orientations about *R so that the *R@solvent → R@solvent + $h\nu$ emissions will be broadened, often leading to a single, featureless band.

In certain cases in solution, some molecular vibrational structure is still apparent in a band corresponding to an single electronic transition. This situation occurs when the couplings of the electronic transitions to the solvent are weak. The most prominent vibrational progression of an electronic absorption or emission band is often associated with a vibration whose equilibrium position is greatly changed by the radiative electronic transition.[13] Thus, a prominent vibrational progression reveals the most important nuclear distortion that occurs during a transition. For "weak" spin-allowed electronic transitions ($f < 10^{-2}$), often the vibration in question is the one that destroys the molecular symmetry to such an extent that a forbidden transition (in idealized perfect molecular symmetry) is caused to become partially allowed via electronic–vibrational interactions. When this is the case, the vibrational structure for absorption provides information on the geometry of the excited state, and the vibrational structure for emission provides information on the geometry of the ground state. [Looking ahead, an experimental example of vibrational structure for an aromatic hydrocarbon, pyrene, is shown in Fig. 4.15. The vibrational structure is a mix of C=C and C—H motions that are involved in the $\pi \rightarrow \pi^*$ transition in going from R → *R in the absorption spectrum, and those involved in the $^*\pi \rightarrow \pi$ transition in going from *R → R in the emission spectrum.]

In some cases, the absorption and emission possess a vibrational structure that can be assigned to a specific vibrational motion. For example, during the n,π^* radiative

transitions of a ketone, in the $R(n^2) + h\nu \rightarrow {}^*R(n,\pi^*)$ transition, an n electron is removed from the HO and is placed in a π^*LU. Thus, in the light absorption process, a π^* electron is produced along the C=O axis so that the C=O bond is suddenly weakened and a C=O vibration is selectively excited. The structure of the C=O vibration of the excited state dominates the vibrational progression absorption spectrum. On the other hand, the ${}^*R(n,\pi^*) \rightarrow R(n^2) + h\nu$ process selectively removes an electron from a π^* orbital (LU) and places it in an n orbital (HO). Consequently, the C=O vibration of the ground state dominates the emission spectrum.

The absorption and emission spectra of benzophenone provide excellent exemplars of the concepts relating vibrational features to the electron configuration associated with radiative transitions. [Again looking ahead, Fig. 4.16 shows that some vibrational structure occurs in the bands of the n,π^* absorption of benzophenone in solution.] The vibrational structure of the $n \rightarrow \pi^*$ transitions of benzophenone corresponds to the two adjacent maxima in Fig. 4.16. The adjacent vibrational levels are separated by $\sim 1200\ cm^{-1}$, which corresponds to the C=O stretching vibration of *R. This value of $1200\ cm^{-1}$ for the *R state is confirmed by direct time-resolved IR measurements of the C=O stretch in R and *R. Figure 4.19a shows the emission spectrum of benzophenone at 77 K. Under these conditions, the vibration bands in the (phosphorescence) emission spectrum of the $T_1(n,\pi^*)$ state of benzophenone are well resolved and show a separation of $\sim 1700\ cm^{-1}$ between adjacent bands. This separation is in good agreement with the energy of the C=O stretching vibration of the *ground-state* benzophenone (as measured by IR spectroscopy). Thus, the separation of the vibrational bands of the absorption spectrum reflects the vibrational structure of *R and the separation of the vibrational bands of the emission spectrum reflects the vibrational structure of R. In passing, we note that the smaller value of $1200\ cm^{-1}$ for the *R state is consistent with weaker bonding in *R, due to the existence of an antibonding electron.

Now, we will see how vibration intensities in electronic absorption and emission spectra are controlled by the Franck–Condon principle.

4.21 The Franck–Condon Principle and Absorption Spectra of Organic Molecules[13]

The Franck–Condon principle (Section 3.10, especially Fig. 3.3) leads to the conclusion that there will be a difference in the probability of vibrational transitions between the wave functions ψ_0 and ${}^*\psi$ (corresponding to the R and *R states, respectively) of a diatomic molecule X—Y. Here, we present examples of the role of the Franck–Condon principle in terms of a *semi*classical model (the vibrations are quantized, but the vibrational wave functions are not considered explicitly). In Fig. 4.8, a situation is shown for which the two potential curves for ψ_0 and ${}^*\psi$ are similar and not displaced vertically; that is, the equilibrium separation $\mathbf{r}_{eq}$ is the same for ψ_0 and ${}^*\psi$. The situation in Fig. 4.8 corresponds to an electronic orbital jump for which the overall bonding is similar in both ψ_0 and ${}^*\psi$. As a result, the equilibrium geometries of R and *R should be similar. In such a situation, the Franck–Condon principle requires that, since absorption must occur vertically, a relatively strong $v = 0 \rightarrow v = 0$ transition (termed a $0 \rightarrow 0$ band) is observed for both absorption and emission (compared with the intensity to other vibrational bands) and the $0 \rightarrow 0$ band of the absorption and emission spectrum overlap significantly. The molecule in R undergoes zero-point motion ($v = 0$) between points A and E. A vertical transition to point B ($v = 4$) is Franck–Condon forbidden, as are transitions to points C and D ($v = 4$). As a result, the $0 \rightarrow 4$ transition is very weak.

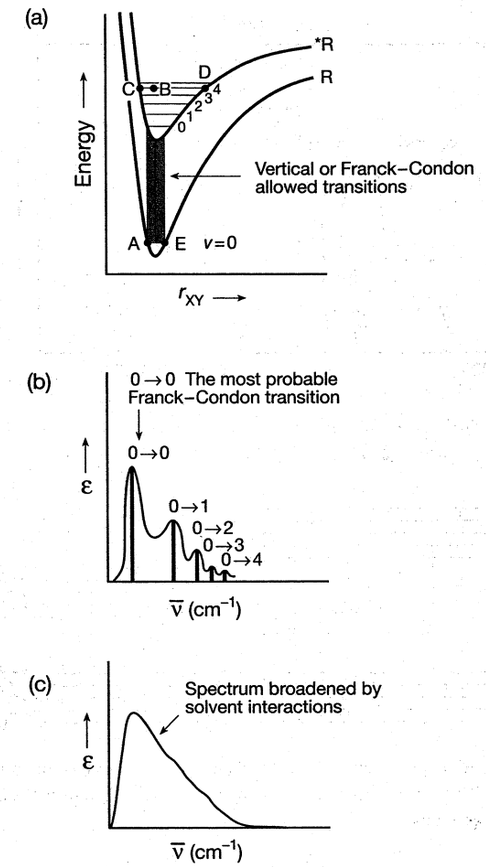

Figure 4.8 (a) Potential energy curves for similar minimum for R and *R showing the Franck–Condon allowed vertical transition for $\mathbf{R} \rightarrow {}^*R$ transitions. (b) Form of the observed absorption spectrum. For an experimental exemplar, see Fig. 4.9. (c) Effect of solvent broadening on the vibrational structure of the absorption spectrum.

Examples of a molecule with a small displacement of the minimum of the energy curves[14] are rigid aromatic hydrocarbons, such as anthracene (Fig. 4.9). In the case of

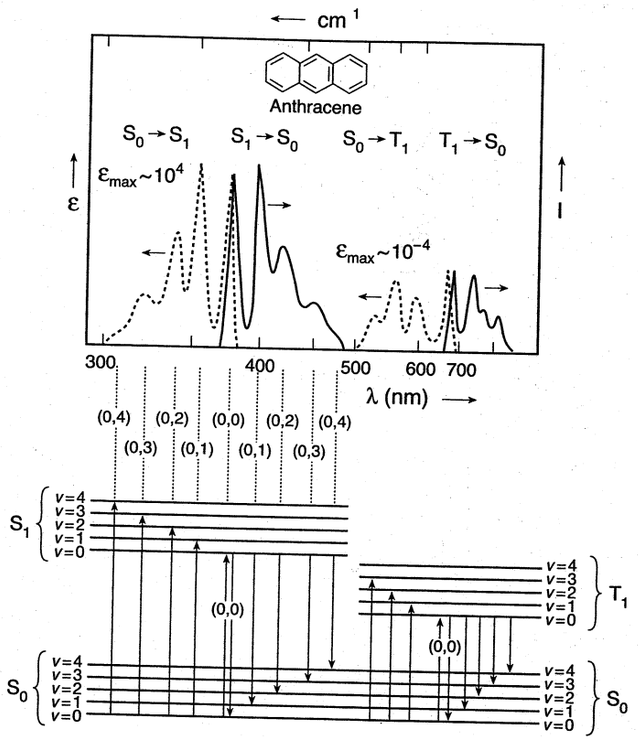

Figure 4.9 Absorption (dotted lines) and emission (solid lines) of anthracene in solution. The lower portion displays an energy level diagram as the basis for vibrational assignments.

anthracene, the excited-state curve minimum is slightly displaced from the ground-state curve minimum because the molecule in the excited state bends slightly to make a "v" shape symmetrical about the 9,10 position of the molecule. In this case, relatively strong $0 \rightarrow 0$ and $0 \rightarrow 1$ vibrational bands are observed in both absorption and emission, and the 0,0 band of absorption and emission overlap. Note that the vibrational patterns for the spin-allowed $S_0 \leftrightarrow S_1$ and spin-forbidden $S_0 \leftrightarrow T_1$ radiative transitions are slightly different. A possible reason is that the vibrations that best mix in triplet character are not exactly the same as those that have the best Franck–Condon factors.

Figures 4.10 and 4.11 represent situations for which the excited curve minima for $^*\psi$ are significantly displaced relative to ψ_0 ($\mathbf{r}_{eq}$ is assumed to be larger in $^*\psi$ than in ψ_0 because the antibonding electron weakens the bonds of *R, and therefore makes the equilibrium geometry, $\mathbf{r}_{eq}$, larger in *R). In Fig. 4.10, the $0 \rightarrow 2$ and $0 \rightarrow 3$ vibrational bands are relatively intense and the $0 \rightarrow 0$ and $0 \rightarrow 1$ vibrational bands are relatively

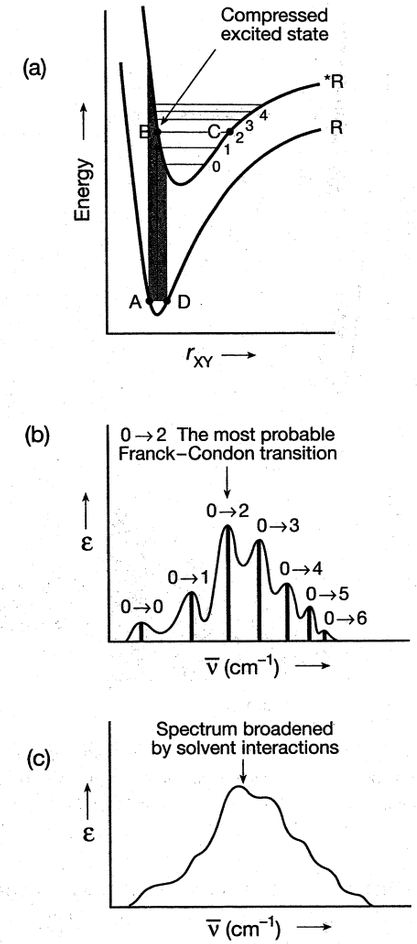

Figure 4.10 (a) Potential energy curves for significantly different minimum for R and *R showing the Franck–Condon allowed vertical transitions for $R \rightarrow {}^*R$ transitions. (b) Form of the observed absorption spectrum (see Fig. 4.15 for an exemplar). (c) Effect of solvent broadening on the vibration structure of the absorption spectrum. A typical example is an aromatic ketone undergoing n,π^* absorption (see Fig. 4.15).

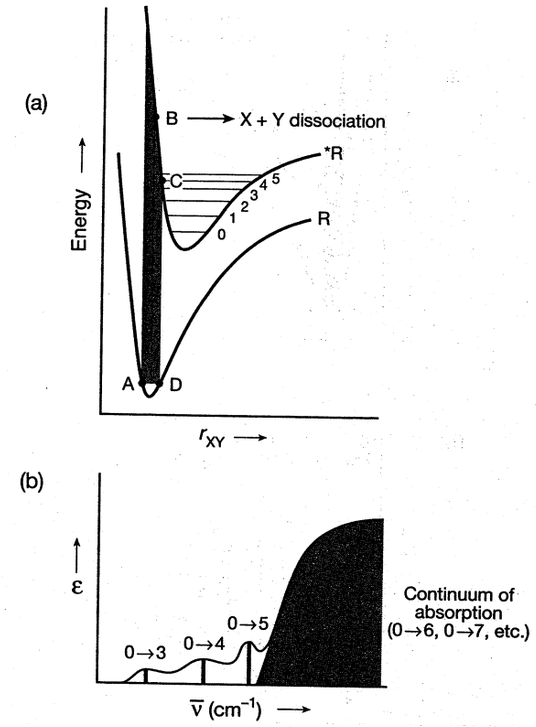

Figure 4.11 The effect of absorption to a dissociative state on the absorption spectrum. A typical example is a molecule possessing a very weak σ bond, for example, CH_3I or CH_3OOCH_3.

weak. In Fig. 4.11, excitation of $^*\psi$ to produce geometries more contracted than point C in the figure (points between B and C) results in dissociation of the diatomic XY molecule into two atoms X + Y. When this happens, there is no vibrational structure in the absorption spectrum since the atoms dissociate immediately after absorbing a photon and do not undergo any vibrations.

4.22 The Franck–Condon Principle and Emission Spectra[13]

In condensed phases, the rate of vibrational and electronic energy relaxation among excited states is very rapid compared to the rate of emission (Chapter 3). As a result, emission will generally occur *only* from the $v = 0$ vibrational level of the lowest excited states of *R. Now, let us apply the Franck–Condon principle to the $^*R \rightarrow R + h\nu$ emission (Fig. 4.12).

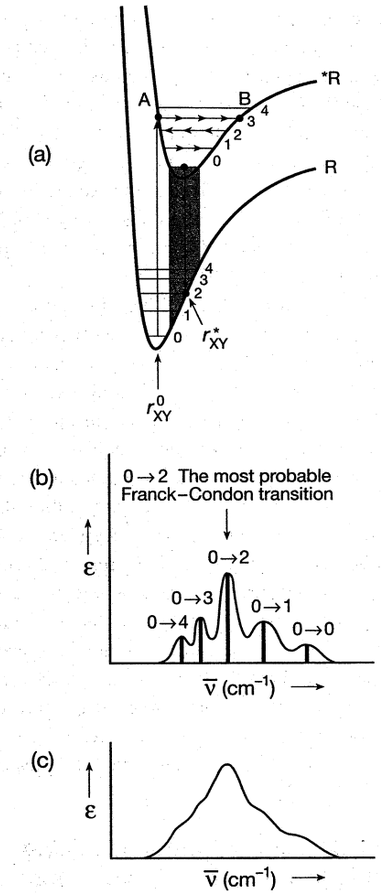

Figure 4.12 (a) Potential energy curves, (b) emission spectrum, and (c) solvent-broadened emission spectrum. As shown, the $0 \rightarrow 2$ emission is the most probable Franck–Condon transition. The most probable absorption is from r_{xy}, and the most probable emission is from r^*_{xy}. Emission from R* produces an elongated ground state.

In analogy to absorption, the most probable emissions will be those that occur "vertically" with the smallest change in the value of the equilibrium geometry of *R, which will generally be those emissions from the $v = 0$ level of *R. The equilibrium separation of the ground-state PE curve minimum is smaller than that of the excited-state curve (because *R possesses an antibonding electron, whereas R does not), so

that the most probable vertical transitions from *R produce an elongated ground state (while absorption produces a compressed excited state) immediately after transition. It is important to note that the frequency (energy) of emission cannot be greater than the frequency (energy) of the $0 \rightarrow 0$ emission, since the emissions from $0 \rightarrow 1$, $0 \rightarrow 2$, and so on emissions correspond to smaller energies than the $0 \rightarrow 0$ emission. Since the energy of the $0 \rightarrow 0$ transition is the maximum energy that can be produced in the $^*R \rightarrow R + h\nu$ transition, this energy is defined as the excitation energy of the state and is given the symbol $^*E_S$ for the energy of $^*R(S_1)$ and the symbol $^*E_T$ for the energy of $^*R(T_1)$. Figure 4.12 shows the emission spectrum expected from a molecule whose PE curves are similar to those in Fig. 4.10.

Consider the two PE curves of Fig. 4.12a. When absorption occurs vertically from the ground-state surface, the excited state is "born" near point A, a turning point for the compressed vibration in $v = 3$. The molecule will begin to vibrate in the $v = 3$ state and, in the absence of any external perturbation (say, in the gas phase at low pressure), the atoms XY would continue to persist in the $v = 3$ state. In solution, however, there are many perturbations induced by collisions, which can also remove energy. In addition, in a polyatomic molecule, vibrations in one part of the molecule may act as a perturbation to vibrations in another part of the same molecule, so that energy is rapidly transferred among vibrational modes (time scales on the order of a few ps or less). Thus, vibrational energy is generally removed very rapidly from upper vibrational levels, and transitions between vibrational levels seem to occur about as fast as vibrational energy can either be removed by the environment or redistribute itself within a molecule. In Fig. 4.12, this decrease in vibrational energy from $v = 3$ to 0 is shown as a sequence of arrows. The mechanisms of removal of vibrational energy from excited energy levels will be discussed in more detail in Chapter 5, which deals with radiationless transitions. This rapid relaxation of vibrational energy in electronically excited states is the fundamental basis for Kasha's rule.

4.23 The Effect of Orbital Configuration Mixing and Multiplicity Mixing on Radiative Transitions[14,15]

In Section 3.4, we saw that the zero-order approximation of electronic states (ignore electron–electron interaction and electron–vibrational interactions) is only a starting point for describing transitions between electronic states, and that we must consider electronic state mixing in order to understand the probability of radiative transitions between electronic states. A basic result of state mixing is to imbue a zero-order state, originally described in terms of a single electronic orbital configuration (or spin multiplicity), with characteristics of a second electronic orbital configuration (or spin multiplicity). We may, of course, consider the mixing of many orbital configurations. Often, however, mixing of only one other orbital configuration (usually the orbital that is closest in energy to the zero-order orbital of interest) is sufficient to interpret a great deal of experimental data. How does mixing affect zero-order predictions? For radiative (and radiationless) transitions, first order mixing is generally a significant

mechanism "allowing" processes that are strictly forbidden in zero-order to occur with measurable probability. We can view the mixing as a interaction between wave functions that are close in energy. Typically, a wave function for which a transition is forbidden in zero-order borrows some of the character of a wave function for which the transition becomes allowed in second order.

As an exemplar, let us consider the radiative processes involving the absorptive transition of an electron from an n orbital to a π^* orbital (or the emissive transition from a π^* orbital to an n orbital). We start with the simple one-electron (zero-order) description of an n and a π^* orbital. This approximation does not include any electron–electron or electron–vibrational interactions. We can term the zero-order wave function that uses these orbitals as a "pure" state (Eq. 4.31a).

Consider the magnitude of f, the oscillator strength (Eq. 4.21), which is directly related to the probability of absorption (ε) and of emission (k_e^0). In zero-order, $f = 0$ for a $S_0 \rightarrow S_1$ (pure n,π^*) radiative transition, since the n and π^* orbitals undergoing transition are strictly orthogonal and therefore there is no orbital overlap. From Eq. 4.21 $< n|P|\pi^* >= 0$, since $<n|\pi^*> = 0$. In first order, we consider that vibrations or electron–electron interactions may "mix" n,π^*, and π,π^* configurations (e.g., compare to Fig. 3.1). The result is that the n and π^* orbitals are no longer orthogonal and the value of $<n|P|\pi^*> \neq 0$. We say that the transition that is forbidden in zero order is "partially" allowed in first order because of vibronic interactions. Including vibronic interactions, Eq. 4.31b is therefore a better description of S_1, which is a state of "mixed" configurations, and the coefficient λ (a mixing coefficient, not a wavelength) is a measure of the extent of mixing.

$$S_1 \text{ (pure)} = n,\pi^* \tag{4.31a}$$

$$S_1 \text{ (mixed)} = n,\pi^* + \lambda(\pi,\pi^*) \tag{4.31b}$$

Since the $S_0 \rightarrow \pi,\pi^*$ transition is generally "allowed" (i.e., in Eq. 4.21 $<P> \neq 0$), a transition $S_0 \rightarrow S_1$ (mixed) is plausible through the contribution of $\lambda(\pi,\pi^*)$ to the wave function describing S_0, although f is expected to be relatively weak compared to a fully allowed transition of the $S_0 \rightarrow \pi,\pi^*$ type. Now, we may estimate the value of f for Eq. 4.32.

$$S_0 \underset{-h\nu}{\overset{+h\nu}{\rightleftarrows}} S_1 \quad \text{(mixed)} \tag{4.32}$$

The expression for f becomes Eq. 4.33:

$$f(S_0 \rightleftarrows S_1) = \lambda^2 f(S_0 \rightleftarrows S_2) \tag{4.33}$$

In other words, the first-order $S_0 \rightarrow S_1$ (mixed) transitions are allowed only to the extent that $S_2(\pi,\pi)$ is mixed into $S_1(n,\pi^*)$. The amount of mixing is given by λ, the coefficient predicted from perturbation theory (Section 3.4). Thus, the observed value of $f(S_0 \rightarrow S_1)$ may be evaluated in terms of the theoretical value of f for the zero-order $S_0 \rightarrow S_2(\pi,\pi^*)$ transition.

According to perturbation theory, the value of λ is given by the value of the matrix element for mixing of S_0 and S_2 divided by the energy gap between S_0 and S_2 (Eq. 4.34).

$$\text{Mixing coefficient} \rightarrow \lambda = \left| \frac{\langle \psi_a | P | \psi_b \rangle}{E_a - E_b} \right| \quad \begin{matrix} \leftarrow \text{Matrix element} \\ \leftarrow \text{Energy separation} \end{matrix} \tag{4.34}$$

If we replace λ in Eq. 4.33 by its equivalent from Eq. 4.34, we produce Eq. 4.35,

$$\begin{matrix} \text{Observed} \\ \text{mixed state} \end{matrix} \quad \begin{matrix} \text{Mixing} \\ \text{coefficient} \end{matrix} \quad \text{Zero-order}$$

$$f(S_0 \rightleftarrows S_1) = \left| \frac{\langle n,\pi^* | P | \pi,\pi^* \rangle}{E_{\pi,\pi^*} - E_{n,\pi^*}} \right|^2 f(S_0 \rightleftarrows \pi,\pi^*) \qquad S_2 = \pi,\pi^* \tag{4.35}$$

where n,π^* and π,π^* refer to the zero-order states, and P corresponds to the interaction that mixes S_1 and S_2.

From Eq. 4.35, we see that the measured value of $f(S_0 \rightarrow S_1)$ reflects both λ (Eq. 4.34) and $f(S_0 \rightarrow \pi,\pi^*)$. The magnitude of $f(S_0 \rightarrow S_1)$ depends on three factors:

1. The magnitude of the matrix element $<n,\pi^*|P|\pi,\pi^*>$.
2. The energy gap ${}^*E_{\pi,\pi^*} - E_{n,\pi^*}$.
3. The zero-order oscillator strength, $f(S_0 \rightarrow \pi,\pi^*)$, of the allowed transition.

In effect, theory predicts that $f[S_0 \rightarrow S_1 + \lambda^2 S_2(\pi,\pi^*)]$ will possess all of the characteristic properties of $S_0 \rightarrow \pi,\pi^*$ transitions except that the probability of the observed transitions will be decreased by the factor λ^2 (Eq. 4.33). For example, the electronic polarization (orientation of the absorbed light relative to the molecular framework) of the $S_0 \rightarrow S_1$ transitions will be derived from the polarization of the $S_0 \rightarrow S_2(\pi,\pi^*)$ transitions. For aromatic molecules, $S_0 \rightarrow S_2(\pi,\pi^*)$ transitions are in-plane polarized.[14] Thus, if S_1 is a mixture of n,π^* and π,π^* states, the $S_0 \rightarrow S_1$ transitions will be in-plane polarized.

Now, we may straightforwardly apply the same ideas of mixing to the qualitative evaluation of a *spin-forbidden* transition, that is, the value of $f(S_0 \rightarrow T_1)$. We assume (Section 3.21) that ${}^3(n,\pi^*)$ and ${}^1(\pi,\pi^*)$ mixing is dominant for a $S_0(n^2) \rightarrow T_1(n,\pi^*)$ transition and that spin–orbit coupling is the dominant interaction that mixes singlet and triplet states, and from perturbation theory we are led to Eq. 4.36:

$$f(S_0 \rightleftarrows T_1) = \left| \frac{\langle {}^3(n,\pi^*) | P_{SO} | {}^1(\pi,\pi^*) \rangle}{E_{\pi,\pi^*} - E_{n,\pi^*}} \right|^2 f(S_0 \rightleftarrows \pi,\pi^*) \tag{4.36}$$

We see that the spin-"forbidden" $S_0(n^2) \rightarrow T_1(n,\pi^*)$ transitions pick up finite oscillator strength via a mechanism that mixes the S and T states. The magnitude of f for $S_0 \rightarrow T_1(n,\pi^*)$ depends on the value of the matrix element and the oscillator strength of the "pure" spin-allowed $S_0 \rightarrow S_n(\pi,\pi^*)$ transitions. Both $S_0 \rightarrow T_1(n,\pi^*)$ absorption and $T_1(n,\pi^*) \rightarrow S_0$ emission are predicted to be in-plane polarized,

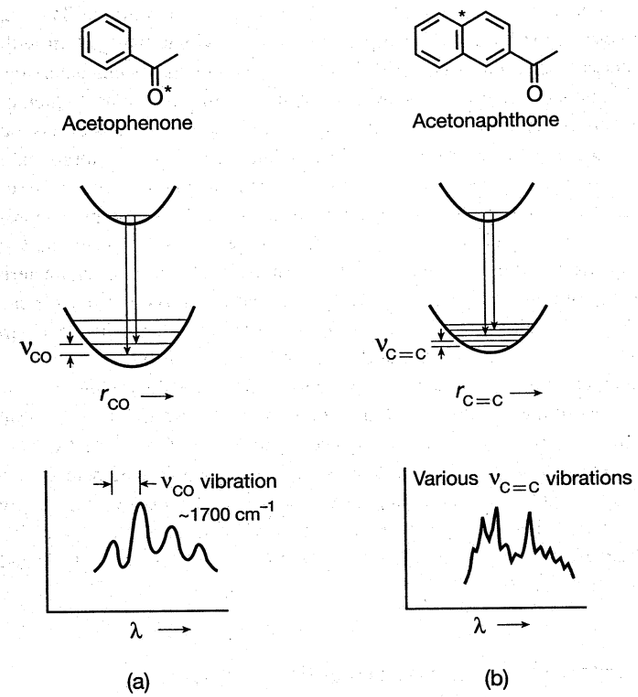

Figure 4.13 (a) Emission of acetophenone possesses a C=O vibrational pattern. (b) Emission of acetonaphthone possesses a C=C vibrational pattern.

because the oscillator strength of the "real" transition is due to the π,π^* state mixed into T_1 and because π,π^* states are generally in-plane polarized.

From the above discussion, it is clear that measurement of "forbidden" absorptions and emissions yield evidence of the identity of the mixing state that provides an interaction mechanism that makes a zero-order forbidden transition allowed in first order. In Section 4.20, we noted that the vibrational structure of absorption and emission bands provides information on the vibrational motions that are induced by orbital transitions. A study of the vibrational structure of an absorption or emission also provides clues as to which molecular motions are most effective in mixing states. For example, like the situation for benzophenone, the vibrational structure of the $S_0 + h\nu \rightarrow S_1(n,\pi^*)$ absorptions of acetophenone shows a regular progression of vibrational bands separated by $\sim 1200\ \text{cm}^{-1}$.[16] This separation corresponds to the energy required to stretch the C=O bond in S_1. The same C=O stretching vibrations are important in mixing allowed π,π^* character into S_1, which is a nominally n,π^* state if it is strictly planar and not vibrating. As soon as the C=O stretch (and bend) is turned on, the S_1 state begins to mix with other states.

In contrast, again like benzophenone, the vibrational structure of $T_1 \rightarrow S_0 + h\nu$ phosphorescence spectrum of acetophenone shows a vibrational pattern with separations between adjacent bands of $\sim 1700\ cm^{-1}$, a value that is characteristic of the C=O vibrational stretch in S_0 (shown schematically in Fig. 4.13a).[16] Such a vibrational pattern is expected for emission from an n,π^* state if the transition is localized on the C=O group; that is, the $\pi^* \rightarrow n$ electron jump leaves excess vibrational energy on the C and O atoms specifically because an antibonding node between these atoms disappears as a result of the orbital jump. On the other hand, the phosphorescence spectrum of acetonaphthone (Fig. 4.13b) does *not* show the characteristic C=O vibrational pattern. Instead, a complicated pattern of C=C vibrations characteristic of the aromatic ring in S_0 is observed. This is expected for emission from a π,π^* state, since the $\pi^* \rightarrow \pi$ electron jump leaves excess vibrational energy between certain C atoms of the aromatic ring as the result of the destruction of a node.

In summary, numerous spectroscopic criteria from absorption and emission exist for the assignment of the electronic configuration to S_1 and T_1. *Photochemical reactivity* can also serve to classify S_1 and T_1 in terms of their electronic configurations. Because of the two correlations, (a) spectroscopic parameters $\Leftrightarrow$ orbital configurations, and (b) orbital configuration $\Leftrightarrow$ photoreactivity, we expect (and will find) correlations between spectroscopic parameters and photoreactivity. The theoretical basis for this relationship will be made via frontier orbital methods and state correlation diagrams (Chapter 6).

4.24 Experimental Exemplars of the Absorption and Emission of Light by Organic Molecules[16]

Now, we will consider a number of experimental examples of the radiative transitions $R + h\nu \rightarrow {}^*R$ and ${}^*R \rightarrow R + h\nu$ (Scheme 4.1). We only consider the lowest excited singlet state (S_1) or the lowest triplet state (T_1) as likely candidates for the initiation of an emission. This generalization, which is based on *Kasha's rule*,[17] results from the experimental observation that the majority of photoreactions and photoemissions studied to date do not appear to involve higher-order electronic states (S_2, T_2, etc.), because rapid radiationless conversions (e.g., $S_n \rightarrow S_1$ and $T_n \rightarrow T_1$) compete favorably with emission from upper electronically excited states (S_n, T_n, $n > 1$). (We will discuss the reasons why this is generally the case in Chapter 5.) Thus, it is the spectroscopy of S_1 and T_1 that is of greatest interest to the organic photochemist, since these two states are the most likely starting point for initiating photophysical and photochemical processes. Accordingly, we consider the following radiative processes in detail:

1. $S_0 + h\nu \rightarrow S_1$ Spin-allowed absorption (singlet–singlet absorption)
2. $S_0 + h\nu \rightarrow T_1$ Spin-forbidden absorption (singlet–triplet absorption)
3. $S_1 \rightarrow S_0 + h\nu$ Spin-allowed absorption emission (fluorescence)
4. $T_1 \rightarrow S_0 + h\nu$ Spin-forbidden emission (phosphorescence)

An exemplar that shows experimental examples of all four of these key radiative transitions has already been given for anthracene in Fig. 4.9. For the allowed radiative

transition, the $S_0 \rightarrow S_1$ absorption occurs at the higher energies (~ 300 to ~ 380 nm), and $S_1 \rightarrow S_0$ fluorescence emission occurs at lower energies (~ 380 to ~ 480 nm). The bands that nearly overlap in $S_0 \rightarrow S_1$ absorption and in $S_1 \rightarrow S_0$ emission near 380 nm correspond to transitions between the 0 vibrational level of S_0 and S_1, that is, the 0,0 *bands for absorption and emission* (see the energy-level diagram below the spectrum of anthracene in Fig. 4.9). At still lower energies, the very weak $S_0 \rightarrow T_1$ absorption (~ 500 to ~ 700 nm) appears. In the spectrum, the signal for this transition is amplified many times in order to be visible. The value of ε_{max} for the $S_0 \rightarrow T_1$ absorption is $\sim 10^8$ *times smaller* than the value of ε_{max} for $S_0 \rightarrow S_1$ absorption. Finally, the $T_1 \rightarrow S_0$ phosphorescence emission is observed at lowest energies.

There are several exemplar chromophores that are representative of the types encountered in most organic photochemical systems. These are

1. The carbonyl chromophore
2. The ethylene chromophore and conjugated polyenes
3. Combinations of the carbonyl and ethylene chromophores (enones)
4. The benzene chromophore and aromatic chromophores and their derivatives

From these exemplar chromophores, we can examine and understand all of the important principles and features of radiative transitions. Building on the knowledge of the photophysics of this set of exemplar chromophores, we can infer the influence of substituted derivatives on the radiative properties of a wide range of organic molecules. In Chapter 5, we consider the radiationless processes of some exemplar chromophores, and in later chapters we examine the photochemistry of the exemplar chromophores.

4.25 Absorption, Emission, and Excitation Spectra

The experimental measurement of an *electronic absorption spectrum* is based on two important principles: Lambert's and Beer's laws.[18] *Lambert's law* states that the proportion of light absorbed by a medium is independent of the initial intensity of the light, I_0. This law is a good approximation for ordinary light sources, such as lamps, but it breaks down when high-intensity lasers are employed. *Beer's law* states that the amount of light absorbed is proportional to the concentration of absorbing molecules in the light path. This law is a good approximation unless molecules begin to form aggregates at higher concentrations. The experimental quantity related to absorption that is conventionally measured is called the *optical density* (OD, Eq. 4.37a), where I_0 is the intensity of incident light falling on the sample and I_t is the intensity of transmitted light through the sample (usually understood to be 1 cm in depth). For example, an OD of 2.0 corresponds to $\sim 1\%$ transmission or $\sim 99\%$ absorption; an OD of 1.0 corresponds to $\sim 10\%$ transmission and 90% absorption; an OD of 0.01 corresponds to $\sim 98\%$ transmission or $\sim 2\%$ absorption. It is important to note that for a sample with an optical density > 2.0, most of the light is absorbed in a very small volume of the sample near to the place where the light impinges on the sample.

An absorption spectrum is completely described by a graph of optical density as the ordinate and the wavelength (λ units typically nm, or Å) of absorbed light as the abscissa (experimental example, Fig. 4.9; schematic examples, Fig. 4.14).

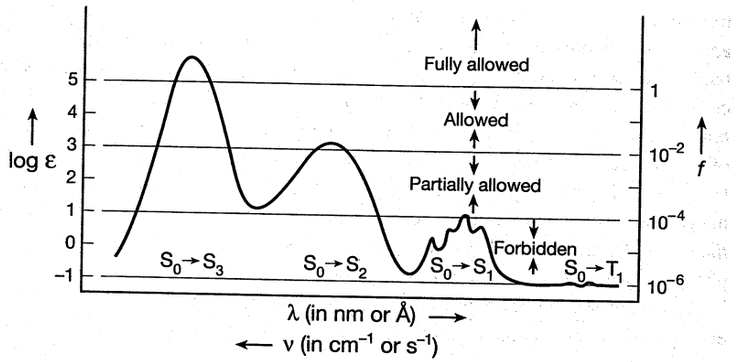

Figure 4.14 Schematic representation of the absorption spectrum of a simple organic molecule. Note the y-axis (left) plots log ε and the y-axis (right) plots f. Often the first ($S_0 \rightarrow S_1$) transition is relatively weak compared to $S_0 \rightarrow S_2$ and $S_0 \rightarrow S_3$ transitions. The $S_0 \rightarrow T_1$ transition, while always present, is often too weak to measure experimentally. Note that the ordinate is a log scale, each entry specifying a power of 10.

In some cases, it is more informative to use energy units (reciprocal wavelength, cm^{-1}, or frequency, s^{-1}) instead of wavelength. Conventionally, the molar extinction coefficient (ε) is employed in such graphs rather than absorption intensity, and is given by Eq. 4.37b.

$$OD = \log (I_0/I_t) \tag{4.37a}$$

$$\varepsilon = [log(I_0/I_t)]/[A] \tag{4.37b}$$

In Eqs. 4.37a and b, I_0 and I_t are the intensity of the incident and transmitted light, respectively; l is the optical path length (usually 1 cm); and [A] is the concentration of absorbing material, A. The coefficient (ε) is a fundamental molecular property and is independent of concentration and path length if Lambert's and Beer's laws hold. Because of the wide variation of the values of ε, absorption spectra are sometimes plotted as log ε versus wavelength (λ, nm), as shown in Fig. 4.14 and as discussed in Section 4.14. The units of ε are $cm^{-1}\,M^{-1}$ (understood as the units of absorption). For comparison with ε, the oscillator strength, f, is plotted on the y-axis to the right of Fig. 4.14. As discussed in Section 4.14, it is interesting to note that ε has the dimensions of *area*/mol (i.e., $cm^{-1}\,M^{-1} = cm^{-1}\,mol^{-1}\,l = cm^2\,mol^{-1}$).

An *emission spectrum* is a plot in nm (or Å) of emission intensity I_e (at a fixed excitation wavelength and constant exciting intensity I_0) as a function of wavelength (or energy) of exciting light. For a weakly absorbing solution (OD < 0.1) of a luminescent molecule A, I_e is given by Eq. 4.38.

$$I_e = 2.3\, I_0 \varepsilon_A\, l \Phi^A [A] \tag{4.38}$$

In Eq. 4.38, ε_A is the extinction coefficient of the absorbing molecule, l is the optical path length, Φ^A is the quantum yield of emission of A (discussed in Section 4.27), and [A] is the concentration of A. The quantum yield of emission, Φ^A, is usually

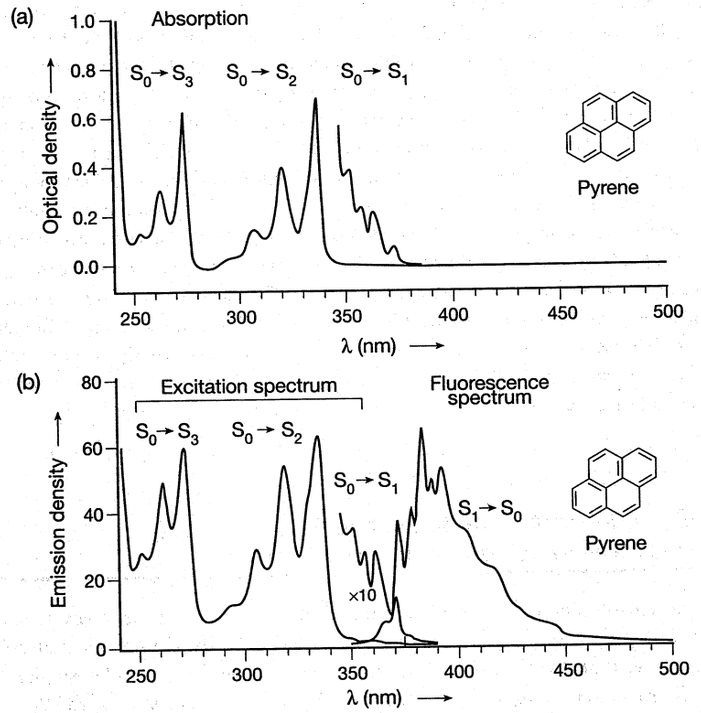

Figure 4.15 (a) Absorption spectrum of pyrene. (b) Excitation spectra of pyrene (left) and fluorescence spectrum of pyrene (right) All spectra are in cyclohexane solvent at room temperature. The insert of bands between 340–380 nm correspond to the $S_0 \rightarrow S_1$ absorption expanded by a factor of 10. This π, π^* transition is symmetry forbidden (Section 4.26) and possesses a much larger extinction coefficient than the shorter wavelength $S_0 \rightarrow S_2$ and $S_0 \rightarrow S_3$ absorptive transitions.

independent of exciting wavelength (Kasha's rule).[17] Thus, from Eq. 4.38, at fixed values of [A], I_0, and l, the intensity of emitted light from a sample, I_e, is directly proportional to the extinction coefficient (ε_A). A plot of I_e as a function of wavelength of exciting light will vary as ε_A is termed an *excitation spectrum* and has the *same spectral shape and appearance as the absorption spectrum.* An advantage of an excitation spectrum over a standard absorption spectrum is the greater sensitivity of luminescence techniques, which often allows observation of an excitation spectra at [A] too low to be directly measured by absorption spectroscopy.

Figure 4.15 is an example of an absorption, fluorescence, and fluorescence excitation spectrum, with pyrene as an exemplar. The excitation spectrum is shown on the lower left portion of the figure together with the fluorescence spectrum to its right. The absorption spectrum of pyrene is shown for comparison directly above the fluorescence excitation spectrum. Notice, as expected from Eq. 4.38, the close

correspondence of the absorption spectrum and the excitation spectrum. Note, also, the relationship of the vibrational spectra of the $S_0 \rightarrow S_1$ absorption and the $S_1 \rightarrow S_0$ fluorescence. Compare this relationship to that shown in Fig. 4.9 for anthracene. Both anthracene and pyrene are examples of aromatic hydrocarbons whose absorption spectra are "mirror images" of the fluorescence spectrum. However, there is an important difference in the $S_0 + h\nu \rightarrow S_1$ transitions: the transition is allowed for anthracene ($\varepsilon_{max} \sim 100{,}000$ for the $S_0 + h\nu \rightarrow S_1$ transition) and is partially forbidden for pyrene ($\varepsilon_{max} \sim 500$, $S_0 \rightarrow S_1$ transition). Because the $S_0 + h\nu \rightarrow S_1$ transition is partially forbidden for pyrene, the $S_1 \rightarrow S_0 + h\nu$ fluorescence transition is also partially forbidden and relatively long lived. The energy gap between energy of the fluorescence transition is easily perturbed by the polarity of solvents.[18c] This sensitivity to solvent polarity makes pyrene fluorescence an excellent probe of the polarity of supramolecular media.

We have seen (Eq. 4.18) that the value of ε_{max} is proportional to the radiative rate of emission. Consequently, the rate constant of fluorescence from anthracene ($\sim 10^8\ s^{-1}$) is much faster than the rate constant for fluorescence of pyrene ($\sim 10^6\ s^{-1}$).

4.26 Order of Magnitude Estimates of Radiative Transition Parameters

By the term "spin-allowed electronic radiative transition," we mean any radiative transition that does not involve a change in spin multiplicity. For organic molecules, spin-allowed electronic radiative transitions are of two types: singlet–singlet and triplet–triplet transitions. Examples are $S_0 \rightarrow S_n$ or $T_1 \rightarrow T_n$ absorptions and $S_1 \rightarrow S_0$ or $T_2 \rightarrow T_1$ emissions.

The probability of spin-"allowed" transitions ranges over four orders of magnitude (Fig. 4.14 and Table 4.3). Thus, we must accept a wide range of "allowedness" in radiative transitions, even for spin-allowed radiative transitions. *We must understand that the terms "allowed" and "forbidden" are relative and not absolute.* We need to think of these terms as the *relative* probability, or rate of one type of process compared to another. It is important in making such comparisons that the processes being compared have similar mechanistic features (analogous forces that induce the transitions). For example, it is not proper to compare the allowed (or forbidden) character of a radiative transition (e.g., $S_1 \rightarrow S_0 + h\nu$) to the allowed (or forbidden) character of a radiationless transition (e.g., $S_1 \rightarrow S_0 +$ heat) since the former involves forces of interactions between the electrons of S_1 and the electromagnetic field and the latter involves forces of interactions between the electrons of S_1 and intramolecular and intermolecular vibrations. We can obtain some insight to the terms allowed and forbidden by considering the classical theory of the interaction of light with molecules, where the "allowedness" or strength of radiative transitions was measured by the oscillator strength (f). Order-of-magnitude estimations of f, ε, and k_e^0 can be made by use of the relationships given in Eq. 4.39.

$$f \propto \int \varepsilon d\nu \sim \varepsilon_{max} \Delta\bar{\nu}_{1/2} \quad \text{and} \quad f \propto k_e^0 (\bar{\nu}^2)^{-1} \tag{4.39}$$

Table 4.4 Some Representative Examples of ε_{max} and f Values for Prototype Transitions[a]

	$k_e(s^{-1})$	Example	Transition type	ε_{max}	f	$\nu_{max}(cm^{-1})$
	10^9	p-Terphenyl	$S_1(\pi,\pi^*) \rightarrow S_0$	3×10^4	1	30,000
Spin	10^8	Perylene	$S_1(\pi,\pi^*) \rightarrow S_0$	4×10^4	10^{-1}	22,850
Allowed	10^7	1,4-Dimethyl-benzene	$S_1(\pi,\pi^*) \rightarrow S_0$	7×10^2	10^{-2}	36,000
	10^6	Pyrene	$S_1(\pi,\pi^*) \rightarrow S_0$	5×10^2	10^{-3}	26,850
	10^5	Acetone	$S_1(n,\pi^*) \rightarrow S_0$	10	10^{-4}	~30,000
	10^4	Xanthone	$T_1(n,\pi^*) \rightarrow S_0$	1	10^{-5}	~15,000
	10^3	Acetone	$T_1(n,\pi^*) \rightarrow S_0$	10^{-1}	10^{-6}	~27,000
Spin	10^2	1-Bromonaph-thalene	$T_1(\pi,\pi^*) \rightarrow S_0$	10^{-2}	10^{-7}	20,000
Forbidden	10	1-Chloronaph-thalene	$T_1(\pi,\pi^*) \rightarrow S_0$	10^{-3}	10^{-8}	20,600
	10^{-1}	Naphthalene	$T_1(\pi,\pi^*) \rightarrow S_0$	10^{-4}	10^{-9}	21,300

a. These values represent orders of magnitude only.

For orders-of-magnitude estimates, we assume that $\Delta\bar{\nu}_{1/2}$, the one-half width of the absorption band (in units of cm^{-1}, called wavenumbers, $\bar{\nu}$, which are directly proportional to energy), is roughly constant for commonly encountered transitions, so that f is proportional to ε_{max} (Eq. 4.17). Thus, a qualitative relationship between the commonly measured experimental quantity ε_{max} and the theoretical quantity f is available. Table 4.4 lists some exemplars of this relationship. "Allowed" transitions ($f \sim 1$) correspond to values of ε_{max} on the order of 10^4–10^5 (exemplars, p-terphenyl and perylene). The strongest spin-"allowed" transitions possess $\varepsilon_{max} \sim 10$ (exemplar, acetone) and therefore correspond to $f \sim 10^{-4}$. Fig. 4.13 compares ε_{max} and f in terms of absorption spectra. Table 4.3 compares values of k_e^0, ε_{max}, and f. Importantly, the value of f is also related to the probability, or rate per unit time, of emission, k_e^0. The more probable the absorption (the larger the value of ε_{max}), the faster the related emission (the larger the value of k_e^0). For values of f close to 1, the fastest rates of emission are on the order of $10^9\ s^{-1}$ (exemplar, p-terphenyl).

For more quantitative comparisons of experiment with theory, we note that the relationship between f and k_e^0 (Eq. 4.27) depends on $\bar{\nu}^2$, the square of the *frequency* of the emission. Thus, the rate of emission depends not only on ε_{max} but also on the wavelength of emission, which determines the frequency of emission. For example (Table 4.4), while 1,4-dimethylbenzene and pyrene possess similar values of ε_{max} (ca. 500–700), they absorb and emit at very different wavelengths (1,4-dimethylbenzene at 277 nm and pyrene at 372 nm). As a result, 1,4-dimethylbenzene and pyrene possess quite different oscillator strengths, f, and values of k_e^0 for fluorescence. Similarly, perylene possesses a slightly larger ε_{max} than p-terphenyl, but the latter possesses a larger f because it possesses a larger $\bar{\nu}_{max}$ of the two compounds.

An important conclusion from the data in Table 4.4 is that *even for spin-allowed transitions, there are factors that cause a certain degree of forbiddenness to absorption and emission.* If we think of a perfectly allowed transition as having an oscillator strength $f_{max} = 1.0$, then we may think of an observed measured f_{obs} value in terms

of the product of the individual "forbiddenness factors" f_i, which *reduce* the value of f_{max} from that of the ideal system, Eq. 4.40:

$$f_{obs} = (f_e \times f_v \times f_s) f_{max} \tag{4.40}$$

where f_e is the prohibition due to electronic factors, f_v is the prohibition due to vibrational (Franck–Condon) factors, and f_s is the prohibition due to spin factors. For a spin-allowed transition, $f_s = 1$, and for a spin-forbidden transition, f_s depends on the spin–orbit coupling available during the transition (typical values of f_s range from 10^{-6}–10^{-11}).

The electronic factor f_e may be subclassified in terms of different kinds of forbiddenness:

1. *Overlap* forbiddenness, which results from poor spatial overlap of the orbitals involved in the HO → LU electronic transition. An exemplar is the n,π^* transition in ketones (Section 2.11), for which the HO and LU are orthogonal to one another in zero-order and the overlap integral $<n|\pi^*>$ is close to zero.
2. *Orbital symmetry* forbiddenness, which results from orbital wave functions (involved in the transition) that overlap in space but have their overlap integral canceled because of the symmetry of the wave functions. Examples are the $S_0 + h\nu \rightarrow S_1(\pi,\pi^*)$ and $S_1(\pi,\pi^*) \rightarrow S_0 + h\nu$ transitions in benzene, naphthalene, and pyrene. Inspection of the details of the phases of HO and LU for these transitions beyond the scope of this text is required for an understanding of orbital forbiddenness. However, some insight is available from classical theory. In order to produce a transition electric dipole moment, the oscillating electric field of the light wave needs to drive an electron back and forth along a molecular axis; that is, a transition oscillating dipole must result from the interaction of the electromagnetic field and the electron. To a good approximation, we need consider only the HO → LU transition as determining the transition dipole along the molecular axis. For molecules possessing high symmetry, quite often for the HO → LU transition, there is no good axis along which a significant transition dipole can be generated. Benzene and pyrene, for example, are very symmetrical molecules for which f is $\sim 10^{-3}$. For *p*-terphenyl, however, a favorable axis exists along the 1,4-positions of the three benzene rings, and $f \sim 1$.

Generally, for *spin-allowed* transitions the electronic factor f_e is the major factor in the determination of the observed values of f. From Table 4.4, note that perylene and *p*-terphenyl possess "strong" $S_0 \rightarrow S_1$ absorptions ($f \sim 1$–10^{-1}, $\varepsilon_{max} \sim 10^5$–$10^4$). These absorptions essentially correspond to fully allowed ($\pi \rightarrow \pi^*$) transitions. For pyrene (and for benzene and naphthalene), the $S_0 \rightarrow S_1(\pi,\pi^*)$ transition is *orbital symmetry forbidden*, and an electronic "forbiddenness factor" of $f_e \sim 10^2$–10^{-3} results in a relatively weak ε_{max} of $\sim 10^2$. For acetone, the $S_0 \rightarrow S_1$ transition corresponds to an $n \rightarrow \pi^*$ transition. This transition is *forbidden by* both *orbital overlap and symmetry* and would be predicted to have $f \sim 0$ if the n orbital were a pure p orbital, and if the molecules were strictly planar. Experimentally, $\varepsilon_{max} \sim 10$ for this $n \rightarrow \pi^*$ transition as the result of vibronic mixing of the n and π^* orbitals.

Let us see how vibronic mixing operates. Out-of-plane vibrations (Fig. 3.1) allow the n orbital to pick up s "character." In the case of benzophenone, "mixing" of the n,π^* state with nearby π,π^* states makes S_1 a hybrid of these two transition types (Eq. 3.9). As a result, the $S_0 \rightarrow S_1$ transition, which is an overlap forbidden n,π^* transition in zero order, picks up finite oscillator strength because of the π,π^* character "mixed" into S_1 (Eqs. 4.31 and 4.35). In a manner of speaking, the S_1 state picks up absorption intensity from its acquired π,π^* character. In the case of acetone, S_1 is more nearly "pure" n,π^* because of the poorer mixing (ΔE *is much larger in the denominator of Eq. 4.35*), and the absorption intensity is correspondingly lower.

Because of the direct relationship between f and the fluorescence rate constant k_F^0, (Eq. 4.27, $k_e^0 = k_F^0$), the factors determining the magnitude of f automatically are proportional to those determining k_F^0. This approximation is a good one for allowed transitions if we can ignore f_v (i.e., rigid molecules) as a major factor determining the value of f or k_F^0. If the nuclear geometry of the equilibrated excited state is very different from that of the initial ground state, then the value of k_F^0 for the $S_1 \rightarrow S_0$ transition will be determined by f_e and by different Franck–Condon factors (see Section 4.22) that relate to f for the $S_0 \rightarrow S_1$ transition. In the special cases for which the equilibrium geometry and predominant vibrational progressions of S_0 and S_1 are similar, a "mirror-image" relationship is sometimes observed for the absorption and related emission spectra (see Figs. 4.9 and 4.15); that is, $S_0 \rightarrow S_1$ "mirrors" $S_1 \rightarrow S_0$ and $S_0 \rightarrow T_1$ "mirrors" $T_1 \rightarrow S_0$.

Based on information from absorption spectra, an orbital configuration may be assigned to the electronic transition responsible for an absorption band. For anthracene, benzene, pyrene, and other aromatic hydrocarbons, the entire π system can be assumed to behave approximately as a single chromophore since the molecular orbitals are delocalized over the molecular framework and only $\pi \rightarrow \pi^*$ transitions are energetically feasible in the 200–700-nm region. For benzophenone and aromatic carbonyl compounds, both $n \rightarrow \pi^*$ (longer wavelength) and $\pi \rightarrow \pi^*$ (shorter wavelength) transitions are possible. Empirically, a number of criteria have been developed that allow an orbital configuration change to be identified from characteristics of absorption and emission spectra; these criteria are presented in Table 4.5.

Consider Fig. 4.16a to be an example for the use of information in Table 4.5 to identify the orbitals involved in radiative transitions that display the spin-allowed absorption spectrum of benzophenone; this spectrum in cyclohexane consists of two major absorption bands, one maximizing at ~ 350 nm and the other maximizing at ~ 250 nm. Note that the n,π^* absorption of a rigid cyclanone (Fig. 4.16b) occurs in a similar wavelength region to that for benzophenone. The relatively low value of ε_{max} (~ 100) for the longer-wavelength band of benzophenone and the wavelength of the maximum allows assignment of an orbitally and spatially forbidden $n \rightarrow \pi^*$ transition to the long wavelength band (see Table 4.5). This assignment is consistent with the "blue shift" of the maximum upon going from cyclohexane to ethanol, since the energy gap between the n and π^* orbitals is expected to be larger (therefore absorption occurs at shorter wavelengths) in ethanol than in cyclohexane. The reason is because

Table 4.5 Empirical Criteria for the Assignment of Orbital Configurations of Ketones

Property	n–π^*		π–π^*	
	$S_0 \rightarrow S_1$	$S_0 \rightarrow T_1$	$S_0 \rightarrow S_1$	$S_0 \rightarrow T_1$
ε_{max}	<200	$>10^{-2}$	>1000	$<10^{-3}$
$k_e(s^{-1})$	10^5–10^6	10^3–10^2	10^7–10^8	1–10^{-1}
Solvent shift	Shorter wavelengths with increasing solvent polarity		Longer wavelengths with increasing solvent polarity	
Vibrational structure	Localized vibrations		Delocalized vibrations	
Heavy atom effect	None		Increases probability of all S → T transitions	
ΔE_{ST}	Small (< 10 kcal mol^{-1})		Large (> 20 kcal mol^{-1})	
Polarization of transition moment	Perpendicular to molecular plane	Parallel to molecular plane	Parallel to molecular plane	Perpendicular to molecular plane
$\Phi_e^{77\,K}$	< 0.01	~0.5	1.0–0.05	< 0.5
E_T	< 75	< 65	Variable	

hydrogen bonding stabilizes the n orbital in S_0 and destabilizes the π^* orbital in S_1. The destabilization of the π^* orbital results from the Franck–Condon excitation of an n electron into a π^* orbital. The ethanol solvent molecules do not have time to reorient during the time scale of the electron orbital jump. As a result, the solvent dipoles are oriented about the carbonyl oxygen atom with their positive ends (hydrogen bonds) pointing toward the oxygen. Immediately after the electron jump occurs, the n orbital is half-filled and is much more electronegative than it was in the ground state. The solvent dipoles are in an unfavorable spatial distribution about the oxygen atom, and this corresponds to an energy increase in the energy of the π^* orbital and a higher energy required for the n → π^* transition in ethanol relative to cyclohexane.

To the photochemist, an idea of the limiting values of k_F^0 is important to calibrate the maximum time allowed for reaction in S_1, because if a reaction from S_1 is to occur efficiently, its rate must be competitive with k_F^0. Otherwise, fluorescence will dominate as a decay pathway for S_0. In terms of numerical benchmarks, note from Table 4.4 that, among organic molecules, a benchmark for the "world's record" for the largest k_F^0 is $\sim 10^9\ s^{-1}$ for *p*-terphenyl (a fully allowed $\pi \rightarrow \pi^*$ transition) and the benchmark for the "world's record" for the smallest k_F^0 is $\sim 10^5\ s^{-1}$ for acetone (a weakly allowed n → π^* transition). These calibration points put the limits on the range of lifetimes limited by the rate of fluorescence in the range of 10^{-9}–10^{-5} s and provide two useful rules for calibration: If an electronically excited organic molecule possesses a lifetime shorter than 10^{-9} s, its lifetime is limited not by fluorescence but by some photophysical or photochemical radiationless process. If an electronically excited organic molecule possesses a lifetime longer than 10^{-5} s, it cannot be a singlet state.

As benchmarks for spin–forbidden transitions, the largest value of the phosphorescence rate constant k_P^0 is on the order of $10^3\ s^{-1}$ (lifetime 10^{-3} s), and the smallest

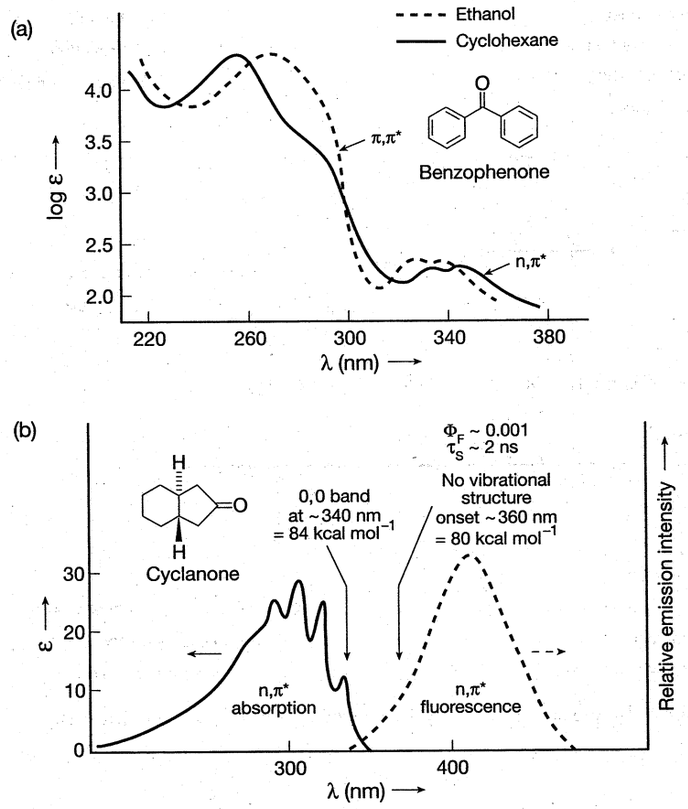

Figure 4.16 (a) Absorption spectrum of benzophenone in ethanol (dashed line) and cyclohexane (solid line). (b) Absorption and emission spectrum of a cyclanone.

value of k_P^0 is on the order of $10^{-1}\ s^{-1}$ (lifetime 10 s). Thus, $^*R(T_1)$ will persist many orders of magnitude longer than $^*R(S_1)$ before emitting a photon. This long-lifetime characteristic of triplets has important implications concerning their photochemistry.

4.27 Quantum Yields for Emission (*R → R + hν)

The rate constants of photophysical and photochemical processes from $^*R(S_1)$ and $^*R(T_1)$ determine the efficiencies of the processes that occur from these electronically excited states. The quantum yield (Φ) is an efficiency parameter measuring the fraction of absorbed photons that produces a specific sequence shown in the paradigm of organic photochemistry (Scheme 2.1). The parameter Φ may be expressed in

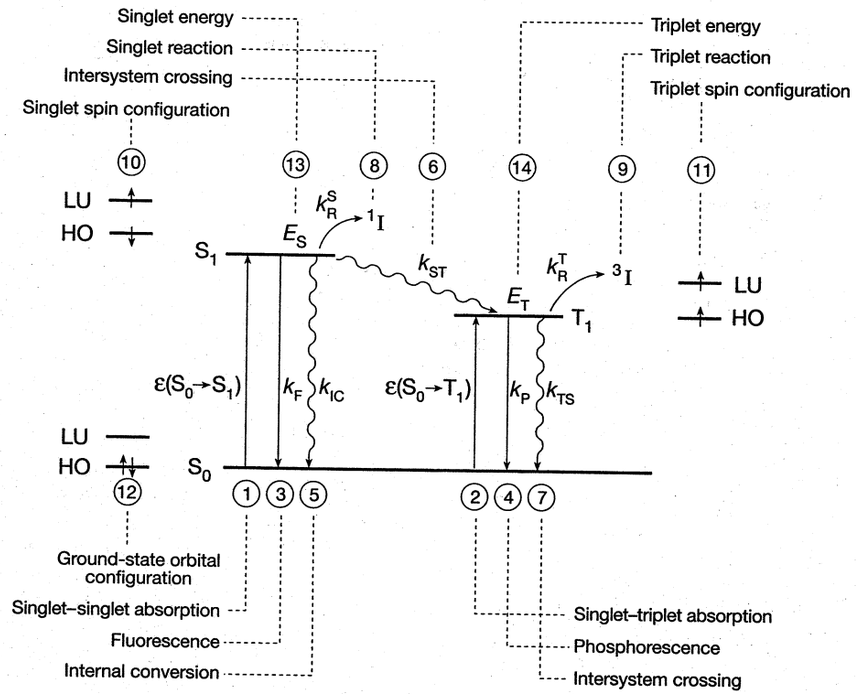

Figure 4.17 The exemplar state energy diagram for molecular organic photochemistry.

molar terms (the number of moles of *R that proceed along a particular pathway in Scheme 2.1 relative to the number of moles of photons absorbed by R) or in kinetic terms (the rate of a pathway of interest from *R compared to the sum of the rates of all pathways for decay of *R). The state energy diagram (Fig. 4.17) serves as a convenient paradigm for bookkeeping of the state electronic configurations, rates radiative and radiationless transitions, energies, and efficiencies of radiative and radiationless photophysical processes. Note that the state energy diagram refers to a nuclear geometry that is very close to the equilibrium geometry of the ground state. In Chapter 6, we discuss an extension of the state energy diagram, namely, the state correlation diagram showing the way the states of R and *R correlate with I and F during photochemical reactions.

The absolute quantum yield of emission for an organic molecule upon absorption of light (Φ_e) is an important experimental parameter containing useful information relating the structure and dynamics of electronically excited states. In addition, emission from organic molecules has become a valuable tool in analytical chemistry and modern photonics in the development of light-operated switches and sensors. Examples of the total (fluorescence and phosphorescence) emission spectra of different types

of organic molecules are given in Figs. 4.18–4.21 for exemplar aromatic lumophores (π,π^* emission) and the ketone lumophore (n,π^* emission).

We noted a number of times that the paradigm for analyzing emission of organic molecules is Kasha's rule,[17] which states that, upon photoexcitation of an organic molecule, only fluorescence from an (thermally equilibrated) S_1 state or phosphorescence from a (thermally equilibrated) T_1 state is observed experimentally. Whether any emission is observed at all from S_1 or T_1 for an organic molecule is determined by the experimental quantum yield for emission (Φ_F for fluorescence and Φ_P for phosphorescence). The value of Φ is a direct and absolute measure of the efficiency of an emission process and is defined as photons out (emitted) versus photons in (absorbed). Although all excited states emit a finite number of photons *in principle*, it is found *in practice* that quantum yields of $< 10^{-5}$ are difficult to measure experimentally and are prone to experimental artifacts. Thus, for practical purposes a molecule is considered to be (measurably) fluorescent or (measurably) phosphorescent if the quantum yield for emission, Φ_e, is $> 10^{-5}$.

A general expression for a quantum yield of emission Φ_e from a specific state, $^*R(S_1)$ or $^*R(T_1)$, is given by Eq. 4.41:

$$\Phi_e = {}^*\Phi k_e^0 (k_e^0 + \Sigma k_i)^{-1} = {}^*\Phi k_e^0 \tau \tag{4.41}$$

where $^*\Phi$ is the formation efficiency of the emitting state, k_e^0 is the rate constant (k_F^0 or k_P^0) for emission from the state, and Σk_i is the sum of all rate constants (unimolecular or pseudo-unimolecular) that radiationlessly deactivate the emitting state; that is, $\tau = (k_e^0 + \Sigma k_i)^{-1}$. The experimental lifetime (τ), and therefore the experimental quantum yield of emission, Φ_e, depend crucially on the magnitude of Σk_i relative to the value of k_e^0. The latter does not usually change very much with experimental conditions, but Σk_i can vary by many orders of magnitude depending on experimental conditions.

For example, in fluid solution at room temperature, bimolecular, diffusional quenching processes (oxygen is a ubiquitous and efficient quencher of electronically excited states), photophysical radiationless deactivations, and photochemical reactions may compete with radiative decay of an excited state (see the state-energy diagram, Fig. 4.17). Thus, Φ_e may be very small *even* if $^*\Phi$ is close to unity.

Thus, in order to observe an electronic emission spectrum routinely, it is usually necessary to minimize Σk_i. This is accomplished by cooling the sample to a very low temperature (77 K, the boiling point of liquid nitrogen, is an experimentally convenient temperature) and/or by making the sample a rigid solid, such as a polymer (all organic solvents are solids at 77 K). Numerous solvents form optically clear solid solutions at 77 K and are called *glasses* at this temperature. The low temperature and sample rigidity cause terms in Σk_i that correspond to the rate constants of processes activated by several kilocalories per mole or more to become small relative to k_e^0. The rigidity of the sample also eliminates terms in Σk_i that are due to bimolecular quenching processes, since diffusion is eliminated in solid solution. In addition to preventing diffusional quenching, a rigid solvent matrix may restrict certain molecular motions (e.g., twisting of C=C bonds or extensive stretching of C—C bonds), which

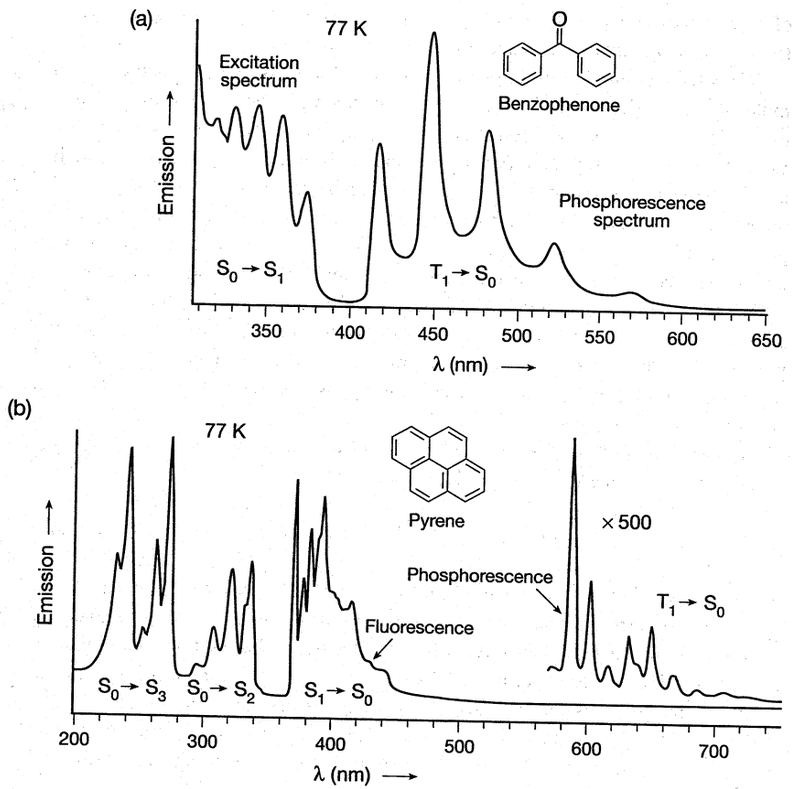

Figure 4.18 Emission spectrum of benzophenone and pyrene at 77 K of (a) benzophenone and (b) pyrene as exemplars for ketones and aromatic compounds. The spectrum of 1-chloronaphthalene (c, opposite) is shown as an exemplar of the heavy atom effect.

are particularly effective at promoting physical and chemical radiationless transitions. Thus, taking an emission spectrum at 77 K usually "quenches" many processes that compete with emission from *R, allowing the quantum yield for emission to reach a value that can be measured experimentally.

Even when fluorescence and phosphorescence spectra of organic molecules are measured at 77 K in organic glasses, the total quantum yields of emission ($\Phi_F + \Phi_P$) are generally < 1.00. Evidently, some radiationless processes from S_1 occur even at 77 K in rigid glasses, as shown in Eq. 4.42.

$$\Phi_F + \Phi_P + \Sigma\Phi_R = 1 \tag{4.42}$$

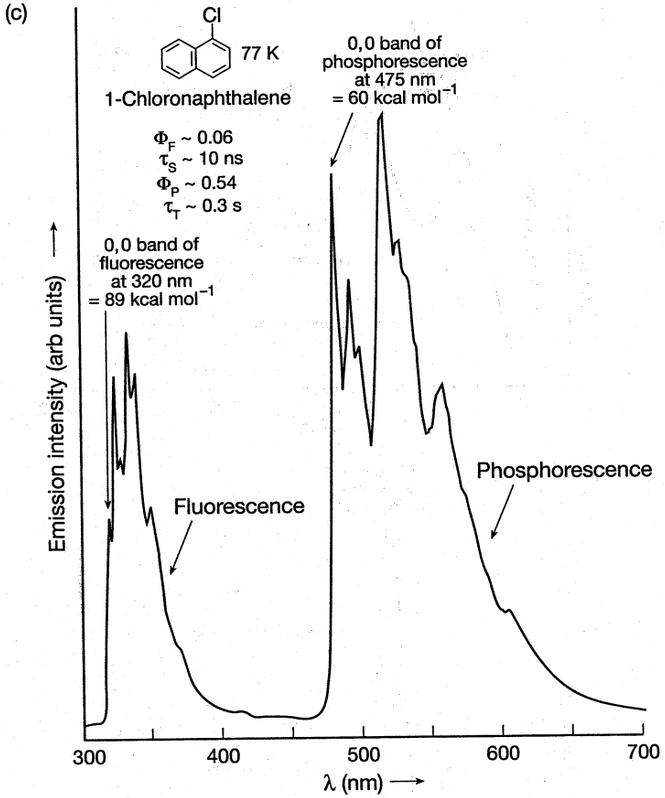

Figure 4.18 *(continued)*

In Eq. 4.42, $\Sigma\Phi_R$ is the sum of quantum yields for photochemical and photophysical radiationless transitions from S_1 and T_1. Identification and evaluation of the radiationless photophysical processes of Φ_R will be discussed in Chapter 5, and the photochemical sources will be discussed in Chapter 6. For our purposes, here we note simply that radiationless processes can compete with k_F for deactivation of S_1 and with k_P for deactivation of T_1, even at 77 K.

Data derived from *fluorescence* spectra at 77 K are conveniently analyzed and interpreted in terms of Eq. 4.43, which is a specific form of Eq. 4.42 ($^*\Phi = 1.00$, since the emitting state is the absorbing state, $k_e = k_F$ and $\Sigma k_i = k_{ST}$).

$$\Phi_F = k_F(k_F + k_{ST})^{-1} = k_F\tau_s \tag{4.43}$$

where τ_S is defined as $(k_F + k_{ST})^{-1}$.

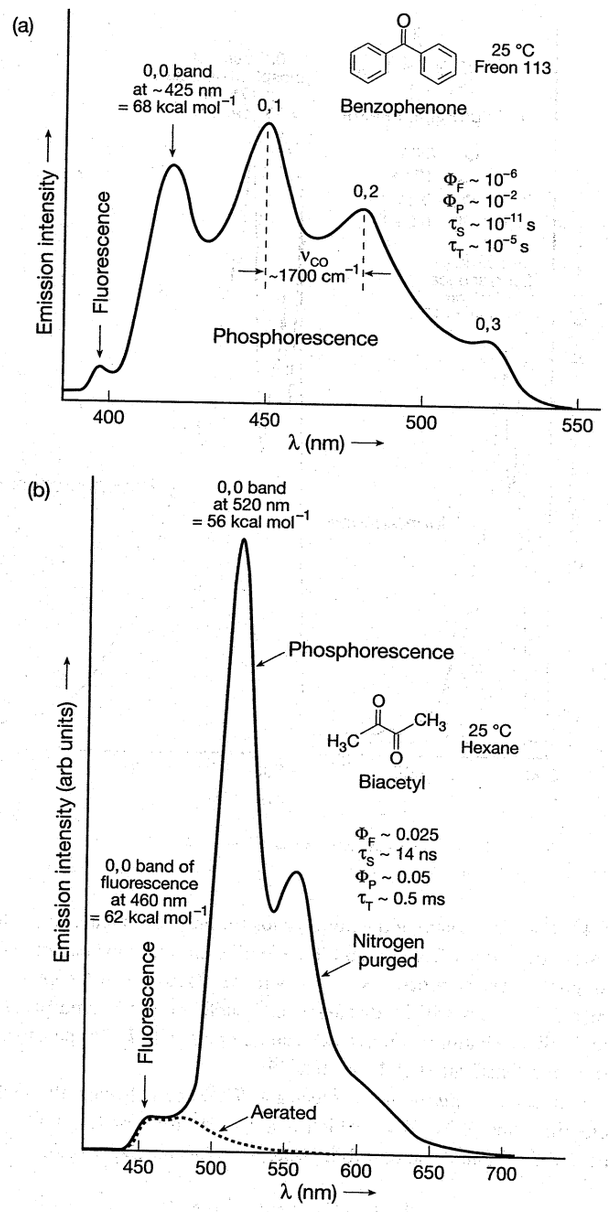

Figure 4.19 Emission spectra of (a) benzophenone in freon113 solvent, (b) biacetyl in hexane solvent, and (c, opposite) 1,4-dibromonaphthalene in acetonitrile solvent at room temperature.

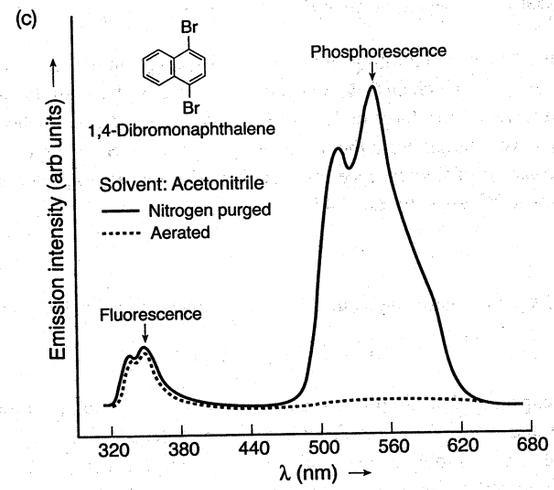

Figure 4.19 *(continued)*

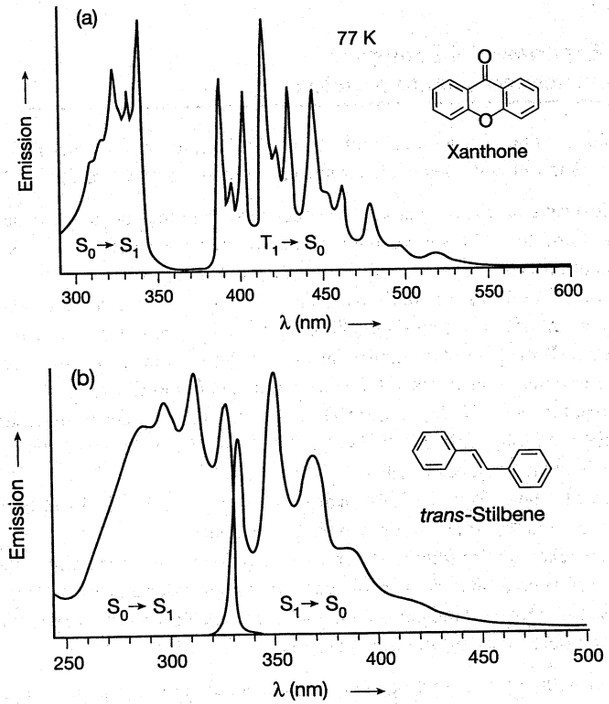

Figure 4.20 Emission spectra (77 K) of (a) xanthone and (b) *trans*-stilbene as exemplars for substituent effects.

Equation 4.43 has two limiting situations: (a) $k_F \gg k_{ST}$, in which case $\Phi_F \sim 1.00$, and (b) $k_{ST} \gg k_F$, in which case $\Phi_F = k_F/k_{ST}$. In terms of these limits, note that Φ_F will $\rightarrow 1$ when k_F is very large or k_{ST} is very small. Also, $\Phi_F \rightarrow 0$ when k_F is very small or k_{ST} is very large. From the limits of ε_{max} for $S_0 \rightarrow S_1$ absorption, the limits of the rate constant of fluorescence for organic molecules are expected to be in the range (Section 4.26) given by Eq. 4.44.

$$10^9\ s^{-1} > k_F > 10^5\ s^{-1} \tag{4.44}$$

The limits of k_{ST} for organic molecules from experiment (Section 4.31) turn out to be

$$10^{11}\ s^{-1} > k_{ST} > 10^5\ s^{-1} \tag{4.45}$$

Thus, it is expected that simply upon consideration of the competition between fluorescence and intersystem crossing from S_1, the value Φ_F can vary over orders of magnitude. For example, in one limiting case the fluorescence is intense and easy to observe; in the other limiting case the fluorescence may be either intense or weak or nonobservable, depending on the values of *both* k_F and k_{ST}.

4.28 Experimental Examples of Fluorescence Quantum Yields

Some data for fluorescence quantum yields (77 K, rigid organic glass) are given in Table 4.6. The following generalizations may be made from the data:

1. Most rigid aromatic hydrocarbons (benzene, naphthalene, anthracene, pyrene, etc.) and their derivatives possess measurable, but variable, fluorescence quantum yields ($1 > \Phi_F > 0.01$), even at 77 K.
2. Low values of Φ_F for nonrigid aromatic hydrocarbons are common and usually the result of competing internal conversion ($S_1 \rightarrow S_0$) or intersystem crossing ($S_1 \rightarrow T_1$) triggered by molecular motion. Spin-allowed and spin-forbidden radiationless transitions will be discussed in detail in Chapter 5.
3. Substitution of Cl, Br, or I, for H on an aromatic ring generally results in a decrease in Φ_F such that $\Phi_F^H > \Phi_F^F > \Phi_F^{Cl} > \Phi_F^{Br} > \Phi_F^I$ (cf. naphthalene with the halonaphthalenes in Table 4.6).
4. Substitution of C=O for H on an aromatic ring generally results in a substantial decrease in Φ_F (cf. benzene with benzophenone).
5. Molecular rigidity (due to structural or environmental constraints) enhances Φ_F (cf. rigid aromatics with stilbene, which possesses a flexible C=C bond).
6. For rigid aromatic molecules, internal conversion does not compete favorably with fluorescence or intersystem crossing.

Starting with aromatic hydrocarbons, which generally possess the highest values of Φ_F, now let us determine how specific values of k_F and k_{ST} contrive to make the value of Φ_F so variable.

For benzene, naphthalene, and pyrene, the $S_0 \rightarrow S_1$ transitions are "orbital symmetry forbidden." These molecules are sufficiently symmetrical that the electric vector

Table 4.6 Some Examples of Fluorescence Quantum Yields and Other Emission Parameters[a]

Compound	Φ_F^a	ε_{max}	k_F^0	k_{ST}	Configuration of S_1
Benzene	~0.2	250	2×10^6	10^7	π,π^*
Naphthalene	~0.2	270	2×10^6	5×10^6	π,π^*
Anthracene	~0.4	8,500	5×10^7	$\sim 5 \times 10^7$	π,π^*
Tetracene	~0.2	14,000	2×10^7	$<10^8$	π,π^*
9,10-Diphenylanthracene	~1.0	12,600	$\sim 5 \times 10^8$	$<10^7$	π,π^*
Pyrene	~0.7	510	$\sim 10^6$	$<10^5$	π,π^*
Triphenylene	~0.1	355	$\sim 2 \times 10^6$	$\sim 10^7$	π,π^*
Perylene	~1.0	39,500	$\sim 10^8$	$<10^7$	π,π^*
Stilbene[b]	~0.05	24,000	$\sim 10^8$	$\sim 10^9$	π,π^*
1-Chloronaphthalene	~0.05	~300	$\sim 10^6$	5×10^8	π,π^*
1-Bromonaphthalene	~0.002	~300	$\sim 10^6$	$\sim 10^9$	π,π^*
1-Iodonaphthalene	~0.000	~300	$\sim 10^6$	$\sim 10^{10}$	π,π^*
Benzophenone	~0.000	~200	$\sim 10^6$	$\sim 10^{11}$	n,π^*
Biacetyl	~0.002	~20	$\sim 10^5$	$\sim 10^8$	n,π^*
Diaza[2.2.2]bicyclooctene	~1.0	~200	$\sim 10^6$	$<10^5$	n,π^*
Acetone	~0.001	~20	$\sim 10^5$	$\sim 10^9$	n,π^*
Perfluoroacetone	~0.1	~20	$\sim 10^5$	$\sim 10^7$	n,π^*
3-Bromoperylene	~1.0	~40,000	$\sim 10^8$	$<10^6$	π,π^*
Pyrene-3-carboxaldehyde	~0.25	~70,000	$\sim 10^8$	$\sim 10^8$	π,π^*
Cyclobutanone	~0.0001	~20	$\sim 10^5$	$\sim 10^9$	n,π^*
Diaza[2.2.1]bicycloheptene	~0.0001	400	$\sim 10^6$	$\sim 10^6$	n,π^*

a. ε_{max} in $M^{-1}cm^{-1}$; k_F^0 and k_{ST} in s^{-1}.

of the light cannot easily find an effective axis along which to oscillate an electron and generate a significant transition dipole. Therefore, these molecules have a relatively low oscillator strength, f, and a relatively low value of ε_{max}. Consequently, for these hydrocarbons, $\varepsilon_{max} \sim 10^2$ and $k_F \sim 10^6\ s^{-1}$. The latter value of k_F is close to the smallest for organic molecules. However, the rate of intersystem crossing from $S_1 \rightarrow T_1$ for aromatic hydrocarbons is also on the order of $\sim 10^6\ s^{-1}$ for both benzene and naphthalene and is somewhat slower for pyrene. Thus, benzene, naphthalene, and pyrene all fluoresce with a moderate quantum yield $\Phi_F > 0.20$. The S_1 molecules that do not fluoresce generally undergo intersystem crossing to T_1 (i.e., $\Phi_{ST} \sim 1.0$).

For anthracene, the $S_0 \rightarrow S_1$ transition is symmetry allowed (the electric vector of light now easily recognizes the long or the short axis of anthracene as an excellent axis for induction of electron oscillation). As a result, $\varepsilon_{max} \sim 10^4$ and $k_F \sim 10^8\ s^{-1}$. In the case of diphenylanthracene, $\Phi_F \sim 1.0$; that is, essentially every excited singlet state formed fluoresces. In this case, a large value of k_F and small values of k_{ST} (poor spin–orbit coupling) and k_{IC} (large energy gap between S_1 and S_0) contibute to produce a value of Φ_F that is close to unity.

Now, consider the decrease in Φ_F that generally accompanies the replacement of H with halogen or C=O functions. The small value of Φ_F (within the framework of

our assumption of negligible internal conversion) means that intersystem crossing is much faster than fluorescence for these molecules; that is, $k_{ST} \gg k_F$. For halogenated naphthalenes, the substitution of halogen for hydrogen affects ε_{max} by a factor of only ~2, whereas Φ_F varies over several orders of magnitude. From the constancy of ε_{max}, we conclude that k_F^0 does not vary much in this series, so that k_{ST} must be the changing variable leading to the radical variation in Φ_F. The enhancement of probability of spin–forbidden transitions that result from the replacement of hydrogen by halogen is known as the "heavy-atom effect," where a "light" atom is defined as any atom in the first two rows of the periodic table (e.g., H, C, N, O, F) and a "heavy" atom is defined as any atom beyond the third row of the periodic table (e.g., Cl, Br, I). The theoretical basis of this effect is due to enhanced spin–orbit coupling induced by heavy atoms (discussed in Section 3.21).

Aromatic ketones (e.g., acetophenone and benzophenone) do not possess heavy atoms, yet generally possess a very small value of Φ_F, implying a relatively fast intersystem crossing compared to the rate of fluorescence. This low value of Φ_F ($\Phi_F \sim$ 0.01–0.0001) is a general feature of the emission of ketones possessing S_1 (n,π^*) states (Figs. 4.18–4.21 and Table 4.6). Since the radiative rate of the orbital symmetry forbidden transition $S_1(n,\pi^*) \rightarrow S_0 + h\nu$ fluorescence is relatively slow ($\sim 10^5\ s^{-1}$ from Table 4.6), the magnitude of k_{ST} need not be much larger than it is for aromatic hydrocarbons. Strikingly however, values of k_{ST} may reach values of $10^{11}\ s^{-1}$ for certain ketones (e.g., benzophenone), implying a very enhanced value of k_{ST} relative to aromatic hydrocarbons (for an explanation of this effect see Section 4.31). Thus, a small value of k_F and a large value of k_{ST} combine to make Φ_F very small for aromatic ketones.

In a few special cases (e.g., unstrained cyclic azoalkanes) a relatively small value of k_F is accompanied by an even smaller value of k_{ST}, so that Φ_F is still ~ 1.0.

The general rule that Φ_F is small for halogenated compounds and carbonyl compounds has exceptions, which are informative to analyze. From Table 4.6, bromoperylene ($\Phi_F \sim 1.0$) and pyrene-3-aldehydes ($\Phi_F \sim 0.70$) are examples. A large energy gap between S_1 and any other T_n states produces a Franck–Condon inhibition to direct $S_1 \rightarrow T_n$ intersystem crossing (Section 4.30), so that the occurrence of a second triplet (usually T_2) that is of lower energy than S_1 is required for state mixing and fast intersystem crossing. In bromoperylene and pyrene-3-aldehyde, k_{ST} is exceptionally slow in spite of the attachment of a bromine atom or an aldehyde function to the aromatic ring, because T_2 lies well above S_1, and state mixing is inhibited.

Anthracene presents an interesting case for which T_2 has an energy that is very close to the energy of S_1. The energy is so close that T_2 may possess a higher energy than S_1 or a lower energy than S_1 depending on the solvent or substitutents. When $^*E(T_2) > E(S_1)$, intersystem crossing is slow and the fluorescence yield is high; when $^*E(T_2) < E(S_1)$, the intersystem crossing rate is fast and the fluorescence yield is low. The effect of the position of T_2 relative to S_1 will be discussed in Chapter 5.

In addition to a competing fast intersystem crossing, Φ_F may be small for molecules that undergo a very fast photochemical reaction in S_1. For example, cyclobutanone ($\Phi_F \sim 0.0001$) undergoes an efficient very fast cleavage of a CO–C bond in S_1 that competes effectively with *both* fluorescence and intersystem crossing.

The lesson to be learned from these examples is that the experimental value of Φ_F represents an *efficiency* that compares *relative* transition *probabilities* and does *not* relate directly to *rates or rate constants*; that is, $\Phi_F \sim 1.0$ for 9,10-diphenylanthracene, for which $k_F \sim 5 \times 10^8\ s^{-1}$, and $\Phi_F \sim 1.0$ for diaza[2.2.2]bicyclooctane, for which $k_F \sim 10^6\ s^{-1}$. In the latter case, Φ_F is high in spite of a low value of k_F because both photophysical or photochemical processes from S_1 are much slower than k_F.

Note that bimolecular quenching processes (oxygen, impurities, solvent, etc.), which are not related to the molecular structure of the fluorescing molecule, may determine the observed value of Φ_F in fluid solution, especially for molecules possessing a long S_1 lifetime.

Saturated compounds[19a,b] and simple alkenes, such as ethylenes[19c] and polyenes,[20] generally do not fluoresce efficiently. For example, tetramethylethylene shows a very broad weak fluorescence ($\lambda_{max}^F \sim 265$ nm), with $\Phi_F \sim 10^{-4}$ and $\tau_S \sim 10^{-11}$ s. Such short lifetimes and low emission efficiencies are typical of "flexible" molecules for which a rapid radiationless deactivation may occur via a stretching motion along a C—C (or C—H) bond or via a twisting motion about a C=C bond.[21] The role of stretching and twisting motions in determining the rates of photophysical radiationless deactivations will be discussed in detail in Chapter 5.

As exemplars of the role of stretching motions in determining Φ_F, consider[22] the aromatic hydrocarbons toluene (**1**) and tert-butyl benzene (**2**). The latter possesses a "looser" side-chain vibration and a lower value of Φ_F than the former. The dissipation of electronic energy through coupling to "loose" stretching vibrational modes has been termed the "loose-bolt effect" of radiationless transitions (see further discussion in Section 5.12).

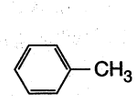

Toluene (**1**)
$\Phi_F = 0.14$

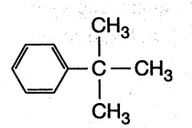

tert-Butyl benzene (**2**)
$\Phi_F = 0.032$

For the role of twisting motions in determining Φ_F, consider the flexible stilbenes **3**[23a] and **4**[23b] and their rigid cyclic derivatives **5** and **6**[23c,d], which provide a nice exemplar of how either molecular structure or environmental rigidity may control the measured values of Φ_F:

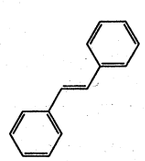

3
trans-Stilbene

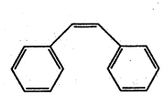

4
cis-Stilbene

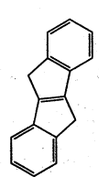

5

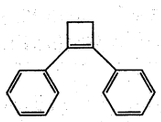

6

Temperature	*trans*-Stilbene **3**	*cis*-Stilbene **4**	**5**	**6**
25 °C	0.05	0.00	1.0	1.0
77 K	0.75	0.75	1.0	1.0

Although *trans*-stilbene (**3**) is only weakly fluorescent ($\Phi_F = 0.05$) and *cis*-stilbene (**4**) is essentially nonfluorescent in fluid solution at room temperature, in a solid solution at 77 K, *both compounds are strongly fluorescent* ($\Phi_F \sim 0.75$). Both temperature and environmental rigidity contribute to this enhancement of fluorescence. For example,[23] the fluorescence efficiency of (**3**) increases by a factor of 3 in going from nonviscous organic solvents ($\Phi_F \sim 0.05$) to viscous glycerol ($\Phi_F \sim 0.15$). Presumably, twisting about the C=C bond induces the radiationless process that competes with fluorescence, and the ability to twist is inhibited in the more viscous solvent and entirely inhibited in rigid solvents. In contrast, the fluorescence yields[23c,d] of the structurally rigid stilbene analogues **5** and **6** are ~1.0 at both 25 °C and 77 K. Here, rigidity is built into the molecular structure, and inhibition of the twisting motion does not require assistance from the external environmental structure or temperature. The dissipation of electronic energy through coupling to "loose" twisting vibrational modes has been termed the "free rotor effect" of radiationless transitions (Section 5.12).

Most ethylenes and polyenes do not display fluorescence or phosphorescence even at 77 K. In several exceptional cases,[20] structured fluorescence emission has been reported from polyenes for which both loose stretching and twisting modes are inhibited by cyclic molecular structures. For example, the rigid 1,3-dienes **7a** and **7b** steroidal compounds sufficiently show structured fluorescence emission. Presumably, structural rigidity of the steroid framework enhances the efficiency of light by inhibiting radiationless processes (especially internal conversion) that compete with fluorescence, and by enhancing k_F by preventing a large Franck–Condon geometry difference between S_1 and S_0 (see Fig. 3.2), as well as by inhibiting a free rotor effect about C=C bonds.

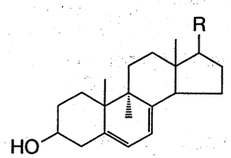

7a
$\lambda_F^{0,0} = 305$ nm
$E_S \sim 95$ kcal mol^{-1}

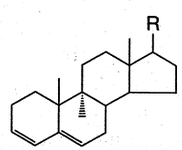

7b
$\lambda_F^{0,0} = 312$ nm
$E_S \sim 92$ kcal mol^{-1}

4.29 Determination of "State Energies" E_S and E_T from Emission Spectra

The electronic energy of *R is an important property since it can be used as free energy to drive photochemical reactions. For example, the higher the energy of *R, the stronger the bonds that can be broken in a primary photochemical process. The electronic energy of *R may be determined *directly* from its emission spectrum. The *highest*-energy (highest frequency, shortest wavelength) vibrational band in an emission spectrum corresponds to the 0,0 transition (Fig. 4.9). The energy gap corresponding to this 0,0 transition characterizes the energy of the excited state, *R, which is responsible for the emission. The energy gap of a 0,0 transition is the *maximum* energy derivable from the excited state if S_0 is regenerated by emission of a photon. The singlet-state energy (E_S) and the triplet-state energy (E_T) are defined as the 0,0 energy gap for fluorescence, S_1 ($v = 0$) → S_0($v = 0$), and phosphorescence, T_1($v = 0$) → S_0($v = 0$), respectively.

Sometimes an emission spectrum does not show sufficiently resolved fine structure for an accurate estimate of E_S of E_T to be made from emission spectra. In this case, the "onset" or the high-energy (short-wavelength portion) of the emission spectrum must be used to estimate the upper limit of E_S or E_T. If vibrational structure appears in the absorption spectrum, the 0,0 band of absorption serves as a safe guide for an upper limit to state energies, even if the emission spectrum is not available. In Figures 4.18–4.21, the 0,0 bands of fluorescence and/or phosphorescence are noted with an arrow, and the values of E_S or E_T derived from the 0,0 vibrational band are given in the associated energy diagrams.

4.30 Spin–Orbit Coupling and Spin-Forbidden Radiative Transitions

The radiative $S_0 \rightarrow T_1$ and $T_1 \rightarrow S_0$ processes are formally "spin-forbidden," but nonetheless are generally observed experimentally because of mixing of T_1 and excited singlet states or mixing of T_1 and S_0. The magnitude of the values of $\varepsilon(S_0 \rightarrow T_1)$ or of k_P^0 ($T_1 \rightarrow S_0$) is directly related to the degree of spin–orbit coupling that mixes S_0 and T. From Section 3.20, the degree of spin–orbit coupling was shown to depend strongly on (a) the ability of the electrons in the HO or LU of *R to approach a nucleus closely, (b) the magnitude of the positive charge (atomic number) of the nucleus that the HO or LU electrons approach and experience, (c) the availability of transitions between orthogonal (or nearly orthogonal) orbitals, and (d) the availability of a "one-atom center" $p_x \rightarrow p_z$ transition that can generate orbital angular momentum that could couple with spin angular momentum.

The degree of spin–orbit coupling between two states of an atom is related to ζ_{SO}, the spin(**S**)–orbit(**L**) coupling constant available from atomic spectra (Section 3.21, Eq. 3.21).[24]

$$\mathbf{H}_{SO} = \zeta_{SO}\mathbf{SL} \tag{4.46}$$

The correlation between the magnitude of spin–orbit coupling within a molecule (as judged from the magnitude of the spin–orbit coupling constant, ζ_{SO}, of atoms) and the magnitude of $\varepsilon(S_0 \rightarrow T)$ absorption and $k_P^0(T \rightarrow S_0)$ emission played a decisive role in establishing the triplet state as an important entity in molecular photochemistry.[25] The oscillator strength of a spin–forbidden radiative transition is expected to be related to the magnitude of ζ_{SO}, since spin–orbit coupling is the major interaction responsible for mixing singlet and triplet states in molecules.[24] This means the value of $\varepsilon(S_0 \rightarrow T)$

Table 4.7 Spin–Orbit Coupling in Atoms[a,b]

Atom	Atomic number	ζ (kcal mol^{-1})	Atom	Atomic number	ζ (kcal mol^{-1})
C[c]	6	0.1	I	53	14.0
N[c]	7	0.2	Kr	36	15
O[c]	8	0.4	Xe	54	28
F[c]	9	0.7	Pb	82	21
Si[c]	14	0.4	Hg	80	18
P[c]	15	0.7	Na	11	0.1
S[c]	16	1.0	K	19	0.2
Cl[c]	17	1.7	Rb	37	1.0
Br	35	7.0	Cs	55	2.4

a. Values are only representative and depend on electron configuration; they are intended here to show only trends.
b. The values are in kilocalories per reciprocal moles. They are rounded off and, strictly speaking, apply to the radical part of ζ. In effect, the angular part of ζ is considered to be close to unity. Values of ζ are for the lowest-energy atomic configurations.
c. Because of substantial configuration interaction for these atoms, the values given are extrapolated from nearby atoms in the periodic table by assuming that ζ varies with atomic number Z^4.

and $k_p^0(T \rightarrow S_0)$ will increase as ζ_{SO} increases, if factors involved in the transition are similar. However, the magnitude of ζ_{SO} depends on the orbital configurations of the states involved (Table 4.7). The important points to be derived from Table 4.7 are (a) there is a rapid increase in the magnitude or spin–orbit coupling parameter, ζ_{SO}, as the atomic number increases; (b) the magnitude of spin-orbit coupling is smaller than the energy of vibrational couplings ($\sim$ 1–5 kcal mol^{-1}) for first- and second-row atoms, such as H, C, N, and O; and (c) for very heavy atoms (Pb, Xe), the magnitude of spin–orbit coupling surpasses the value of vibrational energy levels and begins to approach the value of electronic energy gaps and strong electronic interactions ($\sim$ 20–30 kcal mol^{-1}). For the molecules containing very heavy atoms, spin inversion can occur on a time scale comparable to that of vibrational motions, and the zero-order distinction between singlet and triplet states begins to break down; that is, the mixing between spin states is very strong and the usual zero-order approximation is no longer adequate to describe singlet and triplet states as "pure."

Under certain circumstances, spin–orbit coupling can be very effective even in organic molecules containing only the "light" C, N, O, and H atoms. Effective spin–orbit coupling occurs when the two states involved in mixing are close in energy, so that effective mixing occurs because of the small energy gap, which brings the states close together and allows for effective mixing through resonance. However, in addition to a small energy gap, some other conditions involving the orbitals involved in the intersystem crossing are required for strong spin–orbit coupling involving only light atoms. We discuss these orbital factors in Section 4.31.

4.31 Radiative Transitions Involving a Change in Multiplicity: $S_0 \leftrightarrow T(n,\pi^*)$ and $S_0 \leftrightarrow (\pi,\pi^*)$ Transitions as Exemplars

For spin-forbidden transitions in organic molecules, oscillator strengths are very small and fall in the range $f \sim 10^{-5}$–10^{-9}, whereas the oscillator strengths for spin-allowed transitions are generally much larger and in the range $f \sim$ 1–10^{-3} (Table 4.3). This means that radiative $S_0 \leftrightarrow T$ transitions are strongly forbidden relative to spin-allowed $S_0 \leftrightarrow S$ transitions. We can picture spin forbiddenness as the result of the requirement that the light wave must "catch" the electrons of a molecule in a situation such that spin–orbit coupling is operating on the electron spins at the same time that the electric vector of the light wave is operating on the electron cloud. This situation is generally of low probability unless heavy atoms are involved or the transition involves two states that are strongly spin–orbit coupled because of a small energy gap. More precisely, from the quantum mechanical point of view, the wave functions of the singlet and triplet states of the initial and final states must be mixed by spin–orbit coupling, as the light wave interacts with the singlet portion of the wave function.

Experimentally, it is found that, for a spin-forbidden radiative transition, $S_0(n^2) \leftrightarrow n,\pi^*$ transitions possess a much greater oscillator strength than $S_0(\pi^2) \leftrightarrow \pi,\pi^*$ transitions, as indicated by Eq. 4.47.

$$f[S_0 \leftrightarrow T(n,\pi^*)] \gg f[S_0 \leftrightarrow T(\pi,\pi^*)] \tag{4.47}$$

This is exactly the opposite of the situation for $S_0 \leftrightarrow S_n$ transitions, for which $f(\pi,\pi^*) > f(n,\pi^*)$. Evidently this turnaround in the relative magnitude of the oscillator strength occurs because the spin–orbit force on an electron spin is much more effective when $n^2 \leftrightarrow n,\pi^*$ transitions occur than when $\pi^2 \leftrightarrow \pi,\pi^*$ transitions occur. Let us examine why this should be the case.

The situation may be viewed schematically as follows. The f values of the $S_0(n^2) \leftrightarrow T(n,\pi^*)$ and $S_0(\pi 2) \leftrightarrow T(\pi,\pi^*)$ transitions are composed of three parts (Eq. 4.40): the electronic (f_e), vibrational (f_v), and spin factors (f_S). We know that, in general, $f_e f_v(\pi,\pi^*) > f_e f_v(n,\pi^*)$ because $\varepsilon(\pi,\pi^*) > \varepsilon(n,\pi^*)$ for singlet–singlet transitions for which spin cannot be a contributing factor. This implies that for spin-forbidden radiative transitions, $f_s(n,\pi^*) \gg f_s(\pi,\pi^*)$.

We can obtain a pictorial understanding of the reason why $f_s(n,\pi^*) \gg f_s(\pi,\pi^*)$ from application of the rules for spin–orbit coupling to the $n^2 \leftrightarrow n,\pi^*$ and $\pi^2 \leftrightarrow \pi,\pi^*$ transitions. First, as exemplars, let us consider a radiative $S_0(n^2) + h\nu \rightarrow T(n,\pi^*)$ transition for formaldehyde (Fig. 4.21) and a $S_0(\pi^2) + h\nu \rightarrow T(\pi,\pi^*)$ transition for ethylene (Fig. 4.22). The spin change for formaldehyde is due to an $n \rightarrow \pi^*$ transition, which may be viewed as a jump of an electron from a p orbital localized on oxygen (say, p_x) in the plane of the molecule to a p orbital (say, p_y) perpendicular to the plane of the molecule (i.e., the atomic p orbital on oxygen that makes up one-half of the π^* orbital). The simultaneous $p_x \rightarrow p_y$ orbital jump is thus a one-center jump involving an orbital angular momentum change. *This type of situation is*

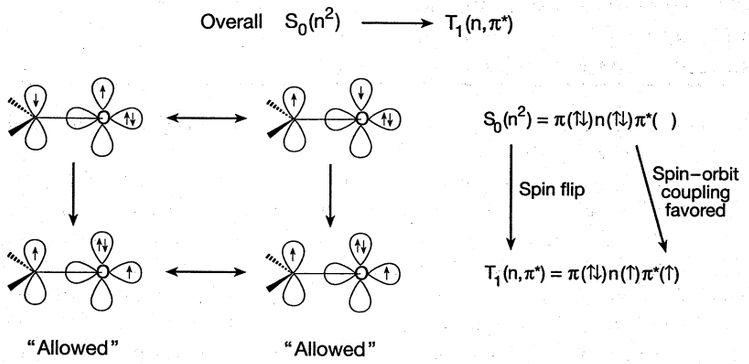

Figure 4.21 Orbital description of the spin–orbit selection rules for a radiative transition involving a spin flip. The $n^2 \rightarrow n,\pi^*$ transition involves an orbital angular momentum change that can be coupled with a spin momentum change on a single (oxygen) atom and is therefore spin–orbit "allowed."

precisely what is required for generating orbital angular momentum and favors strong spin–orbit coupling (Fig. 3.10); that is, the orbital momentum change associated with the $\alpha\beta \rightarrow \alpha\alpha$ (or $\alpha\beta \rightarrow \beta\beta$) spin flip can be coupled with a $p_x \rightarrow p_y$ orbital jump.

Now, let us compare this qualitative picture to the situation for a radiative $S_0(\pi^2) \rightarrow T(\pi,\pi^*)$ transition, for example, for ethylene (Fig. 4.22). It is immediately seen that for a planar ground state, there is no orbital of low energy in the molecular plane into which the π electron can jump (a σ^* orbital is available but has a very high energy, which strongly inhibits spin–orbital coupling); that is, the analogue of the low-energy $p_x \rightarrow p_y$ jump of ketones does not exist for ethylene. Consequently, there are no "one-center" spin–orbit interactions to help flip spins when a light wave interacts with the π electrons of the ethylene, spin–orbit coupling is inhibited, and the oscillator strength of the transition is small.

We conclude that the matrix element for spin–orbit coupling is much larger for $n^2 \rightarrow n,\pi^*$ transitions than for $\pi^2 \rightarrow \pi,\pi^*$ transitions. Since the oscillator strength of a spin-forbidden transition depends directly on the square of the matrix element (Eq. 4.36) corresponding to the perturbation (spin–orbit coupling) that mixes the states undergoing transition, we can conclude that Eq. 4.48 holds.

$$f[S_0(n^2) \leftrightarrow T(n,\pi^*)] \gg f[S_0(\pi^2) \rightarrow T(\pi,\pi^*)] \qquad (4.48)$$

Equation 4.48 (and its extension to other transitions) represents a general situation for organic molecules and is known as El-Sayed's rule.[24c] As seen in the case of ethylene, an aromatic hydrocarbon, such as benzene, cannot invoke an $n \rightarrow \pi^*$ mixing to generate a spin–orbital coupling mechanism.[14] The closest analogous $p_x \rightarrow p_y$ orbital mixing (in-plane to out-of-plane and vice versa) for benzene is of the $\sigma \rightarrow \pi^*$ or $\pi \rightarrow \sigma^*$ type; however, both of these mixings are ineffective because of the large

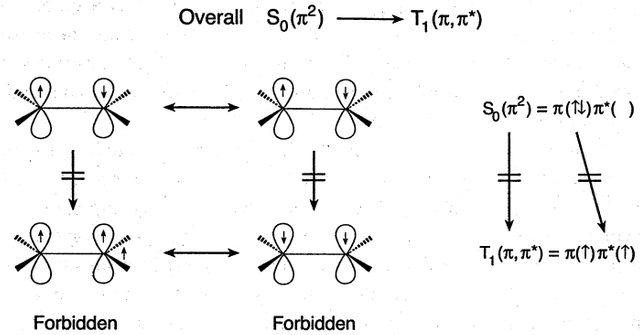

Figure 4.22 Orbital description of the spin–orbit selection rules for a radiative transition involving a spin flip. The $\pi^2 \rightarrow \pi,\pi^*$ transition does not involve an orbital angular momentum change and is spin–orbit "forbidden."

energy gap between the bonding and antibonding orbitals involved. We have seen how out-of-plane vibrations can induce vibronic mixing between an n,π^* and π,π^* state (Fig. 3.1) and can thereby add oscillator strength to a spin-allowed transition that is overlap forbidden in zero order. Now, let us try to picture an analogous theoretical connection among the out-of-plane vibrations, the observation of spin-forbidden phosphorescence emission, and the allowed transitions involving mixing with σ or σ^* orbitals. Consider Fig. 4.23, which shows (a) a planar benzene molecule and one of the p orbitals involved in the π system, and (b) another benzene molecule undergoing out-of-plane C—H vibrations on the carbon atom associated with the p orbital. As long as the molecule is planar, the π,π^* states and, say, the π,σ^* (or σ,π^*) states do not mix, because there is no net orbital overlap between orthogonal orbitals. An out-of-plane C—H vibration, however, destroys the planar symmetry of the molecule and allows mixing of the π,π^* and π,σ^* (or σ,π^*) states. In the extreme case, a substantial out-of-plane C—H vibration would cause a p orbital (originally symmetric above and below the molecular plane) to be transformed into an orbital that possesses an asymmetric

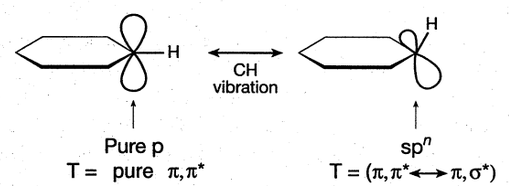

Figure 4.23 Schematic of the effect of an out-of-plane C—H vibration on the hybridization of a carbon atom in benzene. The vibration induces "s character" in the carbon atom and provides a "weak" mechanism for spin–orbit coupling.

electronic distribution relative to the plane of the molecule and that acquires some "s character" as a sp^n hybrid. The mixing of the π,π^* and π,σ^* states means some of the character of the $\pi^* \rightarrow \sigma^*$ transition is mixed into the $\pi \rightarrow \pi^*$ transition so that the latter transitions can "pick up" a certain amount of spin–orbit coupling and the spin-forbidden transition is "weakly" allowed.

This mechanism of inducing spin–orbit coupling is not expected to be particularly effective because of the large amount of energy required to deform the aromatic π electron cloud in this manner and because of the large energy gap between the orbitals involved in the mixing; that is, the matrix element for vibronic mixing, $<\pi,\pi^*|P_{CH}|\pi,\sigma^*>$, is very small. On the other hand, no better mechanism for spin–orbit coupling exists! Indeed, as a result of the very weak spin–orbit coupling, the radiative phosphorescence lifetimes of aromatic hydrocarbons, such as benzene and naphthalene, are very long—on the order of 10 s ($f \sim 10^{-9}$)!

4.32 Experimental Exemplars of Spin-Forbidden Radiative Transitions: $S_0 \rightarrow T_1$ Absorption and $T_1 \rightarrow S_0$ Phosphorescence[25]

Some experimental data for radiative $S_0 \leftrightarrow T_1$ transitions were given in Tables 4.4 and 4.8. The following points may be derived from the data. The oscillator strengths of radiative spin-forbidden $S_0(\pi^2) \leftrightarrow T_1(\pi,\pi^*)$ transitions are very small ($\sim 10^{-7}$–10^{-9}). Indeed, the values of $\varepsilon_{max}(S_0 \rightarrow T_1)$ and k_P for $S_0 \leftrightarrow T_1(\pi,\pi^*)$ transitions are among the smallest observed for organic molecules; that is, $\varepsilon_{max} \sim 10^{-5}$–$10^{-6}$ and $k_P^0 \sim 1$–10^{-1} s. The largest values of $\varepsilon_{max}(S_0 \rightarrow T_1)$ and k_P^0 are found for $T_1(n,\pi^*)$ states or for $T_1(\pi,\pi^*)$ states that possess a heavy atom (e.g., Br or I) conjugated to the π systems or that possess a strong mixing of n,π^* and π,π^* states (heavy atom effect on spin-forbidden transitions). For these systems, $\varepsilon_{max} \sim 10^{-1}$–$10^{-2}$ and $k_P \sim 10$–10^2 s^{-1}. For some organometallic compounds (e.g., tetraphenyl lead), ε_{max} values as high as ~ 10 have been reported.[26a] Generally, there is a wide variation found in the value of Φ_P in going from 77 K to 25 °C; this variation is usually the result of the onset of diffusional quenching of long-lived triplet lifetimes at the higher temperatures (in fluid solutions). The fact that triplet lifetimes at 25 °C in plastic films (a rigid medium that prevents diffusional quenching) are often comparable to those at 77 K is strong support for this conclusion. For example, the lifetime of triphenylene is 16 s at 77 K and is 12 s at 25 °C in a plastic film.[26c]

The substantial difference between the values of ε_{max} (and k_P^0) for π,π^* relative to n,π^* triplet states provides an experimental means of classifying molecules in terms of the orbital configuration of T_1. The rule is as follows. For non–heavy-atom-containing molecules possessing "pure" π,π^* configurations: The value of $\varepsilon_{max}(S_0 \rightarrow T_1)$ and $k_P^0(T_1 \rightarrow S_0)$ will be on the order of 10^{-5}–10^{-6} and 10^2–10^{-1} s^{-1}, respectively. For molecules possessing "pure" n,π^* configurations: The value of $\varepsilon_{max}(S_0 \rightarrow T_1)$ and k_P^0 will be on the order of 10^{-1}–10^{-2} s^{-1} and 10^2–10^1 $cm^{-1}\,M^{-1}$, respectively.

Table 4.8 Quantum Yields for Phosphorescence and Other Triplet Emission Parameters.[a]

Compound	Φ_P 77 K	Φ_P 25 °C	Φ_{ST}	k_P^0	Configuration of T_1
Benzene	~0.2	(<10^{-4})	~0.7	~10^{-1}	π,π^*
Naphthalene	~0.05	(<10^{-4})	~0.7	~10^{-1}	π,π^*
1-Fluoronaphthalene	~0.05	(<10^{-4})		~0.3	π,π^*
1-Chloronaphthalene	~0.3	(<10^{-4})	~1.0	~2	π,π^*
1-Bromonaphthalene	~0.3	(<10^{-4})	~1.0	~30	π,π^*
1-Iodonaphthalene	~0.4		~1.0	~300	π,π^*
Triphenylene	~0.5	(<10^{-4})	~0.9	~10^{-1}	π,π^*
Benzophenone	~0.9	(~0.1)[b]	~1.0	~10^2	n,π^*
Biacetyl	~0.3	(~0.1)[c]	~1.0	~10^2	n,π^*
Acetone	~0.3	(~0.01)[c]	~1.0	~10^2	n,π^*
4-Phenylbenzophenone			~1.0	1.0	π,π^*
Acetophenone	~0.7	(~0.03)[b]	~1.0	~10^2	n,π^*
Cyclobutanone	0.0	0.0	0.0		n,π^*

a. Unless specified, the temperature is 77 K in an organic solvent.
b. In deaerated perfluoromethylcyclohexane at room temperature.
c. In acetonitrile at room temperature.

Some examples of the relation of k_P^0 and orbital configuration (Table 4.8) are available for aromatic ketones. For aromatic ketones, T_1 may be either "pure" n,π^*, pure π,π^*, or a hybrid mixture of the two configurations. An exemplar for a "pure" $T_1(n,\pi^*)$ state is acetone, for which $k_P = 60\ s^{-1}$; an exemplar for a "pure" $T_1(\pi,\pi^*)$ state is naphthalene, for which $k_P = 0.1\ s^{-1}$. Examination of Table 4.8 shows that aromatic ketones may be classified as acetone-like (k_P within an order of magnitude of $60\ s^{-1}$), or naphthalene-like (k_P within an order of magnitude of $0.1\ s^{-1}$). For example, we may assign a nearly "pure" n,π^* configuration to T_1 of benzophenone ($k_P = 20\ s^{-1}$) and a mixed $n,\pi^* \leftrightarrow \pi,\pi^*$ configuration to T_1 of 4-phenyl benzophenone ($k_P \sim 1\ s^{-1}$).

Note in passing that molecular oxygen can enhance the intensity of the $S_0 \rightarrow T_1$ transition of aromatic hydrocarbons.[27] The enhancement of the forbidden transition is explained as the result of charge-transfer interaction of the hydrocarbon with oxygen and mixing of the triplet of the oxygen with the hydrocarbon's singlet state.

As an example of the *internal* heavy-atom effect on a spin-forbidden radiative transition, consider 2-bromobenzene undergoing a $T_1 \rightarrow S_0$ transition. The triplet state may be represented as a set of resonance structures of diradical character (see resonance structures **8a** ↔ **8b**), at least one of which will place the odd electron on the 1-carbon atom, which has a bromine atom attached. Since bromine is capable of expanding its valence octet, some delocalization of the odd electron onto the bromine atom is possible. This finite amount of localization on the "heavy atom" produces a good mechanism for spin inversion because of the strong spin–orbit coupling the π^*

electron experiences when it is on the bromine atom (Chapter 3). The odd electron that undergoes the spin inversion does so by simultaneously jumping from one orbital to another in order to satisfy the requirement of conservation of total angular momentum.

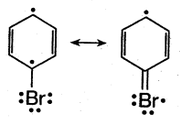

8a **8b**

The heavy-atom effect on absorption spectra strongly enhances $\varepsilon(S_0 \rightarrow T_1)$, but not $\varepsilon(S_0 \rightarrow S_1)$. Because of the relationships between $\varepsilon(S_0 \rightarrow T_1)$ and k_P^0 and between $\varepsilon(S_0 \rightarrow S_1)$ and k_F^0 (Eq. 4.23), we expect that k_P^0, but not k_F^0, will be influenced by heavy-atom perturbation. For example, the shapes of the fluorescence and phosphorescence spectra of molecules **9a**, **9b**, and **10** are very similar in appearance:[28]

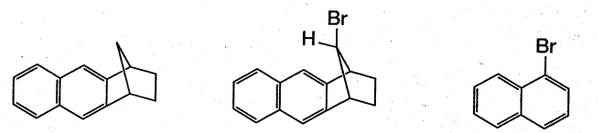

9a
$k_F^0 = 1 \times 10^6\ s^{-1}$
$k_P^0 = 3 \times 10^{-2}\ s^{-1}$

9b
$1 \times 10^6\ s^{-1}$
$500 \times 10^{-2}\ s^{-1}$

10
$1 \times 10^6\ s^{-1}$
$1000 \times 10^{-2}\ s^{-1}$

On the other hand, the fluorescence and phosphorescence *quantum yields* for the molecule **9a**, which contains only "light atoms," are $\Phi_F \sim 0.5$ and $\Phi_P \sim 0.06$, and for **9b** and **10**, $\Phi_F \sim 10^{-3}$ and $\Phi_P \sim 0.6$. Although the values of k_F^0 are essentially constant in this series, the values of k_P^0 are greatly enhanced in the bromine-containing molecules. The much higher values of Φ_P reflect both a greater efficiency of population of T_1 (k_{ST} enhanced by the heavy-atom effect; see Section 5.11) and a greater efficiency of emission from T_1 (k_P^0 is enhanced *more* than k_{TS}).

An example of the *external* heavy-atom effect[29] is shown for 1-chloronaphthalene[30] (Fig. 4.24). When external heavy atoms are contained in the solvent (ethyl iodide as solvent or a high pressure of Xe gas),[31] there is a significant increase in absorption in the region from 350–500 nm. The vibrational structure of the absorption and its mirror-image relationship to the phosphorescence spectrum of 1-chloronaphthalene strongly suggests that the new absorption is due to the enhancement of the $S_0 \rightarrow T_1$ absorption for 1-chloronaphthalene. For the case of 1-chloronaphthalene (Fig. 4.24), the pure liquid exhibits a number of weak absorption bands near 470 nm. A solution of 1-chloronaphthalene in ethyl iodide shows that the weak bands are greatly enhanced in intensity.[30] The 0,0 band of the enhanced $S_0 \rightarrow T_1$ absorption (58 kcal mol^{-1}) occurs at nearly the same energy as the 0,0 band of normal $T \rightarrow S_0$ phosphorescence, confirming that in this case the effect is mainly on the oscillator strength of the spin-forbidden transitions and not on the energies of the states undergoing the transitions.

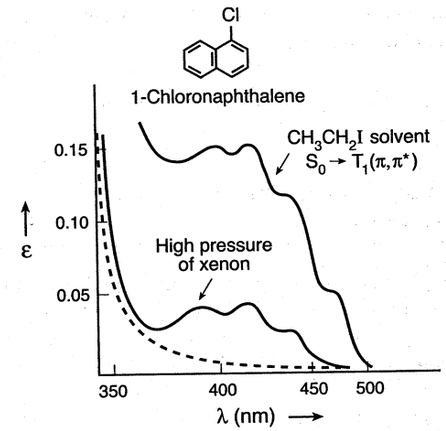

Figure 4.24 Heavy-atom perturbation of the $S_0 \rightarrow T_1$ absorption of 1-chloronaphthalene. The dashed line indicates the absorption spectrum in a "light-atom" solvent.

4.33 Quantum Yields of Phosphorescence, Φ_P: The $T_1 \rightarrow S_0 + h\nu$ Process

A general expression for the quantum yield of phosphorescence (Φ_P) is given by Eq. 4.49.

$$\Phi_P = \Phi_{ST} k_P^0 (k_P^0 + \Sigma k_d + \Sigma k_q[Q]^{-1}) = \Phi_{ST} k_P^0 \tau_T \tag{4.49}$$

In Eq. 4.49, Φ_{ST} is the quantum yield for intersystem crossing, $S_1 \rightarrow T_1$; k_P^0 is the radiative rate of phosphorescence; Σk_d is the sum of the rate constants of all unimolecular radiationless deactivations of T_1 (including photochemical reactions); and $\Sigma k_q[Q]$ is the sum of all bimolecular deactivations of T_1 (including photochemical reactions). By definition, the experimental lifetime of T_1 is given by $\tau_T = (k_P^0 + \Sigma k_d + \Sigma k_q[Q])^{-1}$. From Eq. 4.49, we see that the quantum yield for phosphorescence is the product of a number of factors. Unless these factors can be experimentally identified and controlled, Φ_P is not a reliable parameter for characterizing T_1, although it may be a useful parameter in certain kinetic analyses.

Data for the Φ_P value of molecules at 77 K in rigid glasses (optically clear frozen solvents) is given in Table 4.8. Experimentally, a wide range of values of Φ_P are found for organic molecules. High values of $\Phi_P (\sim 1)$ require that $\Phi_{ST} \sim 1$ and $k_P^0 > (\Sigma k_d + \Sigma k_q[Q])$. At 77 K, it appears that all of the major deactivation processes of bimolecular diffusional quenching ($\Sigma k_q[Q]$ term) are inhibited, so that the main radiationless deactivation of T_1 is $T_1 \rightarrow S_0$ intersystem crossing. In this limiting case, the quantum yield of phosphorescence is simplified to Eq. 4.50; that is, the value

of Φ_P depends only on the value of Φ_{ST} and the competition between the rates of phosphorescence emission and intersystem crossing.

$$\Phi_P = \Phi_{ST} k_P^0 (k_P^0 + k_{TS})^{-1} \quad \text{(at 77 K)} \tag{4.50}$$

4.34 Phosphorescence in Fluid Solution at Room Temperature[32]

The observation of phosphorescence in fluid solution at room temperature was once considered a rare and unusual phenomenon. Now, it is clear that if phosphorescence is observed at 77 K, it can also *generally* be observed at room temperature in fluid solution if two conditions are met:

1. Impurities (e.g., molecular oxygen) and other ground and excited molecules required in the system (R and *R) capable of deactivating triplets by diffusional quenching are rigorously minimized.
2. The triplet does not undergo an activated unimolecular deactivation (photophysical or photochemical) that possesses a rate of greater than $\sim 10^4\ k_P^0$ at room temperature.

The routine experimental observation of measurable phosphorescence requires a value of $\Phi_P \sim 10^{-5}$. The value of Φ_P may be expressed in terms of the rate of phosphorescence and all processes that deactivate T_1. From Eq. 4.48, in the case for which triplet formation from S_1 is efficient, Φ_P is given by Eq. 4.51.

$$\Phi_P \sim \frac{k_P^0}{k_d + k_q[Q] + k_P} \sim \frac{k_P^0}{k_d + k_q[Q]} \quad \text{(in most fluid solutions)} \tag{4.51}$$

In Eq. 4.51, k_d represents the sum of *all* unimolecular deactivations of T_1, and $k_q[Q]$ represents the sum of *all* bimolecular deactivations of T_1.

As discussed above, a typical value of k_P^0 for a "pure" $T_1(n,\pi^*)$ is $10^2\ s^{-1}$, and a typical value of k_P^0 for $T_1(\pi,\pi^*)$ is $10^{-1}\ s^{-1}$. For $\Phi_P \sim 10^{-4}$, we find Eqs. 4.52 and 4.53:

$$k_d + k_q[Q] \sim 10^6\ s^{-1} \quad \text{for} \quad T_1(n,\pi^*) \tag{4.52}$$

$$k_d + k_q[Q] \sim 10^3\ s^{-1} \quad \text{for} \quad T_1(\pi,\pi^*) \tag{4.53}$$

Let us calculate the maximum value for the concentration of a quencher, [Q], that is tolerable for observation of phosphorescence if Q is a diffusional quencher. For a nonviscous organic solvent, the *maximal* rate constant for diffusion is given by $k_{dif} \sim 10^{10}\ M^{-1}\ s^{-1}$. Therefore,

$$\text{if} \quad k_{dif}[Q] < 10^6\ s \quad \text{then} \quad [Q] < 10^{-4}\ M \tag{4.54}$$

and

$$\text{if} \quad k_{dif}[Q] < 10^3\ s \quad \text{then} \quad [Q] < 10^{-7}\ M \tag{4.55}$$

The limit of 10^{-4} M for [Q] is relatively easily obtained, but the limit of 10^{-7} M is more difficult to achieve without very careful purification of solvents and degassing to remove oxygen. These qualitative considerations allow us to understand why compounds that phosphoresce from $T_1(n,\pi^*)$ states are commonly observed in fluid solutions, but phosphorescence from $T_1(\pi,\pi^*)$ is rarely observed, unless extraordinary care is taken to eliminate bimolecular quenching.

The value of k_P^0 may be increased for aromatic hydrocarbons by external or internal heavy-atom perturbation. In certain heavy-atom solvents, the value of k_P^0 is increased to values approaching $10–10^2\ s^{-1}$ (e.g., bromonaphthalene). In these cases, phosphorescence is observed even for aromatic hydrocarbons if the heavy-atom solvent is not itself a triplet quencher.[32e] Examples of phosphorescence data in fluid solutions were given in Table 4.8 and Fig. 4.19. In very favorable or contrived circumstances, phosphorescence from aromatic hydrocarbons occurs even in the vapor phase.[32f] An interesting method to prevent triplet diffusional quenching is to replace a molecular solvent cage with a supramolecular cage (a supercage), such as the hydrophobic core of a micelle.

4.35 Absorption Spectra of Electronically Excited States[33]

We have seen that the electronically excited states $^*R(S_1)$ and $^*R(T_1)$ undergo fluorescence and phosphorescence emission, respectively. Since *R is a "real" molecular structure, it must also possess absorption spectra: a $^*R + h\nu \rightarrow {}^{**}R$ processes (where $^{**}R$ is $S_{n>1}$ or $T_{n>1}$). Indeed, $S_1 + h\nu \rightarrow S_{n>1}$ and $T_1 + h\nu \rightarrow T_n$ radiative transitions can be observed experimentally through very fast excitation and detection methods, termed pulse–probe flash spectroscopy.[33] Since 1950, the speed of detection has increased steadily from $\sim 10^{-3}$ s (ms) and has now approached a limit of $\sim 10^{-15}$ s (fs);[33c] as a result, it is possible under favorable circumstances to detect *R by pulse–probe spectroscopy even when the lifetime of *R is of the order of femtoseconds!

The idea behind flash spectroscopy is to deliver an intense *preparation pulse* (a laser flash) of photons to an absorbing sample to produce *R in as short a period as possible and then, with a weaker *pulse probe* of photons, to detect and characterize the transient species (*R, I, P) that were produced after the preparation pulse *in real time*. These short, intense pulses are readily provided by pulsed lasers. Lasers have been developed that are capable of delivering intense pulses ($10^{16}–10^{18}$ photons) in time periods as short as from 10^{-12} (a ps) to 10^{-15} (a fs) second! In order to gain an appreciation of the time scale implied by a picosecond, consider the following. A bullet traveling 1000 m s^{-1} takes 10^6 ps to travel 1 mm, and light travels 0.3 mm in 1 ps. In a femtosecond, an electron in a Bohr orbit can move only a few angstroms.

Figure 4.25 shows an example[34] of the $T_1 \rightarrow T_{n>1}$ absorption spectra of naphthalene along with the state energy diagram that schematically shows the transitions relative to S_0. Such absorption spectra may be used to characterize the configurations of the states involved in the transitions, but this is a difficult task for various technical and theoretical reasons. However, the use of excited-state absorption spectra in following the concentration of excited states is a very important tool for photochemical kinetics.

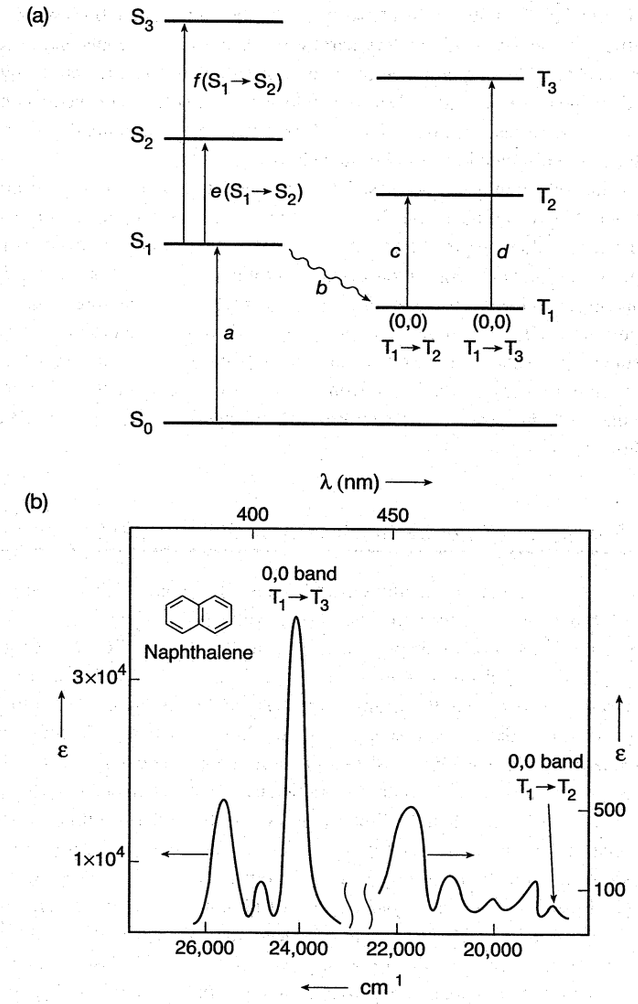

Figure 4.25 The triplet–triplet (T–T) absorption spectrum of naphthalene. (a) A state diagram showing the pathway leading to T–T absorption. Absorption (*a*) is followed by intersystem crossing (*b*) to populate T_1. The latter is capable of absorbing photons and undergoing $T_1 \rightarrow T_2$ and $T_1 \rightarrow T_3$ transitions. (b) The experimental T–T absorption spectrum of naphthalene.

4.36 Radiative Transitions Involving Two Molecules: Absorption Complexes and Exciplexes[35]

Thus far, we have considered absorption and emission processes that involve a single molecule (surrounded by "inert," noninteracting solvent molecules). In certain cases, two or more molecules may participate in *cooperative* absorption or emission; that is, the absorption or emission can only be understood as arising from ground- or excited-state *complexes* of a definite stoichiometry. Such complexes, formed by two or more molecules, are termed *supramolecular* complexes. Commonly, the stoichiometry of such complexes consists of two molecules, so we use this situation as an exemplar. When two molecules act cooperatively to absorb a photon, we say that an *absorption (supramolecular) complex* exists in a ground state and is responsible for the absorption. An excited molecular complex of definite stoichiometry, but which is dissociated in its ground state, is called an *exciplex*. Thus, if two molecules act cooperatively to emit a photon to a dissociative ground state, we say an *exciplex* exists; an exciplex can be detected directly and characterized by the emitted photon. The important conceptual distinction between an absorption complex and an exciplex is that the absorption complex possesses some stability in its ground state, whereas the exciplex does not.

Some significant experimental spectroscopic characteristics of absorption complexes and exciplexes are one or more of the following:

1. *Absorption Complex:* The observation of a new absorption band, usually occurring at longer wavelengths than the absorption of either molecular component, that is characteristic of the complex but not of either of the individual molecular components of the ground-state complex.
2. *Exciplex:* The observation of a new emission band, usually structureless and at longer wavelengths than the absorption for either of the molecular components, that is characteristic of the exciplex but not of the individual components of the exciplex.
3. *Absorption Complex and Exciplex:* A concentration dependence of the new absorption or emission intensity.

In the special case, where the molecular components of the exciplex are the same, the excited molecular complex is termed an "excimer," rather than the more general term "exciplex." Exciplex is reserved for excited-state complexes consisting of two different molecular components. The notion of a specific stoichiometry is included in our definitions of exciplex and excimer because we wish to distinguish these species from those solvated excited molecules for which an undefined number of unexcited solvent molecules provide an environment. Both are examples of *supramolecular assemblies*, which comprise the family of molecules that are held together by intermolecular forces.[36]

4.37 Examples of Ground-State Charge-Transfer Absorption Complexes[37]

Solutions of mixtures of molecules that possess a low ionization potential (electron donors, D) or a high electron affinity (electron acceptors, A) often exhibit absorption bands that are not shown separately by either component. Generally, the new band is due to an electron donor-acceptor (EDA) or charge-transfer (CT) complex in which D has donated an electron (charge) to a certain extent to A. Typical examples[38] of CT spectra are shown in Fig. 4.26. Generally, the absorption band of a CT complex is broad and devoid of vibrational structure. This breadth occurs because the rather small binding energies of EDA complexes allows many different structural configurations for the complex to exist in equilibrium with one another. The absorption energy for each configuration will differ and cause a broadening of the band. Since the bonding is weak and intermolecular, there are no characteristic vibrational bands that appear in the spectra. In addition, the excited complex may be very short lived and not have sufficient time to vibrate in *R.

An important experimental characteristic of an EDA absorption band is its sensitivity-to-solvent polarity. For example, the maxima of the EDA absorption band for enol ethers (donors) and tetracyanoethylene (acceptor) of the molecules shown in Fig. 4.26 vary substantially as solvent polarity is varied.[38] The energy required for

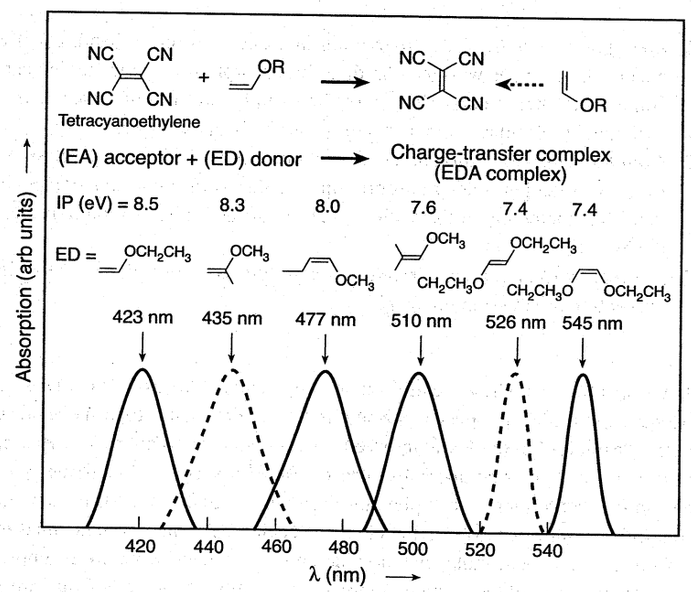

Figure 4.26 The absorption spectra of some EDA complexes of tetracyanoethylene and a variety of enol ethers.

absorption decreases as the solvent polarity increases. This effect is understood in terms of solvent-assisted mixing of the wave functions for the states involved in the EDA transition, which cause a solvent-dependent energy separation of the HO and LU responsible for the CT transition.

4.38 Excimers and Exciplexes[35]

Consider a pair of molecules R and N for which R absorbs a photon to form *R and then *R collides with N. What factors contribute to the stability of an excited-state complex, R-*-N (where excitation is *shared* to some extent by both molecular components) that are missing in the ground-state complex, R/N? An electronically excited-state *R possesses a much stronger electron affinity and a much lower ionization potential than the ground state, because of the occurrence of an electrophilic half-filled HO and a nucleophilic half-filled LU (Chapter 7). Consequently, these orbitals may participate in CT interactions with other polar or polarizable species they encounter intermolecularly. For example, a collision complex between an electronically excited molecular species (R*) with *any* polar or polarizable ground-state molecule, N, will generally be stabilized by some CT interaction involving the HO and the LU or *R with N. This energetic stabilization will in turn cause the R-*-N collision complex to possess a longer lifetime than the corresponding R/N (ground-state) collision complex. The R-*-N collision complex should possess observable spectroscopic and chemical properties that are distinct from those of R*. When this is the case, the R-*-N collision complex can be considered an electronically excited state that is distinct from *R alone; that is, the R-*-N collision complex is a *supramolecular* electronically excited species, held together by attractive intermolecular forces. As mentioned in Section 4.37, such a supramolecular excited complex is termed an *exciplex* if R and N are different molecules (Eq. 4.56a), whereas if R and N are the same molecule (Eq. 4.56b), then the excited complex *R-*-R is termed an *excimer*:

$$*R + N \rightarrow R\text{-}*\text{-}N \quad \text{Exciplex} \tag{4.56a}$$

$$R^* + R \rightarrow R\text{-}*\text{-}R \quad \text{Excimer} \tag{4.56b}$$

A simple theoretical basis for the enhanced stabilization of a R-*-N collision pair relative to a R/N ground-state collision pair is available from the simple theory of MO interactions (Fig. 4.27). If we consider R (or *R) and N colliding, then the major electronic interactions will involve their highest-energy filled (HO) and lowest-energy unfilled (LU) orbitals. According to the rules of perturbation theory, the HO of R will interact with the HO of N to yield two new HOs of the ground-state collision complex or exciplex. Similarly, the LU of R will interact with that of N to produce two new LUs of the collision complex or exciplex. The new HOs and LUs are split in energy relative to the original HOs and LUs of R and N as shown in Fig. 4.27. In both, the collision complex and exciplex, one of the new HOs is lower in energy than the original HOs and one is higher. Similarly, the LUs of the collision complex and exciplex split in energy above and below the original LUs.

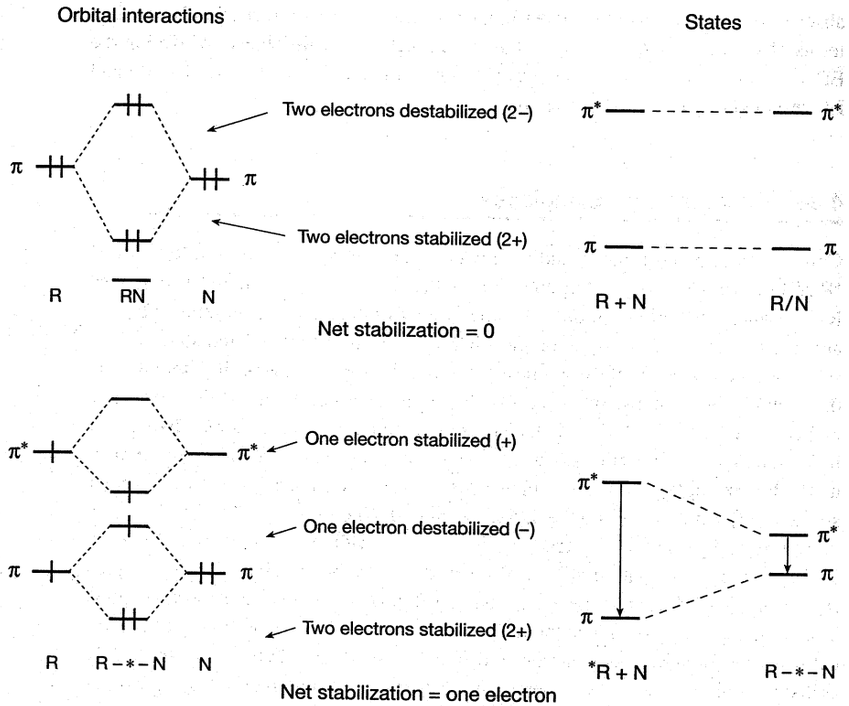

Figure 4.27 Orbital interactions of RN collision pairs and R-*-N exciplexes.

In the collision complex of the ground-state molecules R and N, the four electrons that occupied the HOs of R and N occupy the new set of HOs according to the aufbau principle and fill the lowest-energy orbital. Two electrons are stabilized in the HO and two electrons are destabilized in the LU (Fig. 4.27, top); *thus, no gain in energy is achieved by interaction of R and N during their collisions since the bonding and antibonding interactions are equal and cancel each other*. In the exciplex, however, since one of the partners (*R) is electronically excited, *three* electrons are stabilized (two in the lower-energy HO and one in the lower-energy LU). Only one electron is destabilized (in the higher-energy HO) as the electrons redistribute themselves from their original noninteracting orbitals to the new orbitals of the exciplex (Fig. 4.27, bottom). *Thus, a net gain in energy is always achieved by interaction of *R and N during their collision*! This analysis provides the remarkable conclusion that an electronically excited state has an inherent tendency to form a supramolecular complex with other molecules. The only issue is the strength of the excimer or exciplex binding.

Now, consider the states produced by the collisions corresponding to the collision complex and the exciplex. If there is only a very weak interaction between R* and N, the emission of the collision complex will look very much like that of the monomer

*R, and the energy of the emission will be close to that for the molecular $R^* \rightarrow R + h\nu$ process. If the orbital interactions between the excited molecule and the ground-state molecule are sufficiently strong, the collision complex between *R and N becomes an exciplex (R-*-N), and the energy of the latter *decreases* relative to that of the ground-state complex (R/N). The emission (R-*-N) $\rightarrow$ R/N + $h\nu$ produces the unstable, ground-state collision complex.

As distinct chemical species, exciplexes and excimers are expected to possess distinct and characteristic photophysical and photochemical properties. Perhaps the most general distinguishing characteristic of an electronically excited state is its emission to produce a ground state and a photon. Thus, if exciplexes exist, they should in principle exhibit fluorescence (singlet exciplexes) or phosphorescence (triplet exciplexes). The emission from R-*-N will in general be different from that of R*. Furthermore, since the ground-state collision complex R/N will generally be less bound than R-*-N, emission from the exciplex will usually occur to a weakly bound or dissociative ground state.

Figure 4.28 shows a PE surface description of excimer (or exciplex) formation and emission and relates the energy surface to absorption and emission of photons. The situation shown assumes that the ground-state complex R/N experiences relatively strong repulsions as the two molecules approach each other to close distances, whereas the exciplex (R-*-N) experiences significant stabilizing attractions as the excited ground- and excited-state molecules approach each other. Since exciplexes are typically stabilized by CT interactions, we can replace the symbols R and N with the labels D and A for donor and acceptor molecules, respectively. At large separations of D and A, the absorption spectrum of either component would be identical to that of each monomer; that is, neither component would influence the other. As D and A approach, the absorption spectrum remains constant. Eventually, D and A undergo collisions. If there are no substantial attractions between D and A in their ground states (lower surface), collisions will raise the energy of the system, and very few collision complexes will exist at any given time. Consequently, their concentrations will be quite low and *no new absorption due to the collision complex will be observed*. The "instability" of the ground-state complex is a somewhat arbitrary feature of the excimer and exciplex definitions. The essential idea is that the ground-state DA collision complexes are *unstable*, low-structured species, *not* that they lack a measurable absorption spectrum.

Consider the situation for the approach and collision of D* and A (or A* and D) on the excited surface. At a large separation of D* and A, the emission spectrum is that of the monomer, D*. As the two molecules approach, the bonding between them may increase due to CT or excitation–exchange interactions. These interactions will cause a minimum to occur in the PE curve; if this enthalpy decrease is not offset by an entropy decrease, an excited-state complex (an exciplex) will form. Emission from the exciplex will occur according to the Franck–Condon principle, that is, vertically from the excited-state minimum. If the separation of D and A in the excited-state minimum corresponds to a point on the repulsive part of the ground-state potential curve, Franck–Condon emission will lead exclusively to repulsive states on the ground surface. Immediately after formation, D and A will fly apart. This

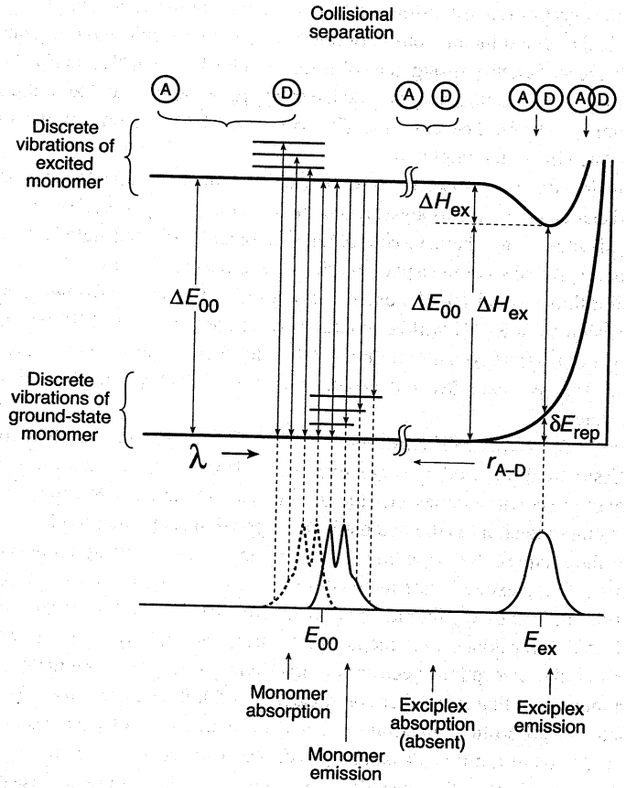

Figure 4.28 Surface interpretation of exciplex emission. Either D or A may be excited on the excited surface.

process is the emission analogue of predissociative or directly dissociative absorption (Fig. 4.11). The short lifetime and indefinite character for the "vibrations" of the final state (collision complex D/A) result in a total absence of *vibrational structure* in the emission spectra of excimers and exciplexes.

Now, we are in a position to appreciate the single most definitive kind of direct spectroscopic evidence for the formation of an excimer or exciplex: the observation of a concentration-dependent, vibrationally unstructured emission spectrum, which occurs on the red (lower-energy, longer-wavelength) of the absorption spectrum of both D and A but does not correspond to the monomer emission spectrum of either D or A.

From Fig. 4.28, we also notice how the important quantities ΔE_{00}, ΔE_{ex}, and ΔH^* are related. The parameter ΔE_{00} is either the excitation energy required to raise the

monomer from $v = 0$ of the ground state to $v = 0$ or the excited state or the excitation energy released when the monomer excited state ($v = 0$) emits a photon and produces the ground state ($v = 0$).

Triplet excimers and exciplexes, while less often directly observed by their emission, are well-established excited-state species.[39] They tend to be more weakly bound and to possess different structures than singlet excimers and exciplexes, probably because of the generally decreased CT character of triplets.

Our theoretical analysis of exciplexes indicates that D-*-A should possess the typical properties of electronically excited states (e.g., emission, radiationless transitions, and photochemistry). The exciplex may be treated stoichiometrically as a supramolecular species and its reactions considered *unimolecular*, although its formation is bimolecular.

4.39 Exemplars of Excimers: Pyrene and Aromatic Compounds

The pyrene excimer serves as a classic exemplar of excimer formation and excimer emission.[35,40] Figure 4.29 shows the *fluorescence* of pyrene in methylcyclohexane as a function of pyrene concentration. At concentrations of $\sim 10^{-5}$ M or less, the fluorescence is concentration independent and is composed of pure pyrene monomer fluorescence (Fig. 4.15), which shows vibrational structure and occurs with a maximum at ~ 380 nm. As the pyrene concentration increases to values in the vicinity of $\sim 10^{-5}$ M, two effects are observed: (1) a new broad, structureless fluorescence emission, due to the pyrene excimer, appears on the longer wavelengths of the monomer emission; and (2) the relative amount of monomer emission-to-excimer emission decreases in intensity. As the concentration of pyrene is increased, the excimer intensity continues to increase relative to the monomer (in Fig. 4.29, the monomer emission is normalized and fixed in order to clearly demonstrate the increase in the excimer emission relative to the monomer emission). At concentrations of pyrene of ~ 0.1 M and greater, only excimer emission is observed.

Let us apply Fig. 4.28 (D = A = pyrene, Py) to describe the formation of a Py excimer. The diagram indicates how the energy of two pyrene molecules varies as a function of their internuclear separation. For the ground-state pair at large distances of separation (~ 10 Å, Fig. 4.28, left) the energy of the pair is constant, since intermolecular interactions are weak at this separation distance. At a separation of ~ 4 Å, which is close to the equilibrium separation of the excimer, the energy of the ground-state collision complex Py/Py rises rapidly due to occupied π orbital repulsions (Fig. 4.28, top). From this figure it is easy to see why the Py excimer emission is structureless and why no absorption is observed that corresponds to Py/Py + $h\nu \rightarrow$ Py-*-Py transitions, since there is essentially a zero concentration of Py/Py pairs. The emission is structureless because the Py-*-Py $\rightarrow$ Py/Py + $h\nu$ emission is to an unstable, dissociative state (the molecule dissociates before it can complete a vibrational cycle). There is no measurable absorption corresponding to

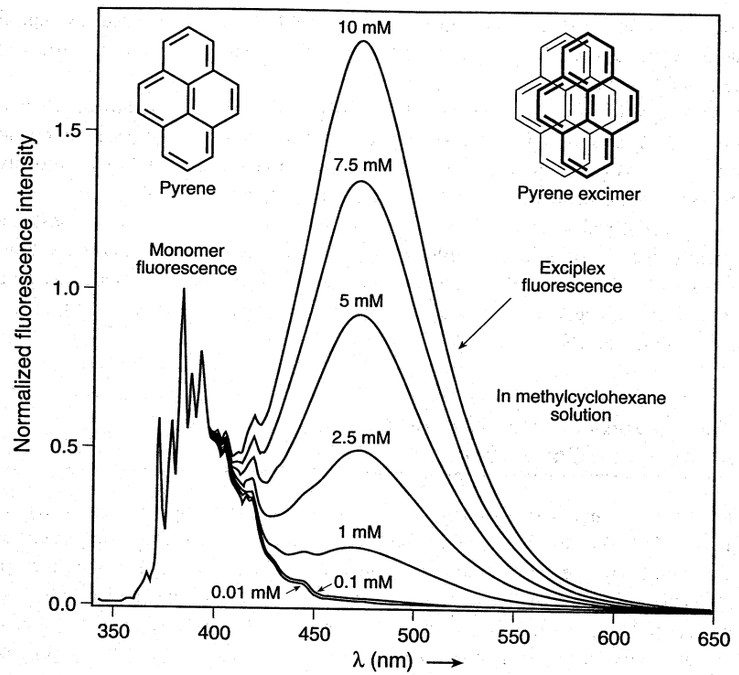

Figure 4.29 Experimental example of the excimer emission of pyrene in methylcyclohexane. The concentrations of pyrene in methylcyclohexane are shown.

the excimer ground state, because too few pairs of Py molecules are in a collision complex at any given instant (the concentration of ground-state complexes of two Py molecules is too small to be measured by absorption of light).

From a spectroscopic analysis of Py excimer emission, and a correlation of this with the emission of Py crystals, it was concluded that the structure of the "face-to-face" Py singlet excimer is favored. This structure is in agreement with expectations based on maximal overlap of π orbitals.

The electronic stabilization energy of the Py excimer is substantial ($\Delta H = -10$ kcal mol^{-1}), but the entropy of formation is quite negative ($\Delta S = -20$ eu; $T\Delta S =$ 6 kcal mol^{-1} at room temperature in a nonpolar solvent).[41] Thus, at ambient temperatures, formation of the excimer is favorable, with $\Delta G \sim -4$ kcal mol^{-1}.

In contrast to the large solvent shifts observed for exciplex emission, the emission wavelength for excimers is usually not very solvent dependent. The reason is because CT interactions are not as pronounced for excimers as for exciplexes. This finding is to be expected from the inherently less polar nature of excimers.

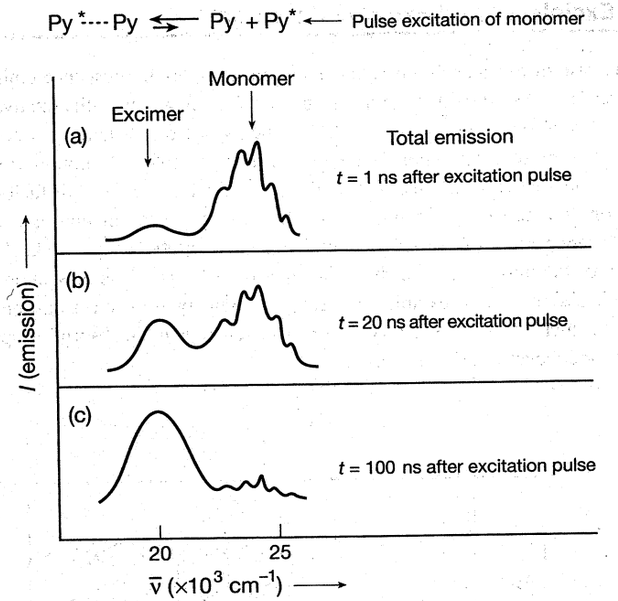

Figure 4.30 The dynamic behavior of Py monomer and excimer emission. (a) After 1 ns, most of the excited Py exists as the monomer. (b) After 20 ms, comparable amounts of excimer and momomer are observed. (c) After 100 ns, most of the excited Py molecules exist in the excimer form.

The time dependence of emission from Py solutions (*time-resolved emission spectroscopy*) provides an excellent confirmation for the dynamic nature of excimer formation.[42] If a solution of pyrene in cyclohexane ($\sim 10^{-3}$ M) is excited with a brief pulse of light, only the excited monomer is produced (the Py/Py collision complex is too low in concentration to absorb). If the *total* emission spectrum is taken after $\sim 1 \times 10^{-9}$ s ($\sim$ 1 ns), the spectrum is mainly that of the *monomer* (Fig. 4.30a); that is, the diffusion of an excited monomer toward a ground-state Py and the formation of an excimer is required for excimer emission, and Py molecules can only move a few angstroms in 10^{-9} s. The small amount of excimer emission results from the formation of excimers by excited Py monomers that happen to encounter Py ground-state molecules during the time of the excitation pulse. After $\sim$ 20 ns, substantial diffusional displacements have occurred, and the concentrations of excimer and monomer become comparable (Fig. 4.30b). After $\sim$ 100 ns, the emission spectrum (Fig. 4.30c) is that which is normally seen under steady-state conditions.

Because of the weaker binding generally found for triplet excimers, excimer phosphorescence is not typically observed.

4.40 Exciplexes and Exciplex Emission[43]

As in the case of excimer fluorescence emission, exciplex fluorescence emission is usually observed as a broad structureless band at longer wavelengths relative to the monomer fluorescence emission (Fig. 4.31). The pyrene-diethylaniline system is an exemplar for exciplex formation and emission. For example, the monomer fluorescence of aromatic hydrocarbons, such as Py, is often quenched at the diffusional rate by electron donors, such as aniline and its derivatives. The quenching is accompanied by the appearance of a broad structureless band $\sim 5000\ \text{cm}^{-1}$ ($\sim 15\ \text{kcal mol}^{-1}$) to the red of the fluorescence of the hydrocarbon monomer. This new fluorescence (Fig. 4.31), assigned to the exciplex, increases in intensity as the electron-donor concentration is increased. There is no corresponding change in the absorption spectrum as the donor concentration is increased.

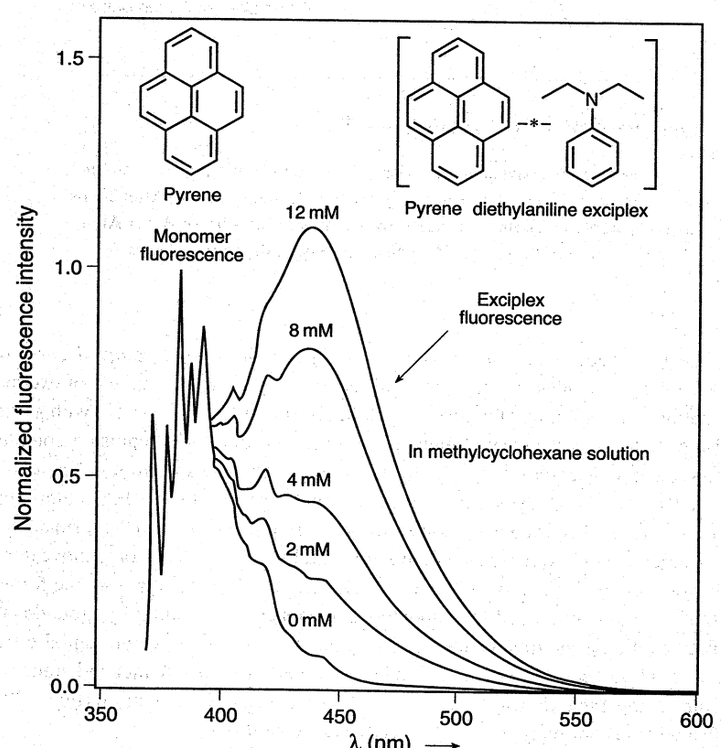

Figure 4.31 Pyrene fluorescence (dotted line) and pyrene–diethylaniline exciplex fluorescence (solid line).

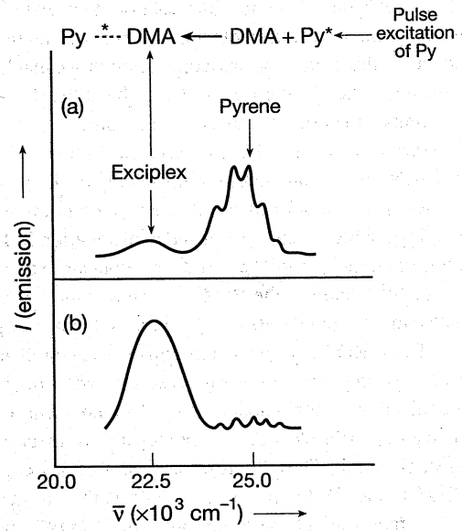

Figure 4.32 Dynamic behavior of the pyrene–dimethylaniline exciplex. (a) After 1 ns, most of the excited Py exists as the monomer. (c) After 100 ns, most of the excited Py molecules exist in the pyrene–dimethylaniline exciplex form.

The dynamic behavior of exciplex formation is nicely demonstrated by time-resolved emission spectroscopy.[43] Figure 4.32 shows the total emission of pyrene-plus-dimethylaniline in cyclohexane: (a) about 1 ns after an excitation of the Py chromophore, and (b) ~ 100 ns after the excitation. It is evident that immediately after the excitation, emission is mainly from the Py monomer, but as time goes on the exciplex begins to increase its contribution to the total.

4.41 Twisted Intramolecular Charge-Transfer States[44]

From the above discussion of radiative transitions, we conclude that, as a rule, for the majority of organic molecules only one fluorescence spectrum should be observed, that is, the $^*R(S_1) \rightarrow R(S_0) + h\nu$ radiative transition. Reactions in which an electronically excited state *R is converted into the excited state of a produce (*P) would correspond to exceptions to this rule, since both $^*R(S_1) \rightarrow R(S_0) + h\nu$ and a $^*P(S_1) \rightarrow P(S_0) + h\nu$ radiative transitions are possible, producing a *dual fluorescence*, from a single initial *R. A *R → *P process occurs entirely on an electronically excited surface and is termed an "adiabatic" photochemical reaction. Excimer formation, *R + N → R-*-N, is an example of a bimolecular adiabatic reaction. There are a

number of cases of unimolecular adiabatic photoreactions that result from the twisting about single bonds. If spontaneous intramolecular rotation occurs in *R and the rotation leads to a product, *P that is in a spectroscopic minimum capable of detection by emission from *P, the photochemical process is detectable if the $^*P \rightarrow P + h\nu$ process occurs, that is, if *P emits a measurable number of photons.

An exemplar[45] of the observation of dual fluorescence due to rotation about a single bond is found for 4-N,N-dimethylaminobenzonitrile, **11**. In the ground state R(**11**) possesses a more or less planar conformation R(**11p**). Upon rotation about the C—N single in bond for R(**11p**), a higher-energy twisted conformation R(**11t**) is produced. Franck–Condon photoexcitation of R(**11p**) produces a planar excited state *R(**11p**). It is not possible to directly photoexcite R(**11t**), since the later conformation is not significantly populated in the ground state. In a nonpolar solvent, a single fluorescence emission is observed from *R(**11p**) with a maximum at ~ 350 nm. However, in polar solvents a second fluorescence emission is observed at ~ 450 nm. The excited state *R(**11p**) may be stabilized by rotation about the C—N bond because of CT from the electron-donor amine group to the electron-acceptor cyano group (an example of a free rotor effect about a single bond). Thus, fluoresce at ~ 350 nm is assigned to emission from the planar *R(**11p**) and the fluorescence at ~ 450 nm is assigned to emission from the product of rotation about the C—N bond of *R(**11p**), the electronically excited twisted intramolecular CT structure, *P(**11t**). Thus, an adiabatic CT reaction *R(**11p**) → *P(**11t**) occurs upon rotation about the C—N bond on the excited surface. Because of its **t**wisted **i**ntramolecular **c**harge-**t**ransfer (TICT) characteristics, *R(**11p**) is termed a TICT state. The planar state has been termed a locally excited (LE) state. A schematic representation of the adiabatic reaction is shown in Fig. 4.33.

Evidence (Fig. 4.34) for the fluorescence assignments for *R (**11p**) and *P(**11t**) is found in the observance of a single fluorescence emission at ~ 350 nm for **12** (which is structurally constrained to be planar) and of a single fluorescence emission at ~ 450 nm for **13** (which is structurally constrained to be twisted). We conclude that a coplanar conformation for which the lone pair is nearly parallel to the carbon p-orbitals of the aromatic π system (**11p**) favors the emission at 350 nm. Twisted

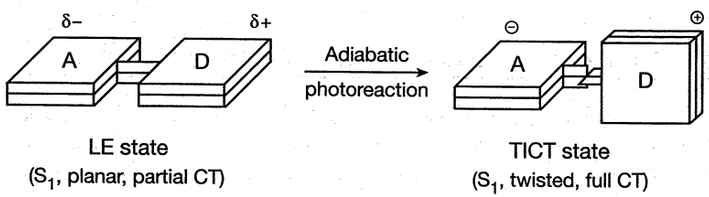

Figure 4.33 A model for formation of a TICT state through an adiabatic *R → *P charge-transfer process. A locally excited planar state, possessing partial charge-transfer characteristics undergoes rotational relaxation toward a twisted conformation that is coupled with intramolecular electron transfer to produce the TICT state.

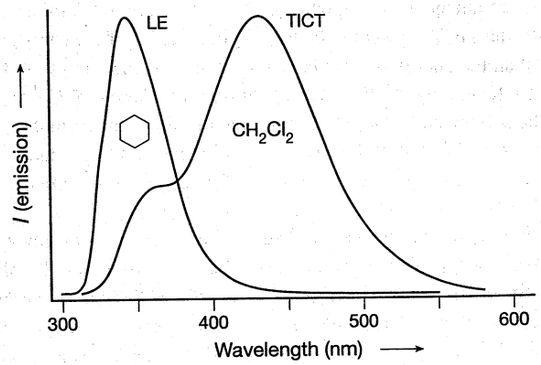

Figure 4.34 Example of the TICT fluorescence of **11t** and **11c**.

structures where the nitrogen lone pair is perpendicular to the π orbital system (**11t**) favor the band at 450 nm.

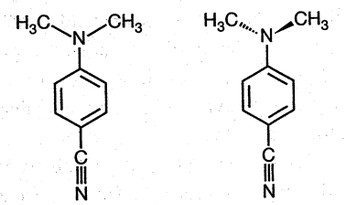

11p
Planar: 350 nm

11t
Twisted: 450 nm

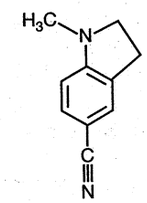

12
350 nm only

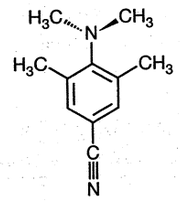

13
450 nm only

The conversion from the planar to the twisted form may involve several barriers: (1) an intramolecular electronic energy reorganization barrier; (2) a thermodynamic barrier if the energy of *R(**11t**) is higher than that of *R(**11p**); and (3) a supramolecular barrier that depends on the friction and electronic reorganization involved in moving

the solvent environment. Thus, depending on the structure of the molecule in nonviscous solvents, the TICT state could be formed irreversibly if the energy of *R(**11t**) is much lower than the energy of *R(**11p**), or reversibly if the energy of the *R(**11t**) is comparable to the energy of *R(**11p**). In addition, the degree of CT depends on the polarity of the solvent and its ability to promote or inhibit the formation of the TICT state. Finally, as the friction of the environment increases, the formation of the TICT state will be kinetically inhibited even if the energy of *R(**11t**) is much lower than the energy of *R(**11p**).

The reaction coordinate for the *R(**11p**) → *R(**11t**) transition involves not only the "gas-phase" energy of the twist but also a certain degree of CT, solvent dipolar relaxation, solvent friction, and probably some rehybridization at the N atom from sp^2 to sp^3. The sensitivity of formation for TICT states to the intramolecular and supramolecular features of a system allow the TICT state to probe the micropolarity and microviscosity of solvents. The large electronic, conformational changes makes them ultrasensitive to supramolecular (solvent cage) effects.

An important characteristic of the exemplar perpendicular TICT state is the structural orthogonality (zero overlap) of the electron donor n orbital for the dimethylamino group and the π orbital system for the acceptor benzonitrile group. This situation can be viewed as one that leads to a dipole moment that is near maximum for full electron transfer from the donor to the acceptor. This feature and the energy minimum for the perpendicular configuration are the essential features of a TICT state. Twisted single and double bonds can be understood within one single theoretical framework, that of diradicaloid states (Chapter 6). An estimation of the energy of *R(**11p**) relative to *R(**11t**) can be obtained from knowledge of electrochemical characteristics of the donor (amine) and acceptor (cyano) groups.

The essence of the TICT phenomenon is the adiabatic transfer of an electron (negative charge) during the *R → *P process. A related phenomenon is the transfer of a proton (positive charge) during the *R → *P process. The latter is termed an "excited state intramolecular proton transfer" (ESIPT). In appropriate cases, the TICT and ESIPT processes can be coupled. The intramolecular hydrogen abstraction of o-hydroxybenzophenone is an exemplar of ESIPT. In this case, the radiationless deactivation of *R(ESIPT) is much faster than emission.

4.42 Emission from "Upper" Excited Singlets and Triples: The Azulene Anomaly

Because of the large number of organic molecules known to obey Kasha's rule[17] (in condensed phases, fluorescence is only observed from S_1 and phosphorescence only from T_1), claims of "anomalous" emission from the S_2, S_3, and so on, and the T_2, T_3, and so on, states of molecules should be viewed with suspicion. To date, examples of emission from $T_n (n > 1)$ are extremely rare. However, well-documented cases of $S_2 \rightarrow S_0 + h\nu$ fluorescence are found for azulene (**12**) and its derivatives.[46] The fluorescence spectrum of **12** reaches a maximum at ~ 374 nm, whereas its $S_0 \rightarrow S_1$

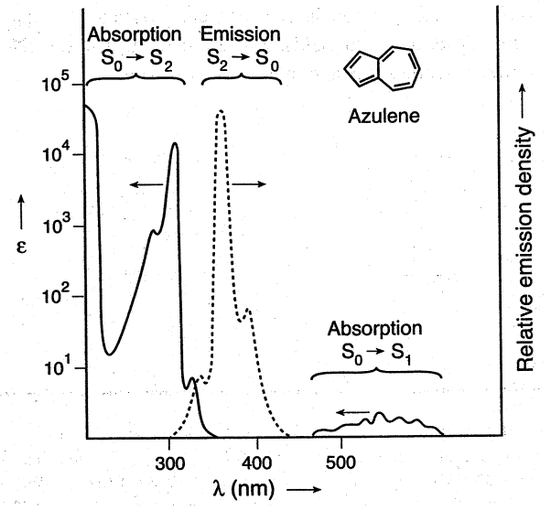

Figure 4.35 The anomalous $S_2 \rightarrow S_0$ fluorescence of azulene. The solid curve shows the $S_0 \rightarrow S_2$ (UV) and the $S_0 \rightarrow S_1$ (vis) absorption of azulene. The fluorescence of azulene (dashed curve) is an approximate mirror image of the $S_0 \rightarrow S_2$.

absorption maximizes at 585 nm (azulene is a blue organic compound). The 0,0 band of the fluorescence and the 0,0 band of $S_0 \rightarrow S_2$ absorption overlap and display an approximate mirror-image relationship to one another (Fig. 4.35). A reason for the observation of an $S_2 \rightarrow S_0$ emission is a large energy gap, which slows down the normally very rapid rate of $S_2 \rightarrow S_1$ internal conversion by decreasing the Franck–Condon factor for radiationless transitions coupled with a fast inherent rate of k_F from S_2. Examples of S_2 emission are known that can be ascribed to thermal population of S_2 from S_1, followed by emission from S_2.

Interestingly, the "normal" $S_1 \rightarrow S_0$ fluorescence from azulene is extremely weak ($\phi_F < 10^{-4}$) and can be obtained only under special conditions.[47] The anomalous lack of normal fluorescence from azulene is understood in terms of a relatively *small* energy gap between S_1 and S_0, which leads to a relatively fast internal conversion. Thus, this explains the anomalous observation of significant fluorescence from S_2 and the virtual lack of emission from S_1 (both are violations of Kasha's rule for emission): Because of its unusual molecular orbitals, the energy gap between S_2 and S_1 is unusually large, leading to a relatively slow internal conversion and the energy gap between S_1 and S_0 is relatively small, leading to a relatively fast internal conversion. As a result, internal conversion can occur in competition with a relatively slow inherent fluorescence.

Substitution of fluorine atoms on the azulene[48] can cause the $S_2 \rightarrow S_0$ fluorescence to increase to significant quantum yields. For example, the azulene **12F** possesses a value of $\Phi_F \sim 0.2$, a significant quantum yield for emission!

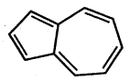

12
Azulene

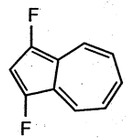

12F

References

1. For excellent nonmathematical discussions of light and its interaction with molecules. (a) R. K. Clayton, *Light and Living Matter, The Physical Part,* McGraw-Hill, New York, 1970. See, for more rigorous treatments (b) H. H. Jaffe and M. Orchin, *Theory and Applications of Ultraviolet Spectroscopy*, John Wiley & Sons, Inc., New York, 1962.
2. For a more detailed discussion, the reader is referred to any elementary textbook of physics. D. Halliday and R. Resnick, *Physics*, John Wiley & Sons, Inc., New York, 1967.
3. For an excellent discussion of light as a wave: W. Kauzman, *Quantum Chemistry*, Academic Press, New York, 1957, p. 546ff.
4. (a) G. W. Robinson, in *Experimental Methods of Physics, Vol. 3.*, L. Marton and D. Williams, eds., Academic Press, New York, 1962, p. 154. (b) W. Heitler, *Quantum Theory of Radiation*, Clarendon Press, Oxford, UK, 1944. (c) G. N. Lewis and M. Calvin, *Chem. Rev.* **25**, 273 (1939).
5. (a) E. J. Bowen, *Quart. Rev.* **4**, 236 (1950). (b) *Chemical Aspects of Light*, Clarendon Press, Oxford, UK, 1946. (c) A. Maccoll, *Q. Rev.* **1**, 16 (1947). (d) D. R. McMillin, *J. Chem. Ed.* **55**, 7 (1978).
6. (a) G. Balavoine, A. Moradpour, and H. B. Kagan, *J. Am. Chem. Soc.* **96**, 5152 (1974). (b) W. Kuhn and E. Knoph, *Z. Phys. Chem.* **7B**, 292 (1930).
7. E. A. Braude, *J. Chem. Soc.* 379 (1950).
8. (a) F. Perrin, *J. Phys. Radium* **7**, 390 (1962). (b) I. B. Berlman, *Mole. Cryst.* **4**, 157 (1968).
9. (a) S. J. Strickler and R. A. Berg, *J. Chem. Phys.* **37**, 814 (1962). (b) W. R. Ware and B. A. Baldwin, *J. Chem. Phys.* **40**, 1703 (1964). (c) J. B. Birks and D. J. Dyson, *Proc. R. Soc.* **A275**, 135 (1963). (d) W. H. Melhuish, *J. Phys. Chem.* **65**, 229 (1961). (e) R. G. Bennett, *Rev. Sci. Instr.* **31**, 1275 (1960). (f) R. S. Lewis and K. C. Lee, *J. Chem. Phys.* **61**, 3434 (1974). (g) D. Phillips, *J. Phys. Chem.* **70**, 1235 (1966).
10. (a) G. N. Lewis and M. Kasha, *J. Am. Chem. Soc.* **67**, 994 (1945). (b) M. Kasha, *Chem. Rev.* **41**, 401 (1948). (c) G. N. Lewis and M. Kasha, *J. Am. Chem. Soc.* **66**, 2100 (1944). (d) S. P. McGlynn, T. Azumi, and M. Kasha, *J. Chem. Phys.* **40**, 507 (1964).
11. (a) B. S. Solomon, T. F. Thomas, and C. Sterel, *J. Am. Chem. Soc.* **90**, 2449 (1968). (b) D. A. Hansen and E. K. C. Lee, *J. Chem. Phys.* **62**, 183 (1975). (c) R. B. Condall and S. Ogilvie, in *Organic Molecular Photophysics*, Vol. 2, J. B. Birks, ed., John Wiley & Sons, Inc., New York, 1975, p. 33.
12. (a) B. S. Neporent, *Pure Appl. Chem.* **37**, 111 (1976). (b) B. S. Neporent, *Opt. Spectrosc.* **32**, 133 (1972). (c) H. Suzuki, *Electronic Absorption Spectra and the Geometry of Organic Molecules*, Academic Press, New York, 1967, p. 79.
13. See this reference for a more rigorous discussion. (a) G. Herzberg, *Spectra of Diatomic Molecules*, Van Nostrand, Princeton, NJ, 1950.
14. (a) S. P. McGlynn, T. Azumi., and M. Kinoshita, *Molecular Spectroscopy of the Triplet State*, Prentice Hall, Englewood Cliffs, NJ, 1969. (b) M. J. S. Deward and R. C. Dougherty, *The PMO Theory of Organic Chemistry*, Plenum, New York, 1974.
15. R. M. Hochstrasser and A. Marzzallo, *Molecular Luminescence*, E. Lim, ed., W. A. Benjamin, New York, 1969, p. 631.
16. The interested reader should see the following references: (a) J. B. Birks, *Photophysics of Aromatic Molecules*, John Wiley & Sons, Inc., New York, 1970. (b) C. A. Parker, *Adv. Photochem.* **2**, 305 (1964). (c) N. J. Turro, *Molecular Photochemistry*, Benjamin, New York, 1967. (d) R. Becker, *Theory and Interpretation of Fluorescence and Phosphorescence*, John Wiley & Sons, Inc., New York, 1969. (e) S. L. Murov, I. Carmichael, and G. L. Hug, *Handbook of Photochemistry,* 2ed., Marcel Dekker, New York, 1993.
17. M. Kasha, *Disc. Faraday Soc.* **9**, 14 (1950).
18. (a) H. H. Jaffe and M. Orchin, *Theory and Applications of Ultraviolet Spectroscopy*, John Wiley & Sons, Inc., New York, 1962. (b) C. A. Parker, *Photoluminescence in Solution*, Elsevier, Amsterdam, The Netherlands, 1968. (c) J. R. Lakowicz, *Principles of Fluorescence Spectroscopy*, Plenum, New York, 1999.
19. (a) F. Hirayama and S. Lipsky, *J. Chem. Phys.* **51**, 3616 (1969). (b) M. S. Henry and W. P. Helman, *J. Chem. Phys.* **56**, 5734 (1972). (c) F. Hirayama and S. Lipsky, *J. Chem. Phys.* **62**, 576 (1975).
20. (a) E. Havinga, *Chimia* **16**, 145 (1962). (b) J. Pusset, and R. Bengelmans, *Chem. Commun.* 448 (1974).
21. (a) M. S. Henry and W. P. Helman, *J. Chem. Phys.* **56**, 5734 (1972). (b) A. M. Halpern and R. M. Danziger, *Chem. Phys. Lett.*, **72** (1972).
22. W. W. Schloman and H. Morrison, *J. Am. Chem. Soc.* **99**, 3342 (1977).
23. (a) S. Sharafy and K. A. Muszkat, *J. Am. Chem. Soc.* **93**, 4119 (1971). (b) D. Gegion, K. A. Muszkat, and E. Fischer, *J. Am. Chem. Soc.* **90**, 12, 3097 (1968). (c) J. Saltiel, O. C. Aafirion, E. D. Megarity, and A. A. Lamola, *J. Am. Chem. Soc.* **90**, 4759 (1968). (d) C. D. De Boer and R. H. Schlessinger, *J. Am. Chem. Soc.* **90**, 803 (1968).
24. (a) R. Hochstrasser, *Electrons in Atoms*, W. A. Benjamin, San Francisco, 1966. (b) D. S. McClure, *J. Phys. Chem.* **17**, 905 (1949). (c) M. A. El-Sayed, *J. Chem. Phys.* **38**, 2834 (1963). (d) M. A. El-Sayed, *J. Chem. Phys.* **36**, 573 (1962); *J. Chem. Phys.* **41**, 2462 (1964).
25. (a) G. N. Lewis and M. Kasha, *J. Am. Chem. Soc.* **67**, 994 (1945). (b) G. M. Lewis and M. Kasha, *J. Am. Chem. Soc.* **66**, 2100 (1944). (c) A. Terenin, *Acta Physicochim. USSR* **18**, 210 (1943).
26. (a) S. R. LaPaglia, *Spectrochim. Acta* **18**, 1295 (1962). (b) N. J. Turro, K.-C. Liu, W. Cherry, M.-M. Liu, and B. Jacobson, *Tetrahedron Lett.*, 555 (1978). (c) R. E. Kellogg and N. C. Wyeth, *J. Chem. Phys.* **45**, 3156 (1966).
27. (a) D. Evans, *J. Chem. Soc.*, 1351 (1957); *J. Chem. Soc.*, 2753 (1959); (b) D. Evans, *J. Chem. Soc.* 1735 (1960); *J. Chem. Soc.*, 1987 (1961). (c) A. Grabowska, *Spectrochim. Acta* **20**, 96 (1966). (d) H. Tsubomura and R. S. Mulliken, *J. Am. Chem. Soc.* **82**, 5966 (1960).
28. G. Kavarnos, T. Cole, P. Scribe, J. C. Dalton, and N. J. Turro, *J. Am. Chem. Soc.* **93**, 1032 (1971).
29. (a) S. P. McGlynn, et al., *J. Phys. Chem.* **66**, 2499 (1962). (b) S. P. Mcglynn, et al. *J. Chem. Phys.* **39**, 675 (1963). (c) G. G. Giachino and D. R. Kearns, *J. Chem. Phys.* **52**, 2964 (1970). (d) G. G. Giachino and D. R. Kearns, *J. Chem. Phys.* **53**, 3886 (1963). (e) N. Christodonleas and S. P. McGlynn, *J. Chem. Phys.* **40**, 166 (1964). (f) D. S. McClure, *J. Chem. Phys.* **17**, 905 (1949).
30. M. Kasha, *J. Chem. Phys.* **20**, 71 (1952).
31. (a) M. R. Wright, R. P. Frosch, and G. W. Robinson, *J. Chem. Phys.* **33**, 934 (1960). (b) A. Grabowska, *Spectrochim. Acta.* **19**, 307 (1963).
32. (a) C. A. Parker and T. A. Joyce, *Trans. Faraday Soc.* **65**, 2823 (1969). (b) W. D. K. Clark, A. D. Litt, and C. Steel, *Chem. Commun.* 1087 (1969). (c) J. Saltiel, H. C. Curtis, L. Metts, J. W. Miley, J. Winterle, and M. Wrighton, *J. Am. Chem. Soc.* **92**, 410 (1970). (d) See this reference for a review of the factors allowing the observation of phosphorescence in fluid solution. N.J. Turro, K.C. Liu, M.F. Chow, and P. Lee, *Photochem. Photobio.* **27**, 500 (1978). (e) K. Kalyanasundaram, F. Grieser, and J. K. Thomas, *Chem. Phys. Lett.* **51**, 501 (1977). (f) H. Gatterman and M. Stockburger, *J. Chem. Phys.* **63**, 4341 (1975).
33. See this reference for a review of the method of flash spectroscopy. G. Porter, *Techniques of Organic Chemistry,* Vol. 8, John Wiley & Sons, Inc., New York, 1963, p. 1054.
34. See this reference for a review of T-T absorption. H. Labhart and W. Heinzelmann, in *Photophysics of Organic Molecules*, Vol. 1, J.B. Birks, ed., John Wiley & Sons, Inc., New York, 1973, p. 297.

35. See these references for reviews of excimers and excliplexes. (a) T. Forster, *Angew. Chem. Int. Ed. En.* **8**, 333 (1969). (b) J.B. Birks, *Photophysics of Aromatic Molecules*, John Wiley & Sons, Inc., New York, 1970, p. 301. (c) H. Beens and A. Weller, in *Organic Molecular Photophysics*, Vol. 2, J. B. Birks, ed., John Wiley & Sons, Inc., New York, 1975, p. 159.

36. J.-M. Lehn, *Supramolecular Chemistry*, VCH, New York, 1995.

37. See this reference for a survey of CT phenomena, including absorption and emission: J. B. Birks, *Photophysics of Aromatic Molecules*, John Wiley & Sons, Inc., New York, 1970, p. 403.

38. M. P. Niemczyk, N. E. Schore, and N. J. Turro, *Mol. Photochem.* **5**, 69 (1973).

39. (a) P. C. Subudhi and E. C. Lim, *J. Chem. Phys.* **63**, 5491 (1975). (b) T. Takemura, M. Aikawa, H. Baba, and Y. Shindo, *J. Am. Chem. Soc.* 98, 2205 (1976). (c) S. O. Kajima, P. C. Subudhi, and E. C. Lim, *J. Chem. Phys.* **67**, 4611 (1977).

40. T. Forster and K. Kasper, *Z. Physik. Chem., N.F.* **1**, 275 (1954).

41. J. B. Birks, *Photophysics of Aromatic Molecules*, John Wiley & Sons, Inc., New York, 1970, p. 357.

42. K. Yoshihara, T. Kasuya, A. Inoue, and S. Nagakura, *Chem. Phys. Lett.* **9**, 469 (1971).

43. (a) A. Weller, *Pure Appl. Chem.* **16**, 115 (1968). (b) H. Knibbe, D. Rehm, and A. Weller, *Ber. Bunsen. Gesell.* **73**, 839 (1969); (c) *Ber. Bunsen. Gesell.* **72**, 257 (1968); *Ber. Bunsen. Gesell.* **73**, 834 (1969). (d) J. B. Birks, *Photophysics of Aromatic Molecules*, John Wiley & Sons, Inc., New York, 1970, p. 403.

44. See this refence for a review of the TICT phenomenon. Z. R. Grabowski, K. Rotkiewicz, and W. Rettig, *Chem. Rev.* 103, 3899 (2003).

45. Z. R. Grabowski and J. Dobkowski, *Pure Appl. Chem.* **55**, 245 (1983).

46. (a) M. Beer and H. C. Longuet-Higgins, *J. Chem. Phys.* **23**, 1390 (1955). (b) G. Viswath and M. Kasha, *J. Chem Phys.* **24**, 757 (1956). (c) J. B. Birks, *Chem. Phys. Lett.* **17** 370 (1972). (d) S. Murata, C. Iwanga, T. Toda, and H. Kohubun, *Ber. Bunsen. Ges. Phys. Chem.* **76**, 1176 (1972).

47. (a) P. M. Rentzepis, *Chem. Phys. Lett.* **3**, 717 (1969). (b) G. D. Gillispie and E. C. Lim, *J. Chem. Phys.* **65**, 4314 (1976).

48. S. V. Shevyakov, H. Li, R. Muthyala, A. E. Asaate, J. C. Croney, D. M. Jameson, and R. S. H. Liu, *J. Phys. Chem. A* 107, 3295 (2003).